





This is to certify that the

dissertation entitled

Applications of Ion-Molecule Reactions for
Distinguishing Organic Isomers in a Tandem
Quadrupole Mass Spectrometer

presented by

Siu H. Stephen Chan

has been accepted towards fulfillment
of the requirements for

Ph.D degree in Chemistry



Major professor

Date Nov. 27, 1991



PLACE IN RETURN BOX to remove this checkout from your record.
TO AVOID FINES return on or before date due.

DATE DUE		
_____	_____	_____
_____	_____	_____
_____	_____	_____
_____	_____	_____
_____	_____	_____
_____	_____	_____
_____	_____	_____

APPLICATIONS OF ION-MOLECULE REACTIONS FOR
DISTINGUISHING ORGANIC ISOMERS IN A TANDEM QUADRUPOLE
MASS SPECTROMETER

By

Siu H. Stephen Chan

A DISSERTATION

Submitted to
Michigan State University
in partial fulfillment of the requirements
for the degree of

DOCTOR OF PHILOSOPHY

Department of Chemistry

1991

DIS

frag

bas

a t

sele

mol

tec

iso

(H)

dif

pre

su

is

in

co

re

m

680-5437

ABSTRACT

APPLICATIONS OF ION-MOLECULE REACTIONS FOR DISTINGUISHING ORGANIC ISOMERS IN A TANDEM QUADRUPOLE MASS SPECTROMETER

By

Siu H. Stephen Chan

Many chemical reactions are isomer-specific whereas simple ionic fragmentation, upon which the specificity of normal mass spectrometry is based, is much less so. The unique location of the collision chamber (Q2) of a tandem quadrupole mass spectrometer (TQMS) provides enhanced selectivity for mechanistic studies and analytical applications of ion-molecule reactions. This can be exploited to develop new analytical techniques for differentiating organic isomers.

Low-energy collisions between the $[M-1]^-$ ions of dichlorobenzene isomers and D_2O or ND_3 are found to produce distinct hydrogen/deuterium (H/D) exchange product patterns that allow the isomers to be clearly differentiated when the traditional mass spectrometric techniques fail. The predominant products observed for o-, m- and p-dichlorobenzene are anions substituted with 3, 2, and 1 deuteriums, respectively. The reactivity of D_2O is about three times that of ND_3 for these reactions. A mechanism involving the formation of a five-membered-ring intermediate is proposed for the exchange reaction and is found to fully explain all the experimental results. The results of computer simulations based on the proposed mechanism are consistent with the observed results.

tetr

[M-

1,3,

proo

rea

dist

form

pro

be c

of t

crea

usi

use

pot

det

Ion-molecule reactions are also explored for analyzing isomers of tetrachlorobenzo-p-dioxin (TCDD). For reactions between D_2O and the $[M-1]^-$ ions of TCDD isomers, 2,3,7,8-TCDD is distinguished from 1,2,3,4-, 1,3,6,8-, 1,2,7,8- and 1,3,7,8-TCDD by its unique formation of a single product having only one H/D exchange. When alcohol molecules are reacted with the $[M-1]^-$ ions from isomeric TCDDs, 2,3,7,8-TCDD is distinguished from the other less toxic isomers by its lower reactivity for the formation of the $[M-1+alcohol]^-$ adduct products.

While ions formed by low-energy ion-molecule reactions in Q2 provide useful information for isomeric differentiation, these ions will not be detected if their mobilities are too low to reach the detector. The detection of these ions can be improved if a gentle longitudinal potential gradient is created along the ion path of Q2. Theoretically, this can be accomplished by using Q2 made of BeO rods on which are winded high-resistance wires used for the generation of the transverse field. The nearly constant potential gradient will provide the ions with a continuous force towards the detector.

to people who strive to make a better world for all human races

hel
his
also
esp
rea

exp
sati
tea
cla

I w
tren
acco
to a
will
tou

tea
con
und
for
The
gra
live

Joe

ACKNOWLEDGEMENTS

I would like to thank my research advisor, Dr. Christie Enke, for his help and guidance that make the completion of my Ph.D a reality. Through his scientific insight, I have learned a lot about being a better scientist. I also would like to thank the other members of my guidance committee, especially Dr. William Reusch who agreed to take on the duty of a second reader for my dissertation just two weeks before my oral defense.

During my graduate school career at Michigan State University, the experience of teaching has provided me a great deal of personal satisfaction. Thanks to all my students who allowed me to enjoy myself as a teacher. Especially during the rough years of my research, seeing my classes was something that I was looking forward to every week.

The most rewarding experience of my life comes from the year when I was a secondary school teacher many years ago. Thanks to the tremendous friendship and help offered by all of my colleagues who accepted me just the way I was. I would also like to extend a special thank to all the kids of my classes who gave me so much fun for being a teacher. I will never forget the hiking trips with all the kids. It certainly was the toughest job I have ever loved.

I also want to express my gratitude to two of my undergraduate teachers, Drs. Paul Merritt and Nick Zevos for their kindness, help and confidence in me that stirred me into the field of chemistry. My undergraduate career at Potsdam, New York, would be less enjoyable if not for the warm hospitality of Mr. & Mrs Sellers during my final year there. Thanks for all the gifts, camping trips and the party in honor of my graduation. You guys have made the cold winter of Potsdam so warm to live in.

I would like to thank my former roommates, David Bell, Andy Teng, Joe Foley and Mark Meyer for their sincere friendship and putting up with

my different moods. Thanks also go to the members of Enke's group for their help. Also I would like to thank Susan Cady for her persistent long-distance friendship and listening to some of my problems.

Over the past many years as a graduate student, I am grateful to have learned many things beside chemistry. Now I understand more about the importance of humanity for the development a mature decent human being. Through appropriate education starting from very young, perhaps, one day we may live in the "dream world" of Dr. Martin L. King Jr..

Although the road to the completion my Ph.D have been a long and tough one, I would like to express my greatest thank to my parents, sisters and brother for their love, moral support and understanding. Finally, I can say with enthusiasm that I am still alive.

LIST

LIST

INTR

Introdu

Collisio

Disting

A

B

TABLE OF CONTENTS

LIST OF TABLES	xi
LIST OF FIGURES	xii

CHAPTER 1

INTRODUCTION	1
Introduction.....	1
Collision Processes in Ion-Molecule Reactions.....	2
Distinguishing Organic Isomers in Tandem Mass Spectrometry.....	8
A. MS/MS in Sector Instruments for Isomeric Differentiation....	9
B. Isomeric Differentiation in MS/MS Instruments Suited for Ion-Molecule Reactions.....	11
a. Tandem Flowing Afterglow-SIFT-Drift.....	12
b. Quadrupole Ion Trap.....	13
c. Fourier Transform Ion Cyclotron Resonance.....	14
d. Triple Quadrupole Mass Spectrometry.....	15

RE
[M
RE

Int

Ex

Res

Con

ME
OF
DE

Intr

Exp

Res

Conc

CHAPTER 2

REACTIVITIES OF DEUTERATED REAGENTS TOWARDS THE [M-1]- IONS OF CHLORINATED BENZENES FOR H/D EXCHANGE REACTIONS.....	27
Introduction.....	27
Experimental.....	28
Result and Discussion.....	29
A. Characterization and Optimization of H/D Exchange Reactions Involving the [M-1]- of o-Dichlorobenzene.....	29
B. H/D Exchange Reactions between Deuterated Reagents and the [M-1]- of o-Dichlorobenzene.....	36
C. H/D Exchange Reactions for the [M-1]- of Isomers of Substituted Chlorobenzenes with D ₂ O.....	39
Conclusions.....	50

CHAPTER 3

MECHANISTIC STUDY OF H/D EXCHANGE BETWEEN [M-1]- IONS OF CHLORINATED BENZENES AND DEUTERATED WATER OR DEUTERATED AMMONIA.....	52
Introduction.....	52
Experimental.....	54
Results and Discussion.....	56
A. Mechanistic Analysis.....	56
B. Collision Pressure Dependence on Products of H/D Exchanges.....	65
C. Reactions with Other Aromatic Isomers.....	86
Conclusions.....	93

**EXPLORATION
MASS SPECTROMETRY
POLYCHLORINATED**

Introduction.....

Experimental.....

Results and Discussion.....

A. General.....

B. Reagents.....

C. Reagents.....

D. Reagents.....

Conclusions.....

**IMPROVEMENTS
A TRIPLE QUADRUPOLE
CONSIDERATIONS**

Introduction.....

Designs for the
Instrument.....

Conclusions.....

CHAPTER 4

EXPLORATION OF ION-MOLECULE REACTIONS IN TANDEM MASS SPECTROMETRY FOR DISTINGUISHING ISOMERS OF POLYCHLORO-DIBENZO-P-DIOXINS.....	99
Introduction.....	99
Experimental.....	101
Results and Discussion.....	102
A. Generation of Reactant Ions.....	102
B. Reactions with D ₂ O.....	103
C. Reactions with Alcohols.....	112
D. Reactions with O ₂	115
Conclusions.....	116

CHAPTER 5

IMPROVEMENT TO THE DETECTION OF LOW-ENERGY IONS IN A TRIPLE QUADRUPOLE MASS SPECTROMETER - A THEORETICAL CONSIDERATION.....	120
Introduction.....	120
Designs for the Second Quadrupole Collision Chamber of a TQMS Instrument.....	122
Conclusions.....	140

CONCLUSION

APPENDIX

CHAPTER 6

CONCLUSIONS AND SUGGESTED FUTURE EXTENSIONS..... 142

APPENDIX..... 145

Table 2-1

Table 3-1

Table 4-1

Table 4-2

LIST OF TABLES

Table 2-1	Total ion intensity of all products and ion intensity for the 3-D substituted product at different collision pressure settings. The optimum collision offset energy is shown right next to each pressure.....	35
Table 3-1	Maximum number of H/D exchanges for the [M-1] ⁻ ions of isomers of chlorinated benzenes (in cases of no isomerization).....	92
Table 4-1	Ion intensity ratios for m/z 319 and m/z 320 derived from the ammonia NCI mass spectra of the selected TCDD isomers.....	106
Table 4-2	Percentages of the [M-1+alcohol] ⁻ adducts based on 100% of the [M-1] ⁻ reactants.....	113

Figure 1-1

Figure 1-2

Figure 2-1

Figure 2-2

Figure 2-3

Figure 2-4

Figure 2-5

Figure 2-6

(
I
Y
i
t
P
I
S
b
I
f
A
c
a
th
D
P
th
se
p
is
d
P
re
(n
re
ex
S
D
P
of
wi

LIST OF FIGURES

Figure 1-1	Center-of-mass axial kinetic energy spectrum of protonated α -hydroxyisobutyrate ethyl ester. The yield of adduct ions, m/z 150 (●), and the most intense fragment, m/z 115 (■), were recorded against the experimental center-of-mass energy of the protonated molecular ion (m/z 133). (Adapted from Ref. 18).....	7
Figure 1-2	Schematic of a triple quadrupole mass spectrometer based on the Finnigan TSQ-70B model.....	17
Figure 2-1	Ion intensity as a function of collision energy offset at Q2 for the $[M-1]^-$ of <i>o</i> -dichlorobenzene.....	31
Figure 2-2	A plot of optimum collision energy as a function of collision pressure of D_2O . At a specific pressure value, an optimum collision energy is obtained by varying the collision offset voltage of the instrument until the D_3 -substituted product is optimized.....	33
Figure 2-3	Percent of detected ions that have exchanged with three deuteriums at different collision pressure settings. Offset energy is the optimum for each pressure. The percent detected D_3 -substituted product is based on 100% for the total ion intensity of all detected ions.....	34
Figure 2-4	Product mass spectra obtained from H/D exchange reactions between the $[M-1]^-$ of <i>o</i> -dichlorobenzene (m/z 145) and different deuterated reagents. The reagents that do not produce any observable H/D exchange peaks are not shown in the figure.....	37
Figure 2-5	Selected isomers for H/D exchange reactions with D_2O	40
Figure 2-6	Product mass spectra for the $[M-1]^-$ ion of the isomers of chloroaniline upon H/D exchange reactions with D_2O	41

Figure 2-7

Figure 2-8

Figure 2-9

Figure 2-10

Figure 2-11

Figure 2-12

Figure 3-1

Figure 3-2

Figure 3-3

Figure 3-4

Figure 2-7	Product mass spectra for the [M-1] ⁻ ion of the isomers of chlorophenol upon H/D exchange reactions with D ₂ O...	42
Figure 2-8	Product mass spectra for the [M-1] ⁻ ion of the isomers of chlorobenzaldehyde upon H/D exchange reactions with D ₂ O.....	43
Figure 2-9	Product mass spectra for the [M-1] ⁻ ion of the isomers of chlorotoluene upon H/D exchange reactions with D ₂ O.....	44
Figure 2-10	Product mass spectra for the [M-1] ⁻ ion of the isomers of chloroanisole upon H/D exchange reactions with D ₂ O.....	45
Figure 2-11	Product mass spectra for the [M-1] ⁻ ion of the isomers of chlorobenzoic acid upon H/D exchange reactions with D ₂ O.....	46
Figure 2-12	Product mass spectra for the [M-1] ⁻ ion of the isomers of chloronitrobenzene upon H/D exchange reactions with D ₂ O.....	47
Figure 3-1	Product spectra obtained from the H/D exchange reactions between the [M-1] ⁻ ions of the individual isomers of dichlorobenzene and deuterated water and deuterated ammonia. The reactant ions are at m/z 145. Peaks at higher mass unit are due to one or more H/D exchange reactions.....	57
Figure 3-2	The possible charge sites for the [M-1] ⁻ ions of dichlorobenzene isomers and the consequent location and number of exchangeable hydrogens according to the proposed reaction mechanism.....	62
Figure 3-3	Plots for normalized relative product intensity vs collision pressure for H/D exchange reactions between the [M-1] ⁻ ions of dichlorobenzene isomers and D ₂ O molecules.....	66
Figure 3-4	Plots for normalized relative product intensity vs collision pressure for H/D exchange reactions between the [M-1] ⁻ ions of chlorobenzene isomers and ND ₃ molecules.....	70

Figure 3-5

A
a
c
s
r
c

Figure 3-6

T
o
o

Figure 3-7

A
r
p
T
e
s
o

Figure 3-8

T
o
o

Figure 3-9

T
st
up

Figure 3-10

A
re
pr
co
H
m
D
as
ar

Figure 3-11

A
re
pr
co
H/
p-e
NI

Figure 3-5	A simulated collision-dependence plot that represents a composite of individual collision-product plots for different percentages of reactive collision. The simulation is based on the proposed H/D exchange reaction mechanism between the structure II of o-dichlorobenzene and D ₂ O or ND ₃ molecules.....	73
Figure 3-6	The reaction pathway for the structure II anions of o-dichlorobenzene upon reactive collisions with D ₂ O or ND ₃ molecules.....	75
Figure 3-7	A simulated collision-dependence plot that represents a composite of individual collision-product plots for the different percentages of reactive collision. The simulation is based on the proposed H/D exchange reaction mechanism between the structure I anions of o-dichlorobenzene and D ₂ O or ND ₃ molecules.....	77
Figure 3-8	The reaction pathway for the structure I anion of o-dichlorobenzene upon reactive collision with D ₂ O or ND ₃ molecules.....	80
Figure 3-9	The reaction pathway for the structure III (top) and structure IV (bottom) anions of o-dichlorobenzene upon reactive collisions with D ₂ O or ND ₃ molecules.....	82
Figure 3-10	A simulated collision-dependence plot that represents a composite of individual collision-product plots for different percentages of reactive collision. The simulation is based on the proposed H/D exchange reaction mechanism between a mixture of different m-dichlorobenzene anions and D ₂ O or ND ₃ molecules. The mixture of anions is assumed to contain 50% structure IV, 25% structure V and 25% structure II.....	84
Figure 3-11	A simulated collision-dependence plot that represents a composite of individual collision-product plots for different percentages of reactive collision. The simulation is based on the proposed H/D exchange reaction mechanism between p-dichlorobenzene anions (structure VI) and D ₂ O or ND ₃ molecules.....	87

Figure 3-12
L
i
L
[
M
t

Figure 3-13
A
b
L
s
P

Figure 4-1
M
c
r

Figure 4-2
M
c
c
a

Figure 4-3
P
T
e
a
th

Figure 5-1
A
d

Figure 5-2
A

Figure 5-3
T
Q
ap

Figure 5-4
T
Q
ap

Figure 5-5
T
Q
ap

Figure 5-6
T
Q
ap

Figure 3-12	Product spectra for the tetra and trichlorobenzene isomers that produce H/D exchange ion products. The H/D exchange products are due to reactions between the [M-1] ⁻ ions of the isomers indicated and D ₂ O molecules. No H/D exchange products are observed for the other tetra and trichlorobenzene isomers.....	90
Figure 3-13	A product spectrum for H/D exchange reactions between the [M-1] ⁻ ions of 1-chloronaphthalene and D ₂ O molecules. Reactant ions having five hydrogens substituted with deuteriums are the predominant products.....	94
Figure 4-1	Mass spectra of TCDD isomers derived from negative chemical ionization (NCI) using ammonia as a reagent.....	104
Figure 4-2	Mass spectra of 1,2,4,7,8- and 1,2,3,7,8-penta-chlorodibenzo-p-dioxin derived from negative chemical ionization (NCI) using ammonia as a reagent.....	107
Figure 4-3	Product mass spectra of [M-1] ⁻ ions derived from TCDD isomers upon hydrogen/deuterium (H/D) exchange reactions with D ₂ O. The exchange products are indicated by peaks at one or more m/z units above the reactant ions.....	110
Figure 5-1	A potential contour diagram for the extraction lens design.....	123
Figure 5-2	A design of segmenting the second quadrupole rods.....	125
Figure 5-3	The configuration of a potential contour diagram for Q2 made of 6-segmented rods with a 5-V potential applied.....	126
Figure 5-4	The configuration of a potential contour diagram for Q2 made of 11-segmented rods with a 5-V potential applied.....	127
Figure 5-5	The configuration of a potential contour diagram for Q2 made of 21-segmented rods with a 5-V potential applied.....	128
Figure 5-6	The configuration of a potential contour diagram for Q2 made of 26-segmented rods with a 5-V potential applied.....	129

Figure 5-7

Figure 5-8

Figure 5-9

Figure 5-10

Figure 5-11

Figure A-1

Figure A-2

Figure A-3

Figure A-4

Figure A-5

Figure A-6

Figure A-7

Figure 5-7	The configuration of a potential contour diagram for Q2 made of 35-segmented rods with a 5-V potential applied.....	130
Figure 5-8	Potential along the ion path for the designs of Q2 made of different numbers of segments when a potential difference of 5 V is applied.....	131
Figure 5-9	The 1st derivative plots representing potential gradient vs spatial distance into the Q2 ion path.....	134
Figure 5-10	A design of modifying the second quadrupole using the non-circular zig-zag wire-winding technique. Dash lines represents wires winded on the back side of the rod.....	137
Figure 5-11	Room temperature thermal conductivity of BeO compared to various materials. (Adapted from literature data compiled by Ceradyne, Inc., Costa Mesa, CA).....	139
Figure A-1	A simulated collision-product plot for the structure I of o-dichlorobenzene based on an H/D exchange reactivity of 5% reactive collision.....	146
Figure A-2	A simulated collision-product plot for the structure I of o-dichlorobenzene based on an H/D exchange reactivity of 10% reactive collision.....	147
Figure A-3	A simulated collision-product plot for the structure I of o-dichlorobenzene based on an H/D exchange reactivity of 20% reactive collision.....	148
Figure A-4	A simulated collision-product plot for the structure I of o-dichlorobenzene based on an H/D exchange reactivity of 25% reactive collision.....	149
Figure A-5	A simulated collision-product plot for the structure I of o-dichlorobenzene based on an H/D exchange reactivity of 30% reactive collision.....	150
Figure A-6	A simulated collision-product plot for the structure I of o-dichlorobenzene based on an H/D exchange reactivity of 35% reactive collision.....	151
Figure A-7	A simulated collision-product plot for the structure I of o-dichlorobenzene based on an H/D exchange reactivity of 40% reactive collision.....	152

Figure A-20

Figure A-21

Figure A-22

Figure A-23

Figure A-24

Figure A-25

Figure A-26

Figure A-27

Figure A-28

Figure A-29

Figure A-8	A simulated collision-product plot for the structure I of o-dichlorobenzene based on an H/D exchange reactivity of 45% reactive collision.....	153
Figure A-9	A simulated collision-product plot for the structure I of o-dichlorobenzene based on an H/D exchange reactivity of 50% reactive collision.....	154
Figure A-10	A simulated collision-product plot for the structure I of o-dichlorobenzene based on an H/D exchange reactivity of 55% reactive collision.....	155
Figure A-11	A simulated collision-product plot for the structure I of o-dichlorobenzene based on an H/D exchange reactivity of 60% reactive collision.....	156
Figure A-12	A simulated collision-product plot for the structure I of o-dichlorobenzene based on an H/D exchange reactivity of 65% reactive collision.....	157
Figure A-13	A simulated collision-product plot for the structure I of o-dichlorobenzene based on an H/D exchange reactivity of 70% reactive collision.....	158
Figure A-14	A simulated collision-product plot for the structure II of o-dichlorobenzene based on an H/D exchange reactivity of 5% reactive collision.....	159
Figure A-15	A simulated collision-product plot for the structure II of o-dichlorobenzene based on an H/D exchange reactivity of 10% reactive collision.....	160
Figure A-16	A simulated collision-product plot for the structure II of o-dichlorobenzene based on an H/D exchange reactivity of 20% reactive collision.....	161
Figure A-17	A simulated collision-product plot for the structure II of o-dichlorobenzene based on an H/D exchange reactivity of 25% reactive collision.....	162
Figure A-18	A simulated collision-product plot for the structure II of o-dichlorobenzene based on an H/D exchange reactivity of 30% reactive collision.....	163
Figure A-19	A simulated collision-product plot for the structure II of o-dichlorobenzene based on an H/D exchange reactivity of 35% reactive collision.....	164

Figure A-37

Figure A-38

Figure A-39

Figure A-40

Figure A-41

Figure A-42

Figure A-43

Figure A-30	A simulated collision-product plot for a mixture of dichlorobenzene anions originated from m-dichlorobenzene. The calculations are based on an H/D exchange reactivity of 25% reactive collision. The mixture contains anions of 50% structure VI, 25% structure V and 25% structure II.....	175
Figure A-31	A simulated collision-product plot for a mixture of dichlorobenzene anions originated from m-dichlorobenzene. The calculations are based on an H/D exchange reactivity of 30% reactive collision. The mixture contains anions of 55% structure VI, 25% structure V and 20% structure II.....	176
Figure A-32	A simulated collision-product plot for a mixture of dichlorobenzene anions originated from m-dichlorobenzene. The calculations are based on an H/D exchange reactivity of 30% reactive collision. The mixture contains anions of 50% structure VI, 25% structure V and 25% structure II.....	177
Figure A-33	A simulated collision-product plot for a mixture of dichlorobenzene anions originated from m-dichlorobenzene. The calculations are based on an H/D exchange reactivity of 35% reactive collision. The mixture contains anions of 55% structure VI, 25% structure V and 20% structure II.....	178
Figure A-34	A simulated collision-product plot for a mixture of dichlorobenzene anions originated from m-dichlorobenzene. The calculations are based on an H/D exchange reactivity of 35% reactive collision. The mixture contains anions of 50% structure VI, 25% structure V and 25% structure II.....	179
Figure A-35	A simulated collision-product plot for a mixture of dichlorobenzene anions originated from m-dichlorobenzene. The calculations are based on an H/D exchange reactivity of 40% reactive collision. The mixture contains anions of 55% structure VI, 25% structure V and 20% structure II.....	180
Figure A-36	A simulated collision-product plot for a mixture of dichlorobenzene anions originated from m-dichlorobenzene. The calculations are based on an H/D exchange reactivity of 40% reactive collision. The mixture contains anions of 50% structure VI, 25% structure V and 25% structure II.....	181

Figure A-44

Figure A-45

Figure A-46

Figure A-47

Figure A-48

Figure A-49

Figure A-50

Figure A-51

Figure A-52

Figure A-53

Figure A-54

re A-44	A simulated collision-product plot for a mixture of dichlorobenzene anions originated from m-dichlorobenzene. The calculations are based on an H/D exchange reactivity of 20% reactive collision. The mixture contains anions of 50% structure VI, 25% structure V and 25% structure II.....	189
re A-45	A simulated collision-product plot for the structure VI of p-dichlorobenzene based on an H/D exchange reactivity of 5% reactive collision.....	190
re A-46	A simulated collision-product plot for the structure VI of p-dichlorobenzene based on an H/D exchange reactivity of 10% reactive collision.....	191
re A-47	A simulated collision-product plot for the structure VI of p-dichlorobenzene based on an H/D exchange reactivity of 20% reactive collision.....	192
re A-48	A simulated collision-product plot for the structure VI of p-dichlorobenzene based on an H/D exchange reactivity of 25% reactive collision.....	193
re A-49	A simulated collision-product plot for the structure VI of p-dichlorobenzene based on an H/D exchange reactivity of 30% reactive collision.....	194
re A-50	A simulated collision-product plot for the structure VI of p-dichlorobenzene based on an H/D exchange reactivity of 35% reactive collision.....	195
re A-51	A simulated collision-product plot for the structure VI of p-dichlorobenzene based on an H/D exchange reactivity of 40% reactive collision.....	196
re A-52	A simulated collision-product plot for the structure VI of p-dichlorobenzene based on an H/D exchange reactivity of 45% reactive collision.....	197
re A-53	A simulated collision-product plot for the structure VI of p-dichlorobenzene based on an H/D exchange reactivity of 50% reactive collision.....	198
re A-54	A simulated collision-product plot for the structure VI of p-dichlorobenzene based on an H/D exchange reactivity of 55% reactive collision.....	199

Figure A-55

Figure A-56

Figure A-57

Figure A-55	A simulated collision-product plot for the structure VI of p-dichlorobenzene based on an H/D exchange reactivity of 60% reactive collision.....	200
Figure A-56	A simulated collision-product plot for the structure VI of p-dichlorobenzene based on an H/D exchange reactivity of 65% reactive collision.....	201
Figure A-57	A simulated collision-product plot for the structure VI of p-dichlorobenzene based on an H/D exchange reactivity of 70% reactive collision.....	202

Introduction

Solvent
occurring in
reactions are
complete labo
technique req
required for si

J. J. Th
1913 (1). The
by today's stan
numerous ion-
generally trea
mass spectro
reactions was
Interest in io
1960s. Over t
useful for car
briefly describ

CHAPTER 1

INTRODUCTION

Introduction

Solvent molecules often play an important role in ionic reactions occurring in solution. The effects of solvation can be eliminated if the reactions are carried out in the gas phase. A mass spectrometer can be a complete laboratory for studying ion-molecule reactions. The gas phase technique requires only a small fraction of the sample amount normally required for similar studies in the condensed phase.

J. J. Thomson first reported the products of ion-molecule reactions in 1913 (1). The vacuum technology in Thomson's day is considered primitive today's standard. As a result of poor vacuum in the mass spectrometer, numerous ion-molecule reactions often took place; and the reactions were generally treated as a nuisance. With the advent of better vacuum and mass spectrometric technology, a systematic study of ion-molecule reactions was begun in 1952 with the work of Tal'roze and Ljubimova (2). Interest in ion-molecule reactions has been widespread since the early 1950s. Over the past three decades, numerous techniques have been found useful for carrying out ion-molecule reactions. These techniques will be fully described in the latter part of this chapter.

The ma
molecule re
compounds.
selection of a
selected reagi
many MS/MS
quadrupole m
ion-molecule r
of other techn
reactions as a

Collision Proc

The first
ion and a neu
exchange betw
depend very r
treatment of c
results can b
mechanics. TH
in detail by S
translational e
the collision p
ion and molecu
states. Deper
excitations ca

The main objective of this dissertation is the application of ion-molecule reactions for distinguishing among isomers of organic compounds. A tandem mass spectrometric system (MS/MS) allows selection of a specific mass ion from the ion source for reaction with selected reagent molecules in an isolated reaction chamber. Although many MS/MS systems exist today, the unique features of a triple quadrupole mass spectrometer are well suited for analytical applications of ion-molecule reactions. In this thesis, these features are compared to those of other techniques with emphasis on the applicability of ion-molecule reactions as analytical tools.

Collision Processes in Ion-Molecule Reactions

The first step in an ion-molecule reaction is a collision between an ion and a neutral molecule. The collision causes energy or momentum to be transferred between the interacting species. The results of the collision depend very much on the collision energy involved. Although an exact treatment of collision processes is quantum mechanical (3), most collision results can be sufficiently explained by models based on classical mechanics. The classical ion-molecule collision theory has been discussed in detail by Su and Bower (4). In general, a fraction of the relative translational energy prior to collision is converted into internal energy of the collision partners. The internal energy gained may promote both the ion and molecule to some new excited electronic, vibrational and rotational states. Depending on the energy within the interacting systems, the collisions can cause fragmentation, ion-molecule reactions and even

photon emission
energy can also

Most studies
energy regime
and magnetic
collisions at high
typically monochromatic
MIKES, for studies
regime, momentum
induced by the
the short interaction
are often not
ions resulting
charge exchange

In contrast
energy collision
low energy "binary"
momentum transfer
those in the
processes, the
extremely high
Because the efficiency
with increased
means to promote
, the interaction

photon emission. For vibrationally excited ions, collisions at thermal energy can also result in the reduction of internal energy.

Most studies of ion-molecule collisions have been performed in high-energy regimes (over 1 KeV) or low-energy regimes (below 100 eV). Electric and magnetic sector instruments have been used almost exclusively for the collisions at high energy (> 1 KeV). The products of these collisions are typically monitored in mass-analyzed ion kinetic energy spectrometry, or MAIKES, for structural elucidation of ionic species (5). In this high-energy regime, momentum transfer is minimal. The direct electronic excitation induced by the collisions often causes unimolecular decay (6). Because of the short interacting time for the collision species, ion-molecule reactions are often not observed during high energy collisions. However, products resulting from dissociation, charge stripping, charge inversion and charge exchange may be formed.

In contrast to the high-energy collisions, the energy involved in low-energy collisions can not efficiently promote electronic excitation. These low-energy "billiard ball" collisions involve mostly vibrational excitation by momentum transfer, and produce large scattering angles compared to those in the high collision energy regime. During these low energy collisions, the energy conversion efficiency from translational to internal is extremely high. In many cases, efficiencies close to 100% are observed (7). Because the efficiency of collisionally activated dissociation (CAD) increases with increased internal energy, low energy collisions are an efficient means to promote CAD. When collisions occur at very low energies (< 3 eV) the interaction time between ions and neutral molecules can be several

vibrational p
reactions inv
Collisions at
studies of ion
studied in sec
use of a com
devices can a
these reaction
and ion cyclot

In mos
designated fo
instrument, n
thermal energ
the kinetic en
or energy in la
between the
energy and mo
available for e
effective collis
center of mass
times the ratio
masses of the
the equation as

ational periods long. During this long interaction time, ion-molecule reactions involving the formation of new chemical bonds may occur. Reactions at thermal or near thermal energies are typically used for studies of ion-molecule reactions; thus, these reactions are not easily studied in sector instruments. Although hybrid instruments involving the use of a combination of sector (magnetic and electric) and quadrupole mass filters can also be used for low-energy ion-molecule reactions, most of the reactions have been studied in quadrupole, ion trap, flowing afterglow, and ion cyclotron resonance instruments.

In most experiments, a well-defined collision cell or region is designated for ion-molecule reactions. In the case of a quadrupole mass filter instrument, neutral molecules are injected into the collision cell under thermal energy. The collision energy for ion-molecule reactions is due to the kinetic energy of the ions entering the collision cell. The kinetic energy in laboratory frame (E_{lab}) is derived from the potential difference between the ion source and the collision cell. However, conservation of energy and momentum in a collision requires that only a fraction of E_{lab} is available for excitation of the interacting species (8). This fraction is the relative collision energy (E_{cm}) in a coordinate system moving with the center of mass of the collision partners. As such, E_{cm} is defined as E_{lab} multiplied by the ratio of the mass of the neutral molecule (M_n) and the sum of the masses of the neutral molecule and the reactant ion (M_i). It is described by the following equation as:

$$E_{cm} = E_{lab} [M_n / (M_n + M_i)]$$

This equation
energy can be
relative to the
heavier neutro
into internal
neutral mole

The av
pressure of n
multiple colli
increases over
internal energ
molecule coll
frequency of i
yield from su
multiple collis
intermediates
products. Cle
order sequenti

Most io
energies. Alt
thermoneutral
studied (12-15)
differs for end
orientation (Al
formation of a

This equation implies that for a collision with a specific ion, the effective energy can be varied by either changing the potential of the collision cell relative to the ion source or changing the mass of the neutral molecules. A heavier neutral molecule provides a more efficient means to convert E_{lab} into internal energy. In the case of electron impact, the large mass ratio of a neutral molecule to an electron makes E_{lab} nearly equal to E_{cm} .

The average rate of collisions can be increased by raising the pressure of neutral collision gas in the collision cell. Generally, under multiple collision conditions, the average internal energy of ions often increases over that of single collision conditions (9,10). This increase in internal energy may improve the yield of CAD products. For reactive ion-molecule collisions, multiple collision conditions result in a higher frequency of ion-molecule interactions, which in turn increase the product yield from such reactions. When collisions occur at thermal energies, multiple collision conditions may also have a stabilizing effect on reaction intermediates which are often needed for the formation of final ion products. Clearly, for reaction products arising from second or higher order sequential reactions, multiple collisions are necessary.

Most ion-molecule reactions occur at thermal or near thermal energies. Although the majority of these reactions are exothermic or thermoneutral, some endothermic ion-molecule reactions have also been studied (12-15). The dependence of product yield on translational energy differs for endothermic and exothermic reactions (16). Average dipole orientation (ADO) theory predicts that ion-molecule reactions proceed via formation of a long-lived collision complex (17). Accordingly, product ion

yield of an
approaching
may be expla
complex lives
complex becom
adduct ions is
energy for ad
available for
However, the
exothermic re
cases, the ex
chemical bond

Ion frag
valuable struc
and efficiency
vibrational ene
of the low-ene
increases some
increase levels
For a large m
due to the larg
for a large ion
because each
internal energ
fragmentation,

Yield of an exothermic reaction is greatest for ion kinetic energy approaching zero and decreases with increasing ion kinetic energy. This may be explained assuming that products are formed only if the collision complex lives long enough. As kinetic energy increases, the life-time of the complex becomes too short to form products. The formation of ion-molecule adduct ions is particularly energy sensitive (18,19). The optimum kinetic energy for adduct ion formation is often barely positive; the energy range available for these reactions is extremely narrow (see Figure 1-1). However, there are many instances where adduct ions formed through exothermic reactions may not be observed as final products at all. In such cases, the excess energy released is large enough to cause rupture of chemical bonds.

Ion fragmentation derived from ion-molecule collisions provides valuable structural information regarding the original molecule. The yield and efficiency of the fragmentation depend largely on the amount of excess vibrational energy in the chemical bonds. For collisions at the very low end of the low-energy regime, the total internal energy deposited to an ion increases somewhat linearly with an increase in collision energy. This increase levels off as the collision energy increases up to a certain level. For a large molecule, the internal degrees-of-freedom is a large number relative to the large number of chemical bonds. The fragmentation efficiency for a large ion is extremely low, even at very high collision energies, because each chemical bond shares only a small fraction of the total internal energy gained (20,21). As an alternative, to collision-induced fragmentation, ion-molecule reactions may be explored for structural

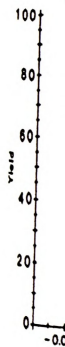


Figure 1-1 Ca
α-
m
re
th

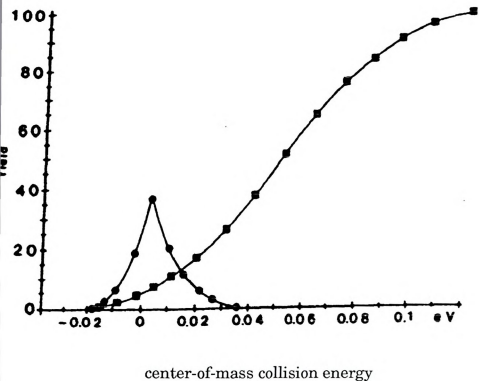


Figure 1-1 Center-of-mass axial kinetic energy spectrum of protonated α -hydroxyisobutyrate ethyl ester. The yield of adduct ions, m/z 150 (●), and the most intense fragment, m/z 115 (■), were recorded against the experimental center-of-mass energy of the protonated molecular ion (m/z 133) (Adapted from Ref. 18)

information t
simple ionic fr

Distinguishing

Mass sp
samples that
Many example
equipped with
produce suffici
certain organic
very similar ma
particular, the
compounds are
notorious comp
polychlorodiben
of different app
spectral differe
framework of M
dimension to all
include metast
(CAD), photodi
demonstrated t
particular, the s
the fragmentatio

formation that is often much more structure-specific than the result of simple ionic fragmentation (22,23).

Distinguishing Organic Isomers in Tandem Mass Spectrometry

Mass spectrometry (MS) has been the method of choice for analyzing samples that demand low detection limits and structural information. Many examples may be found where a single stage mass spectrometer equipped with electron ionization (EI) or chemical ionization (CI) is used to produce sufficiently distinct mass spectra to allow the differentiation of certain organic isomers. Still many isomers are found to have identical or very similar mass spectra when the traditional MS techniques are used. In particular, the differentiation of many positional isomers of aromatic compounds are known to be extremely difficult. These isomers include various compound types such as polychlorinated biphenyls (PCBs) and polychlorodibenzo-p-dioxins (PCDDs). Over the past few decades, a number of different approaches have been adapted in order to increase the mass spectral differences of some isomers. These are primarily within the framework of MS/MS, which provides an additional mass spectrometric dimension to allow extra processes for the ions. These extra processes may include metastable decomposition, collisionally activated dissociation (CAD), photodissociation and ion-molecule reactions. All have been demonstrated to be useful in differentiating organic isomers. In particular, the specificity of ion-molecule reactions has been useful when fragmentation techniques failed (24).

A. MS/MS in

The ap
described by S
A two-sector in
decomposition
the extent of
differentiate th
MS/MS for dis
instruments.
different instr
analytical appl
next section.

The appl
McLafferty et a
the same instru
as stereoisome
differentiated o
metastable ions
often do not pro

The yield
to have collision
instrument. Su
cause CAD to o
energetic collision

MS/MS in Sector Instruments for Isomeric Differentiation

The application of MS/MS for isomeric differentiation was first described by Shannon and McLafferty (25) for analyzing isomers of $C_2H_5O^+$. A non-sector instrument was used to monitor ions derived from metastable decompositions in the field-free region between sectors. The differences in the extent of the competing decomposition pathways were used to differentiate the isomers of $C_2H_5O^+$. Since this beginning, the application of MS/MS for distinguishing isomers has been extended to different types of instruments. Different processes have also been applied to each of the different instruments for differentiating isomers. The features and practical applications of non-sector instruments will be discussed in the next section.

The application of metastable decomposition was further extended by McLafferty et al. (26) to differentiate isomers of $C_2H_6N^+$ and $C_3H_8N^+$ using the same instrumental settings as described before. Larger molecules such as stereoisomers of 2-acetamido-2-deoxyhexose were also successfully differentiated on the basis of differences in the relative abundances of the metastable ions (27). Despite these successes, metastable decompositions do not produce useful information for isomeric differentiation.

The yield of ionic fragmentation can be improved if ions are allowed to undergo collisions with neutral molecules in the field-free region of a sector instrument. Such collisions increase the internal energy of the ions and lead to CAD to occur. In order to reduce the effect of scattering due to elastic collisions, neutral molecules with low molecular weight such as

He are introd
have used
differentiation
al, have empte
differentiate C
ion source ur
molecule reac
three different
 $C_4H_7N^+$ adduc
four-sector ins
isomers to be
are almost ind

The inte
with photons.
region of a re
differentiate iso
ylene, the diff
function of pho
isomers of ethy
photons. Diffe
[M-OH]⁺ ions w

Although
ion-molecule re
charge strippin
Burgers et al.

are introduced into the field-free region to induce CAD. Kiremire et al. used CAD to produce diagnostic fragments that allow the differentiation of pyranococumarin isomers (28). Recently, McLafferty et al. have employed a combination of both ion-molecule reactions and CAD to differentiate $C_4H_4^+$ isomers (29). In this case, NH_3 was introduced into the source under EI conditions to produce distinctive products of ion-molecule reactions for three different $C_4H_4^+$ structures originated from different hydrocarbons. The ion products at m/z 69, presumably the $C_4H_4N^+$ adduct, were subjected to CAD with He in the field-free region of a sector instrument. The distinctive spectra thus obtained allow the isomers to be distinguished. The CAD spectra of unreacted $C_4H_4^+$ isomers are almost indistinguishable.

The internal energy of an ion can also be increased by interaction with photons. The process of photodissociation was applied in the field-free region of a reversed geometry double focusing mass spectrometer to differentiate isomers of xylene and ethylnitrobenzene (30,31). In the case of xylene, the difference in translational energy released by the $[M]^+$ ions as a function of photon energy was used to differentiate the isomers. For the isomers of ethylnitrobenzene, $[M-OH]^+$ ions were selected to interact with photons. Differences in the relative photoabsorption cross-sections of the $[M]^+$ ions were used for isomeric differentiation.

Although the energetic processes in sector instruments do not allow ion-molecule reactions involving the formation of new chemical bonds, charge stripping (32,33) and charge exchange reactions (34,35) do occur. Kiremire et al. (36) have used the charge stripping reactions to analyze

isomers of C_2
collision with
spectra permit
charge exchange
differentiate
exchange a cl
singly charged

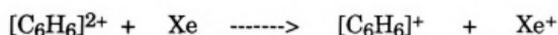
[C

The isomers of
abundances of

B. Isomeric Di Reactions

Ion-mole
ion-molecule co
is well suited f
fragmentation
collision energi
favored. With
take place in
reactions. With
ion-molecule re
be on ion-molec

mers of $C_2H_5O^+$ ions. Stripping of an electron from $C_2H_5O^+$ by energetic collision with He generates a doubly charged ion. The resulting mass spectra permit the clear identification of four distinct $C_2H_5O^+$ species. The charge exchange reactions were explored by Guilhaus et al. (37) to differentiate isomers of $[C_6H_6]^{2+}$ ions. The doubly charged ion can exchange a charge with Xe atoms in a high-energy collision to form two singly charged ions. These processes can be represented as :



Isomers of $[C_6H_6]^{2+}$ were distinguished primarily by the relative abundances of $[C_6H_6]^+$ ions formed by the charge exchange.

Ionic Differentiation in MS/MS Instruments Suited for Ion-Molecule Reactions

Ion-molecule reactions can be performed on instruments that allow molecule collisions at low energies (a few eV or less). A technique that is well suited for ion-molecule reactions can still allow CAD, because some fragmentation occurs even at very low energies. Thus, by adjustment of the collision energies, either ion-molecule reactions or CAD products can be studied. With the advent of laser technology, photodissociation can also take place in instruments that are primarily used for ion-molecule reactions. With this in mind, applications of CAD, photodissociation and ion-molecule reactions will be discussed in this section. The emphasis will be on ion-molecule reactions and their potential in analytical applications.

Curren

commonly us
flowing after
(38), fourier
quadrupole
quadrupole m
will be descri
analytical app
isomers.

a. Tandem Flo

Tandem

developed in 1
afterglow sour
mass-selected
tube, where ne
Helium buffer
carry them to
detected by a
In fact, this in
quadrupole ma
design and con
the FA-SIFT t
phenomena of i
with such instr

Currently, there are four different MS/MS techniques that are commonly used to perform ion-molecule reactions. They are tandem flowing afterglow-selected ion flow tube (SIFT)-drift (or tandem FA-SIFT) (38), fourier transform ion cyclotron resonance (or FTMS) (39-41), quadrupole ion trap mass spectrometry (ITMS) (42-45) and triple quadrupole mass spectrometry (TQMS) (46-48). The unique features, which will be described later, of TQMS are utilized in this dissertation to explore analytical applications of ion-molecule reactions for distinguishing organic isomers.

Tandem Flowing Afterglow-SIFT-Drift

Tandem FA-SIFT is an extension of the flowing afterglow technique developed in 1963 by Ferguson et al. (49). In this technique, the flowing afterglow source is used to generate the reactant ions. These ions are then mass-selected by the selected ion flow tube (SIFT) to enter the flow-drift tube, where neutral reagents are added to carry out ion-molecule reactions. Helium buffer gas is used in the flow-drift tube to thermalize the ions and carry them to the reaction regions. The ionic reactants and products are detected by a quadrupole mass filter coupled with an electron multiplier. In fact, this instrumental configuration is very similar to that of a triple quadrupole mass spectrometer. The major differences of the two are in the design and configuration of the ion source and the collision region. So far, the FA-SIFT technique has been limited to fundamental studies of the phenomena of ion-molecule reactions. Only a few laboratories are equipped with such instruments, and they are not commercially available. Perhaps,

the popularity
and greater so

b. Quadrupole

Althou
described by I
ion trap (ITM
in 1987 (42).
cap electrode
radiofrequenc
determines th
the field and
background p
damp the m
ionization (CI
pressures orde
(51-53). Photo
56, 58) have be
few years, the
is particularly
the future, ut
applications in

popularity of this technique is overshadowed by the higher versatility and greater sensitivity of the TQMS for analytical applications.

Quadrupole Ion Trap

Although the basic concept of a quadrupole ion trap was first described by Paul and Steinwedel in the 1950s (50), the use of a quadrupole ion trap (ITMS) as an MS/MS instrument was first reported by Louris et al. (51, 52) (42). This three-dimensional quadrupole device consists of two endcap electrodes and a central ring electrode to which direct current and radiofrequency voltages can be applied. The radiofrequency voltage determines the mass-to-charge ratios of ions which can be trapped within the trap and can be used to selectively eject ions from the traps. A high vacuum pressure of helium (10^{-3} torr) is normally used in the trap to dampen the motion of stored ions for optimum operation. Chemical ionization (CI) with a variety of CI reagents can also be carried out at pressures orders of magnitude less than those employed in traditional CI (53). Photodissociation (54), CAD (55-57) and ion-molecule reactions (53, 54) have been performed in the MS/MS mode of an ITMS. Over the past few years, the popularity of ITMS has grown tremendously. The technique is particularly well suited for ion-molecule reactions. Its versatility will, in the future, undoubtedly allow for the development of many analytical applications in a wide range of areas.

c. Fourier Tr

Fourier

It is an exten

by E. O. Law

in ICR by Cor

for ion-molec

typical FTMS

cell at a total

due to the ef

trajectory. Af

reactions with

larger orbits b

motion of all e

receiver plate

computer for

spectrum (60,

except for a c

resolving pow

instrument.

studies of ion-

Althoug

processes (62,6

The feasibility

isomers has b

isomers includ

Fourier Transform Ion Cyclotron Resonance

Fourier transform ion cyclotron resonance is also known as FTMS, an extension of ion cyclotron resonance (ICR) that was first described by J. O. Lawrence in 1930 (59). The introduction of Fourier transformation ICR by Comisarow and Marshall (39) has made FTMS the best technique for ion-molecule experiments requiring ultra-high mass resolution. In a typical FTMS experiment, ions are generated by electron impact in a cubic cell at a total pressure of 1 to 100 μ torr. These ions are trapped in the cell by the effects of magnetic and electric fields and follow a circular trajectory. After a certain time, referred to as trapping time, during which collisions with neutral molecules can take place, the ions are then excited to higher orbits by a fast frequency-swept radiofrequency pulse. The coherent motion of all excited ions induces image currents in a circuit shunting two detector plates. These currents are amplified and transmitted to a computer for Fourier transformation to generate an interpretable mass spectrum (60,61). The basic features of FTMS are quite similar to ITMS, except for a difference in resolving power and operational pressure. A resolving power of over a million is achievable with a modern FTMS instrument. The technique is particularly well suited for fundamental studies of ion-molecule reactions.

Although some of the first papers about ICR were related to CAD processes (62,63), the technique was mostly used for ion-molecule reactions. The feasibility of using ion-molecule reactions to differentiate organic compounds has been demonstrated by numerous reports (64-76). These reports include $C_2H_5O^+$ (68,71), $C_5H_{10}^+$ (69), $C_6H_6O^+$ (70), trans- and cis-4-

tert-butylcyclohexanone (73),
were motivated by the
sufficient mass resolution
success of the method
specificity of the method
addition to ion
FTMS to differentiate
of $C_4H_9O_2^+$ (74) and
may be used for the

d. Triple Quadrupole

The development of the
Yost and Enke ion trap
widespread in the field
involves three stages:
(Q1) and the ion
combination of the
applied. Mass resolution
the DC and RF fields
behavior of ion
differential equation
interacting with
(Q2) is used to
potential is applied
during the MS

tert-butylcyclohexyl acetate (75), C_8H_{10} (72), C_7H_8O (72), trans- and cis- α -calone (73), $C_3H_3^+$ (76) and tautomers of $C_3H_8N^+$ (74). Most of the studies are motivated by the fact that the majority of these isomers do not give sufficient mass spectrometric information for isomeric differentiation. The success of these examples demonstrates the usefulness of the high specificity of ion-molecule reactions compared to the other processes. In addition to ion-molecule reactions, photodissociation has also been used in MS to differentiate isomers. Under irradiation by a laser beam, isomers $C_4H_9O_2^+$ (77,78) and $C_5H_6^+$ produce characteristic fragment patterns that may be used for their differentiation.

Triple Quadrupole Mass Spectrometry

The development of a triple quadrupole mass spectrometer (TQMS) by Fenn and Enke (46,47) for general MS/MS applications has stimulated widespread interest in MS/MS techniques. The instrumentation of TQMS involves three quadrupole devices positioned in series. The first quadrupole (Q1) and the third quadrupole (Q3) are used as mass-filters to which a combination of direct-current (DC) and radiofrequency (RF) potentials are applied. Mass selection and mass scanning are accomplished by sweeping the DC and RF potentials applied to the four poles of Q1 and Q3. The behavior of ions traveling through a quadrupole is described by the Mathieu differential equations (79,80) that describe the stable trajectory of ions interacting with the fields inside the quadrupoles. The second quadrupole (Q2) is used as a non-mass-selective collision chamber where only RF potential is applied. The processes of ion-molecule interactions occur in Q2 during the MS/MS operation. The main function of the RF potential applied

to Q2 is to fo
properties an
mass filter ha
al. (82). Th
operational
information.
discussed in
Enke (83). O
reactions will

All the
performed on
instrument.
experiments w
adapt the des
traditional lin
due to the for
the curved c
difference in th
fact, technical
quadrupole sy
chamber. The
imparted by th
(85). The oper
Figure 1-2. B
enter the collis

Q2 is to focus ions scattered by the collision processes. The transmission properties and the ion containment efficiency of an RF-only quadrupole filter have been discussed in detail by Miller et al. (81) and Dawson et al. (82). The versatility of a TQMS instrument allows a variety of operational modes, which provide different types of MS and MS/MS information. All the possible modes of a TQMS have been reviewed and discussed in depth by others, including colleagues and students of Dr. C. G. Dawson (83). Only the mode used for the experiments involving ion-molecule reactions will be discussed.

All the experimental work described in this dissertation was performed on either a Finnigan TSQ-70B or a Finnigan TSQ-700 TQMS instrument. Except for some of the work described in Chapter 3, all the experiments were performed on the TSQ-70B model. Both Finnigan models feature the design of a curved collision chamber that is different from the traditional linear design. It is believed that the curved design reduces noise due to the formation of neutral products that cannot be transmitted beyond the curved chamber (84). In addition, there is also a fundamental difference in the design of Q2 between the TSQ-70B and TSQ-700 models. In principle the TSQ-700 model should not be considered as a triple quadrupole system because it uses an octopole design for the collision chamber. Theoretically, the octopole design can reduce the radial energy imparted by the RF potential and allow a higher ion transmission efficiency. The operational mode used for all MS/MS experiments is depicted in Figure 1-2. Briefly, ions created in the source are mass-selected by Q1 to enter the collision chamber (Q2) where neutral reagents are introduced for



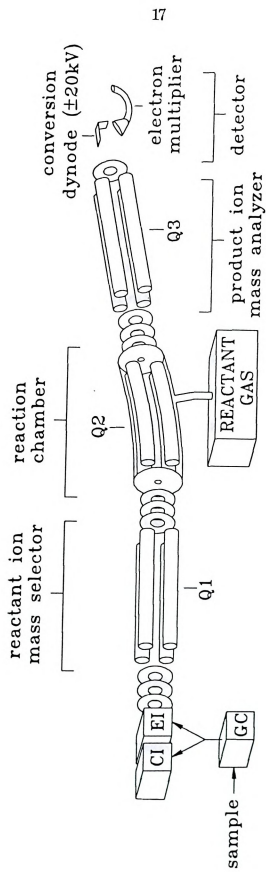


Figure 1-2 Schematic of a triple quadrupole mass spectrometer based on the Finnigan TSQ-70B model

interaction
analyzed by

The ve
techniques.
bombardment
contrast, on
SIFT, ITMS
unit mass re
with high se
TQMS is co
important fo
greatest adv
unique loca
simultaneous
molecule reac
are spatially
a setting ens
collision char
scanning all
can be introd
In contrast, I
and mass sca
When an ion
function as a
allowing suffi

action with the ions. Product ions emerging from Q2 are then mass-filtered by Q3 for product mass spectra.

The versatility of this TQMS allows for very wide range of ionization techniques. They include, but are not limited to, CI, EI, fast atom bombardment, atmospheric pressure ionization and electrospray. In contrast, only limited ionization techniques are allowed in Tandem-FA-MS, ITMS and FTMS. The capacity of a TQMS to provide independently high mass resolution to both mass filtering stages results in an instrument with high selectivity. An even higher selectivity can be achieved when a TQMS is coupled with gas or liquid chromatography. This capacity is important for trace analysis of environmental samples. Perhaps, the two greatest advantages of a TQMS over the ion trapping techniques are the location of its collision chamber and the independent and simultaneous operation of the three quadrupoles. In a TQMS, ion-molecule reactions take place in a region where the ions and the molecules are spatially separated from the ion source by a mass filtering device. Such design ensures that only ions with a specific m/z value can enter the reaction chamber. Since ion selection, ion-molecule reaction and mass filtering all occur simultaneously in different regions, analytical samples can be introduced continuously into the system without any interruptions. In contrast, ITMS and FTMS require the ionization, ion-molecule reaction and mass scanning to be processed in the same region at different times. In an ion trapping instrument is in its trapping mode, it loses its capability as a mass analyzer. Finally, a TQMS has the advantage of providing sufficient control of a wide range of axial kinetic energies. The

capability of
studies of bo

Despi
disadvantag
all, the resid
short compar
prohibit the
intermediate
undetermine
applied to th
is believed t
spectra obtai
Q3, they are
in the collisi
ions derived
and high col
discussed in g

The p
quadrupole s
significantly
isomers, infor
permit their
natural morp
distinguished

ability of controlling collision energy is important for energy-resolved studies of both endothermic and exothermic reactions.

Despite all the advantages described above, there are some disadvantages in using a TQMS to study ion-molecule reactions. First of all, the residence time of the reactant ions in the collision chamber is very short compared to those of ITMS and FTMS. This short residence time may inhibit the formation of some ion products which require long-lived intermediates and have slow kinetics. Second, an ion can also gain an indeterminate amount of radial kinetic energy due to the RF potential applied to the collision chamber. The octopole design of the TSQ-700 model is believed to minimize this problem. Finally, because the product mass spectra obtained from the TQMS represent only the ions transmitted into the detector, they are not necessarily truly representative of the product distribution in the collision chamber. This could be a problem when sampling product ions derived from ion-molecule reactions conducted under thermal energy and high collision pressure conditions. This particular problem will be discussed in greater detail in Chapter 5.

The primary ion-molecule interaction used in most tandem quadrupole systems is CAD. The CAD efficiency in a TQMS is often significantly higher than that of a multisection instrument. For some cases, information provided by CAD in a TQMS is selective enough to permit their differentiation (86-88). Isomers of dimethoxyindole (87), acetyl morphinan (86) and o/p bisphenol-A (88) have been successfully distinguished by CAD. However, when CAD fails to produce useful

information

reactions ma

The u

Yost et al. (8)

differentiate

reported suc

Bursey et al.

of 1,2-cyclop

(92). The sa

reactions and

1,2-cyclopent

used by Jalor

isomers. Ko

differentiate

Heath et al

differentiate

Despite

reactions in

successes dem

triple quadru

specificity of i

TQMS, we ha

distinguishing

dissertation.

formation for isomeric differentiation, the specificity of ion-molecule reactions may be useful.

The use of the TQMS for ion-molecule reactions is relatively new. *et al.* (89) first explored the use of ion-molecule reactions in a TQMS to differentiate isomeric structures. Since then, several laboratories have reported successes in using ion-molecule reactions to differentiate isomers. *ey et al.* used ammonia as the neutral reagent to differentiate isomers 2-cyclopententanediol (90) $C_2H_5O^+$ (91) and hexachlorinated biphenyl

The same group also explored the use of endothermic proton transfer reactions and trimethylsilyl ions to differentiate isomers of $C_6H_6^+$ (93) and 2-cyclopententanediol (94), respectively. Buta-1,3-diene and benzene were used by *Jalonen* (95) to differentiate the structures of $C_2H_5O^+$ and $C_2H_3O^+$ ions. *Kostianinen et al.* (96,97) have explored the use of oxygen to differentiate several isomers of tetrachlorodibenzo-p-dioxin. Recently, *h et al.* (98) have reported success in using dimethyl ether to differentiate $C_7H_7^+$ isomers.

Despite the applications described above, the use of ion-molecule reactions in the TQMS is still limited to only a few laboratories. Their successes demonstrate the analytical potential of ion-molecule reactions in quadrupole mass spectrometry. By taking the advantages of the specificity of ion-molecule reactions and the sensitivity and selectivity of the TQMS, we have explored novel applications of ion-molecule reactions for distinguishing organic isomers, which will be described in this section.

References

1. Thom
to Che
2. Tal'ro
209.
3. Berry,
4. Su, T.
Ed., A
5. McLaf
Am. C
6. Yamac
7. Michael
8. Bernst
Claren
9. Todd, I
44, 37.
10. Wysoch
Spectra
11. White,
22, 132.
12. Orland
Anal. C
13. Orland
24, 1033
14. Orland
Spectro
15. Orland
25, 485.
16. Kinter,
17. Bowers,

ferences

- Thomson, J. J., " Rays of Positive Electricity and Their Applications to Chemical Analysis ", Longmans : London, England, 1913.
- Tal'roze, V. L.; Ljubimova, A. K., *Dokl. Akad. Nauk SSSR*. **1952**, 86, 209.
- Berry, M. V.; Mount, K. E., *Repts. Prog. Phys.* **1972**, 35, 315.
- Su, T.; Bower, M. T. " Gas Phase Ion Chemistry, Vol ", Bower, M. T. Ed., Academic Press : New York, 1979.
- McLafferty, F. W.; Bente, P. F.; Kornfeld, R.; Tsai, S.-C.; Howe, I., *J. Am. Chem. Soc.* **1973**, 95, 2120.
- Yamaoka, H.; Pham, D.; Durup, J., *J. Chem. Phys.* **1969**, 51, 3465.
- Michael, K. T.; Bursey, M. M., *J. Am. Chem. Soc.* **1986**, 108, 1797.
- Bernstein, R. B.; Levine, R. D., " Molecular Reaction Dynamics ", Clarendon Press : Oxford, England, 1974.
- Todd, P. J.; McLafferty, F. W., *Int. J. Mass Spectrom. Ion Phys.* **1982**, 44, 37.
- Wysocki, V. H.; Kenttamaa, H. I.; Cooks, R. G., *Int. J. Mass Spectrom. Ion Processes* **1987**, 75, 181.
- White, E. L.; Tabet, J.-C.; Bursey, M. M., *Org. Mass Spectrom.* **1987**, 22, 132.
- Orlando, R.; Murphy, C.; Fenselau, C.; Hansen, G.; Cotter, R. J., *Anal. Chem.* **1990**, 62, 215.
- Orlando, R.; Fenselau, C.; Cotter, R. J., *Org. Mass Spectrom.* **1989**, 24, 1033.
- Orlando, R.; Fenselau, C.; Cotter, R. J., *Rapid Commun. Mass Spectrom.* **1990**, 4(7), 259.
- Orlando, R.; Fenselau, C.; Cotter, R. J., *Org. Mass Spectrom.* **1990**, 25, 485.
- Kinter, M. T.; Bursey, M. M., *Org. Mass Spectrom.* **1987**, 22, 775.
- Bowers, M. T.; Su, T.; Anicich, V. G., *J. Chem. Phys.* **1973**, 58, 5175.

18. Schm
1985,
19. Schm
493.
20. Craig
21. Bente
Chem.
22. Hudsc
1984, 4
23. McAd
24. Kinter
1988, 1
25. Shann
26. Lersen
27. Fourni
28. Kirem
Rodigh
29. Wesde
Spectro
30. Mukht
Mass S
31. Morgan
Mass S
32. Maque
Menu,
33. Bowen,
34. Beynon
1971, 5,
35. Beynon
36. Burgers
1982, 17

- Schmit, J. P.; Dawson, P. H.; Beaulieu, N., *Org. Mass Spectrom.* **1985**, 20, 269.
- Schmit, J. P.; Beaudet, S.; Brisson, A., *Org. Mass Spectrom.* **1986**, 21, 493.
- Craig, A. G.; Derrick, P. J., *J. Am. Chem. Soc.* **1985**, 107, 6707.
- Bente, P. F.; McLafferty, F. W.; McAdoo, D. J.; Lifshitz, C., *J. Phys. Chem.* **1975**, 79, 713.
- Hudson, C. E.; McAdoo, D. J., *Int. J. Mass Spectrom. Ion Processes* **1984**, 59, 325.
- McAdoo, D. J.; Hudson, C. E., *Org. Mass Spectrom.* **1987**, 22, 615.
- Kinter, M. T.; Bursey, M. M., *Biomed. Environ. Mass Spectrom.* **1988**, 15 583.
- Shannon, T. W.; McLafferty, F. W., *J. Am. Chem. Soc.* **1966**, 88, 5021.
- Lersen, K.; McLafferty, F. W., *J. Am. Chem. Soc.* **1974**, 96, 139.
- Fournie, J.-J.; Puzo, G., *Anal. Chem.* **1985**, 57, 2287.
- Kiremire, B. T.; Chiarello, D.; Traldi, P.; Vettori, U.; Guiotto, A.; Rodighiero, P., *Rapid Commun. Mass Spectrom.* **1990**, 4, 117.
- Wesdemiotis, C.; Zhang, M.-Y.; McLafferty, F. W., *Org. Mass Spectrom.* **1991**, 26, 671.
- Mukhtar, E. S.; Griffiths, I. W.; Harris, F. M.; Beynon, J. H., *Org. Mass Spectrom.* **1981**, 16, 51.
- Morgan, T. G.; Kingston, E. E.; Harris, F. M.; Beynon, J. H., *Org. Mass Spectrom.* **1982**, 17, 594.
- Maquestiau, A.; Van Haverbeke, Y.; Flammang, R.; De Meyer, C.; Menu, A., *Org. Mass Spectrom.* **1977**, 12, 706.
- Bowen, R.; McLafferty, F. W., *Org. Mass Spectrom.* **1980**, 15, 51.
- Beynon, J. H.; Mathias, A.; Williams, A. E., *Org. Mass Spectrom.* **1971**, 5, 303.
- Beynon, J. H., *Anal. Chem.* **1970**, 42, 97A.
- Burgers, P. C.; Terlouw, J. K.; Holmes, J. L., *Org. Mass Spectrom.* **1982**, 17, 369.

37. Guilh
Mass
38. Van I
J. Ma
39. Comis
40. Marsl
1979,
41. McIve
42. Louris
C., Jr.
43. March
Spectr
York,
44. Berbe
Mass
45. March
46. Yost, I
47. Yost, I
48. Yost, I
49. Fehsen
Phys. J
50. Paul, V
1956.
51. Boswe
Ion Pr
52. Johns
Mass S
53. Berber
Mass S
54. Louris
Ion Pr

Guilhaus, M.; Kingston, R. G.; Brenton, A. G.; Beynon, J. H., *Org. Mass Spectrom.* **1985**, 20, 424.

Van Doren, J. M.; Barlow, S. E.; Depuy, C. H.; Bierbaum, V. M., *Int. J. Mass Spectrom. Ion Phys.* **1987**, 81, 85.

Comisarow, M. B.; Marshall, A. G., *Chem. Phys. Lett.* **1974**, 25, 282.

Marshall, A. G.; Comisarow, M. B.; Parisod, G., *J. Chem. Phys.* **1979**, 71, 4434.

McIver, R. T., *Amer. Lab.* **1980**, 12, 18.

Louris, J. N.; Cooks, R. G.; Syka, J. E. P.; Kelley, P. E.; Stafford, G. C., Jr.; Todd, J. F. J., *Anal. Chem.* **1987**, 59, 1677.

March, R. E., Hughes, R. J., " *Quadrupole Storage Mass Spectrometry (Chemical Analysis Series, Vol. 102)* ", Wiley : New York, 1989.

Berberich, D. W.; Hail, M. E.; Johnson, J. V.; Yost, R. A., *Int. J. Mass Spectrom. Ion Phys.* **1989**, 94, 115.

March, R. E., *Org. Mass Spectrom.* **1991**, 26, 627.

Yost, R. A.; Enke, C. G., *J. Am. Chem. Soc.* **1978**, 100, 2274.

Yost, R. A.; Enke, C. G., *Anal. Chem.* **1979**, 51, 1251A.

Yost, R. A.; Enke, C. G., *American Lab.* **1981**, June, 88.

Fehsenfeld, F. C.; Ferguson, E. E.; Schmeltekopf, A. L., *J. Chem. Phys.* **1966**, 44, 3022.

Paul, W.; Steinwedel, H., US Pat. 2939952, 1960; German pat. 944900, 1956.

Boswell, S. M.; Mather, R. E.; Todd, J. F. J., *Int. J. Mass Spectrom. Ion Processes.* **1990**, 90, 139.

Johnson, J. V.; Berberich, D. W.; Pedder, R. E.; Yost, R. A., *Adv. Mass Spectrom.* **1989**, 11A 276.

Berberich, D. W.; Hail, M. E.; Johnson, J. V.; Yost, R. A., *Int. J. Mass Spectrom. Ion Processes* **1989**, 94, 115.

Louris, J. N.; Brodbelt, J. S.; Cooks, R. G., *Int. J. Mass Spectrom. Ion Processes* **1987**, 75, 345.

55. John
Chem
56. Louri
G. J.;
96, 11
57. Evan
1991,
58. Brodt
59. Lawr
60. McIve
61. Hunt,
E., *Ar*
62. Kapla
63. Henis
64. Henis
65. Burse
66. Benez
67. Burse
Anal.
68. Beauc
69. Gross
70. Nibbe
71. Staley
Am. C
72. McIve
73. Henio
1975, 5
74. Tomer

Johnson, J. V.; Yost, R. A.; Kelley, P. E.; Bradford, D. C., *Anal. Chem.* **1990**, *62*, 2162.

Louris, J. N.; Brodbelt, J. S.; Cooks, R. G.; Glish, G. L.; Van Berkel, G. J.; McLuckey, S. A., *Int. J. Mass Spectrom. Ion Processes* **1990**, *96*, 117.

Evans, C.; Traldi, P.; Mele, A.; Sottani, C., *Org. Mass Spectrom.* **1991**, *26*, 347.

Brodbelt, J. S.; Cooks, R. G., *Analytica Chimica Acta* **1988**, *206*, 239.

Lawrence, E. O.; Edlefsen, N. E., *Science* **1930**, *72*, 376.

McIver, R. T., Jr.; *Rev. Sci. Instrum.* **1970**, *41*, 555.

Hunt, D. F.; Shabanowitz, J.; McIver, R. T.; Hunter, R. L.; Syka, J. E., *Anal. Chem.* **1985**, *57*, 765.

Kaplan, F., *J. Am. Chem. Soc.* **1968**, *90*, 4483.

Henis, J. M. S., *J. Am. Chem. Soc.* **1968**, *90*, 844.

Henis, J. M. S., *Anal. Chem.* **1969**, *41*, 22A.

Burse, M. M.; Hoffman, M. K., *Can. J. Chem.* **1971**, *49*, 3395.

Benezra, S. A.; Bursey, M. M., *J. Am. Chem. Soc.* **1972**, *94*, 1024.

Burse, M. M.; Kao, J.-I.; Henion, J. D.; Parker, C. E.; Huang, T.-I., *Anal. Chem.* **1974**, *46*, 1709.

Beauchamp, J. L.; Dunbar, R. C., *J. Am. Chem. Soc.* **1970**, *92*, 1477.

Gross, M. L.; Lin, P.-H.; Franklin, S. T., *Anal. Chem.* **1972**, *44*, 974.

Nibbering, N. M. M., *Tetrahedron* **1973**, *29*, 385.

Staley, R. H.; Corderman, R. R.; Foster, M. S.; Beauchamp, J. L., *J. Am. Chem. Soc.* **1974**, *96*, 1260.

McIver, R. T., *Org. Mass Spectrom.* **1975**, *10*, 396.

Henion, J. D.; Kao, J.-I.; Nixon, W. B.; Bursey, M. M., *Anal. Chem.* **1975**, *47*, 689.

Tomer, K. B., *Org. Mass Spectrom.* **1974**, *9*, 686.

75. Burse
76. Auslo
77. Bayku
 Soc. 15
78. Asam
 1988, 1
79. McLae
 Oxford
80. Mathi
81. Miller
 1986, 7
82. Dawsc
 1982, 4
83. Vincen
 G., Or
84. Syka,
 1990, 3
85. Syka,
 Matus
 Analyt
86. Pelton
87. Emary
 Comm
88. Charle
 Spectro
89. Fetterc
 19, 104
90. Meyerl
 169.
91. Kinter,
92. White,
 13, 413.

- Bursey, M. M.; Hass, J. R.; Stern, R. L., *Anal. Chem.* **1975**, *47*, 1452.
- Ausloos, P. J.; Lias, S. G., *J. Am. Chem. Soc.* **1981**, *103*, 6505.
- Baykut, G; Watson, C. H.; Weller, R. R.; Eyler, J. R., *J. Am. Chem. Soc.* **1985**, *107*, 8036.
- Asamoto, B.; Dunbar, R. C., *Int. J. Mass Spectrom. Ion Processes* **1988**, *86*, 387.
- McLachlan, N. W., "Theory and Application of Mathieu Function", Oxford University Press : New York, 1947.
- Mathieu, E., *J. Math. Pures Appl.* **1868**, *13*, 137.
- Miller, P. E.; Denton, M. B., *Int. J. Mass Spectrom. Ion Processes* **1986**, *72*, 223.
- Dawson, P. H.; Fulford, J. E., *Int. J. Mass Spectrom. Ion Processes* **1982**, *42*, 195.
- Vincenti, M.; Schwartz, J. C.; Cooks, R. G.; Wade, A. P.; Enke, C. G., *Org. Mass Spectrom.* **1988**, *23*, 579.
- Syka, J. E. P.; Schoen, A. E., *Int. J. Mass Spectrom. Ion Processes* **1990**, *96*, 97.
- Syka, J. E. P.; Schoen, A. E.; Stafford, G. C., Jr.; Hail, M. E.; Matuszak, K. P., Abstract Book of Pittsburgh Conference on Analytical Chemistry and Applied Spectroscopy, 1990, Abstract #151.
- Peltonen, K.; Kostianen, R., *Org. Mass Spectrom.* **1988**, *23*, 278.
- Emary, W. B.; Allegri, G.; Costa, C.; Frison, G.; Traldi, P., *Rapid Commun. Mass Spectrom.* **1989**, *3*, 413.
- Charles, B.; Cole, R. B.; Bruneton, J.; Tabet, J.-C., *Org. Mass Spectrom.* **1989**, *24*, 445.
- Fetterolf, D. D.; Yost, R. A.; Eyler, J. R., *Org. Mass Spectrom.* **1984**, *19*, 104.
- Meyerhoffer, W. J.; Bursey, M. M., *Org. Mass Spectrom.* **1989**, *24*, 169.
- Kinter, M. T.; Bursey, M. M., *J. Am. Chem. Soc.* **1986**, *108*, 1797.
- White, E. L.; Bursey, M. M., *Biomed. Environ. Mass Spectrom.* **1989**, *18*, 413.

93. Kinte
94. Meyer
246.
95. Jalone
96. Kostia
97. Kostia
135.
98. Heath
1991,

Kinter, M. T.; Bursey, M. M., *Org. Mass Spectrom.* **1987**, *22*, 775.

Meyerhoffer, W. J.; Bursey, M. M., *Org. Mass Spectrom.* **1989**, *24*, 246.

Jalonen, J., *J. Chem. Soc., Chem. Commun.* **1985**, 872.

Kostiainen, R.; Auriola, S., *Org. Mass Spectrom.* **1990**, *25*, 255.

Kostiainen, R.; Auriola, S., *Rapid Commun. Mass Spectrom.* **1988**, *2*, 135.

Heath, T. G.; Allison, J.; Watson, J. T., *J. Am. Soc. Mass Spectrom.* **1991**, *2*, 270.

REACTI

THE [M

Introduction

The a
reactions w
differentiat
employed ch
that would
The extent o
and tertiary
later reporte
compounds v
from many
reactions w
reactions v
spectrometri
analytical p
with [M-1]
between the
reagents . T
different de

CHAPTER 2

REACTIVITIES OF DEUTERATED REAGENTS TOWARDS THE [M-1]⁻ IONS OF CHLORINATED BENZENES FOR H/D EXCHANGE REACTIONS

Introduction

The analytical potential of hydrogen/deuterium (H/D) exchange reactions was first demonstrated by Hunt and co-workers (1) for differentiating primary, secondary and tertiary amines. This early work employed chemical ionization (CI) using ND₃ as a reagent to produce ND₄⁺ which would then undergo H/D exchange reactions with amine molecules. The extent of the degree of H/D exchange is different for primary, secondary and tertiary amines. Based on a comprehensive study, the same group has reported H/D exchange reactions on the [M-1]⁻ ions of several aromatic compounds with deuterated reagents (2). Although protonated molecules in many aromatic compounds were also found to have H/D exchange reactions with deuterated reagents (2,3), thus far only H/D exchange reactions with [M-1]⁻ ions were shown to produce useful mass spectrometric information for differentiating aromatic isomers (4). Such analytical potential encourages further studies on H/D exchange reactions with [M-1]⁻ ions. This chapter will describe the H/D exchange reactions between the [M-1]⁻ ions of various chlorinated benzenes and deuterated reagents. The focus of this chapter is a study of relative reactivities for different deuterated reagents with different types of [M-1]⁻ ions. The

mechanistic
will be disc

Experiment

A trip
was used to
of the triple
the experim
to enter the
mass resolu
tuned for sli
into the ion
produced by
and the ma
respectively.
the experim
collision ene
instrument)
consistency i
in terms of r
Duplicate ru
same. The
average of th

kinetic details for the reactions of anions of dichlorobenzene isomers are discussed in Chapter 3.

Experimental

A triple quadrupole mass spectrometer (Finnigan TSQ-70B model) was used to perform all the experiments. The operation and configuration of the triple quadrupole system have been described in Chapter 1. During the experiments, only $[M-1]^-$ ions were allowed by the first quadrupole (Q1) to enter the collision chamber for reactions with deuterated reagents. Unit mass resolution was maintained in the third quadrupole whereas Q1 was set for slightly better than unit mass resolution. Samples are introduced into the ion source by a direct insertion probe. The $[M-1]^-$ ions were generated by CI using NH_3 as a reagent. The temperature of the ion source and the manifold of the spectrometer were set at 150 °C and 70 °C, respectively. The pressure of the CI source and the collision chamber for the experiments were maintained at 1.5 torr and 4 mtorr, respectively. A collision energy of 2.8 eV (according to the Q2 offset voltage reading of the instrument) was used. All the experiments were performed twice to test for consistency in the results. The replicates were compared for discrepancies in relative peak ratios and the absence or presence of stray peaks. Separate runs consistently gave spectra that were approximately the same. The data shown come from one set of results rather than the average of the replicates.

All the
Company,
purchased from
which was
chemicals were
purification

Results and

A. Character

Involving

Many
very narrow
even ionic pro
be observed
appropriate
satisfactory j
ion-molecule
efficiency of th
These factors
tuning progra
two factors in
Since H/D exc
this section is
of collision en

All the chlorinated benzenes were purchased from Aldrich Chemical Company, Inc., Milwaukee, WI. All the deuterated reagents were purchased from Cambridge Isotopes Laboratory, Woburn, MA except ND_3 which was obtained from MSD Isotopes, Montreal, Canada. All the chemicals were the best purity available and were used without further purification.

Results and Discussion

Characterization and Optimization of H/D Exchange Reactions Involving the $[\text{M}-1]^+$ of o-Dichlorobenzene

Many ion-molecule reactions have been found to occur only within very narrow collision energy ranges (5,6). In a triple quadrupole system, the ionic products derived from successful ion-molecule reactions may not be observed if the instrumental parameters of the system are not set at appropriate values. Usually, the standard tuning program can do a satisfactory job in optimizing many instrumental parameters. For a given ion-molecule reaction system, the two major factors that control the efficiency of the reaction system are collision energy and collision pressure. These factors must be optimized in addition to the optimization by the standard tuning program. Sometimes, compromises have to be made between the two factors in order to achieve a maximum yield of a certain ion product. The H/D exchange reactions are the main theme of this research work, and the present section is devoted to the characterization and optimization of the effects of collision energy and collision pressure on the exchange reactions. The

study is ba
dichloroben

The
controlled b
collision cha
chamber if t
complex inst
an ion as it
can affect it
the offset po
1. This figu
collision cha
derivative pl
with a width
about 3.0 V.
would be litt
the offset po
occurring at
ionic dissocia
potentials ar
chamber coul
transmission
but it will alm

Ion-mol
and D₂O prod

y is based on the H/D exchange reactions between the [M-1]⁻ of o-dichlorobenzene and D₂O.

The kinetic energy of an ion entering the collision chamber is controlled by the offset voltage potential between the ion source and the collision chamber. Theoretically, no ion should be able to enter the collision chamber if the offset voltage potential is set at zero or less. In reality, for a complex instrument such as the Finnigan TSQ-70B, the kinetic energy of an ion as it leaves the source, as well as other instrumental parameters, affect its transmission. The ion transmission efficiency as a function of offset potential for the [M-1]⁻ of o-dichlorobenzene is shown in Figure 2. This figure demonstrates that some ions can still manage to enter the collision chamber even at an offset potential below zero. From the relative plot, the transmission window of the ions centers at around 1.8 V with a width of about 3 V. Transmission of the ion reaches a maximum at about 3.0 V. This information is important because it suggests that there would be little or no gain in ion transmission into the collision chamber if the offset potential is increased beyond 3.0 V. For ion-molecule reactions occurring at high collision pressures, a higher collision energy would favor dissociation and increase the chance of ion scattering. If the offset potentials are set at below 3.0 V, ion transmission into the collision chamber could be reduced significantly. Optimum is balance between ion transmission and reaction efficiency. It may be different for each reaction; however, it will almost always be in the low energy region.

Ion-molecule reactions between the [M-1]⁻ ions of o-dichlorobenzene and D₂O produce H/D exchange ion products. All three hydrogens on the

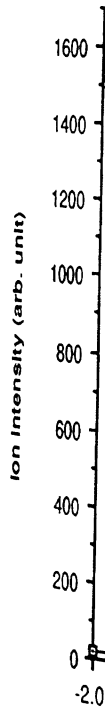
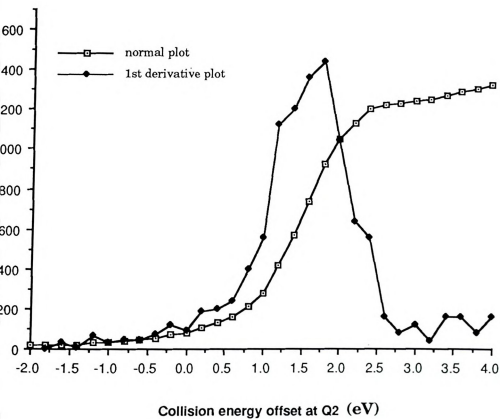


Figure 2-1 Ion Intensity (arb. unit)



2-1 Ion intensity as a function of collision energy offset at Q2 for the $[M-1]^-$ of *o*-dichlorobenzene.

anions of
resulting from
a specific reaction
collision energy
potential energy
At collision
no H/D exchange
optimum collision
as a function of
optimum collision
until the peak
product spectrum
the collision
causes a high
pressure as shown
product reaction
increased to
reduce the ion
increase of collision
ion transmission
3.0 to 4.0 mtorr
increases from
merely 6%.
between the
of the reactants
deuteriums.
substituted with

ns of o-dichlorobenzene are exchangeable, but the ion products
ting from the exchange of all three hydrogens are detected only within
pecific range of collision energy and collision pressure. The values of
ion energy and collision pressure were obtained from the offset voltage
tial and the pressure gauge reading of the instrument, respectively.
llision energies above 5.0 eV or at collision pressure below 0.3 mtorr,
D exchange products of any kind were observed. Figure 2-2 shows the
imum collision energies for the formation of the D₃-substituted product
function of collision pressure. At a specific collision pressure, the
imum collision energy is determined by varying the collision energy
the percentage distribution of the D₃-substituted product in the
ct spectrum is optimized. The optimum collision energy increases as
ollision pressure is increased. An increase in collision pressure also
s a higher relative yield of the D₃-substituted product up to around 4.0
as shown in Figure 2-3. The relative yield of the D₃-substituted
ct reaches a maximum of about 85% when the collision pressure is
sed to 4.0 mtorr. Further increases of the collision pressure only
e the ion transmission efficiency (see Table 2-1). For example, an
se of collision pressure from 4.0 to 5.0 mtorr would reduce the total
nsmission by 60%. However, for a collision pressure increase from
4.0 mtorr, the percentage distribution of the D₃-substituted product
ses from 65% to 85%, but the total ion transmission is reduced by
6%. The results suggest that for the H/D exchange reactions
n the [M-1]⁻ of o-dichlorobenzene and D₂O, a maximum of about 85%
reactant ions passing through Q2 are substituted with three
iums. The rest of the reactant ions are either nonreactive or
uted with only one or two deuteriums. The optimum collision energy

optimum offset collision energy (lab in eV)

Figure 2.

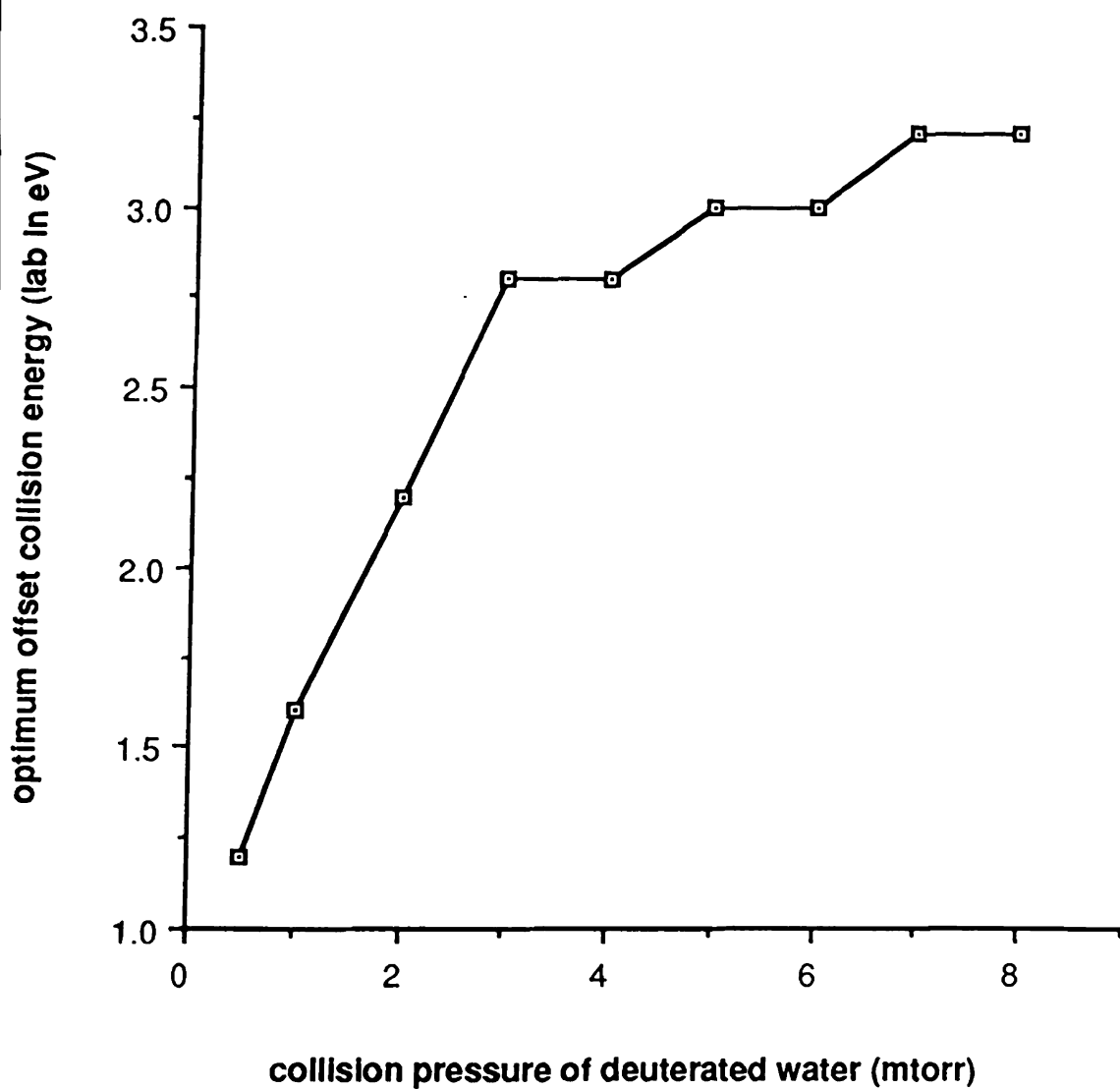


Figure 2-2 A plot of optimum collision energy as a function of collision pressure of D_2O . At a specific pressure value, an optimum collision energy is obtained by varying the collision offset voltage of the instrument until the D_3 -substituted product is optimized.

detected 3-D substituted product (%)

Figure

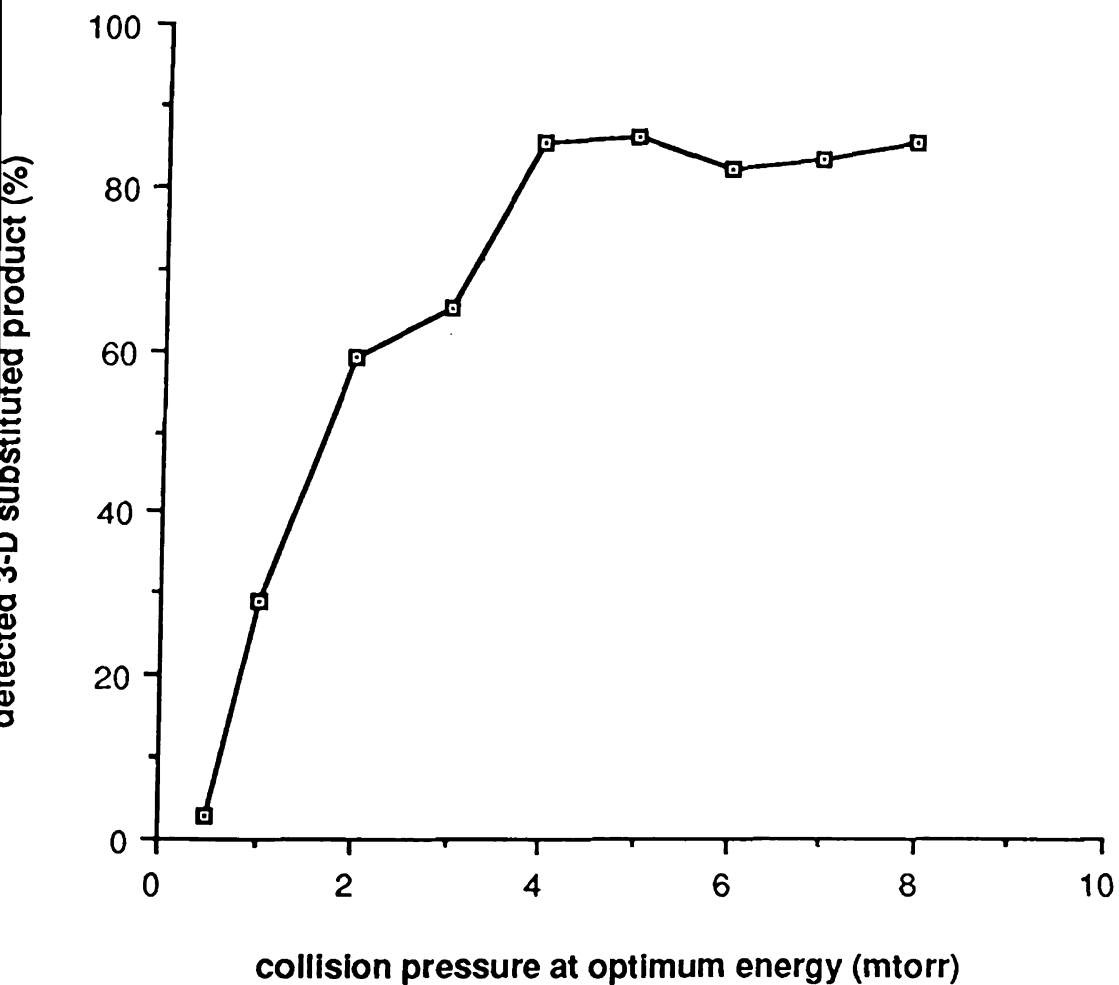


Figure 2-3 Percent of detected ions that have exchanged with three deuteriums at different collision pressure settings. Offset energy is the optimum for each pressure. The percent detected D₃-substituted product is based on 100% for the total ion intensity of all detected ions.

Table 2-1 Total ion intensity of all products and ion intensity for the D₃-substituted product at different collision pressure settings. The optimum collision offset energy is shown right

different collision pressure settings. The optimum collision offset energy is shown right next to each pressure.

collision pressure (mtorr) (optimum collision energy)	total ion intensity of all products	ion intensity for the D ₃ -substituted product
0.5 (1.2 eV)	47,400,000	1,400,000
1.0 (1.6 eV)	47,500,000	13,800,000
2.0 (2.2 eV)	22,600,000	13,300,000
3.0 (2.8 eV)	18,800,000	12,200,000
4.0 (2.8 eV)	17,600,000	14,900,000
5.0 (3.0 eV)	7,500,000	6,500,000
6.0 (3.0 eV)	4,100,000	3,300,000
7.0 (3.2 eV)	2,200,000	1,900,000
8.0 (3.2 eV)	1,000,000	800,000

and collision
mirror, resp

B. H/D Exchange

o-Dichloro

Alth
reactions,
undergo H
compounds
approxima
difference,
deuterated
systems.
exchange i
than 20 kc
react with
H/D excha
deuterated

The
 C_2H_5OD , C
(pyridine).
 CD_3SOCD_2
The reagent
Figure 2-4.
potentials

collision pressure for the exchange reactions are at 2.8 eV and 4.0 eV respectively.

Exchange Reactions between Deuterated Reagents and the [M-1]⁻ of o-dichlorobenzene

Although D₂O has been widely used as a reagent for H/D exchange reactions, a number of other deuterated reagents have also been found to undergo H/D exchange reactions with both anions and cations of organic compounds (2,7). An H/D exchange reaction requires reagents of approximately equal relative acidity or proton affinity (2,7). For large differences, the preferred reaction is proton transfer; thus, no single reagent is universally effective for all kinds of H/D exchange reactions. For negative ions reacting with a deuterated reagent, H/D exchange is generally not observed if the difference in acidities is greater than 10 kcal (7). In this section, different deuterated reagents are used to study the [M-1]⁻ of o-dichlorobenzene for H/D exchange reactions. The exchange reactivities and efficiencies are compared among the reagents employed.

The deuterated reagents chosen for this study are D₂O, ND₃, CH₃OD, CDCl₃, CD₃COCD₃, CD₃CN, CD₃SOCD₃, CD₄, C₆D₆ and C₅D₅N (7). Among these reagents, CDCl₃, CD₃COCD₃, CD₃CN and ND₃ were found in this study to produce no H/D exchange products. Reagents that have produced H/D exchange products are shown in Table 4. All the spectra were obtained under optimized collision offset and collision pressure settings except for ND₃ which could not be

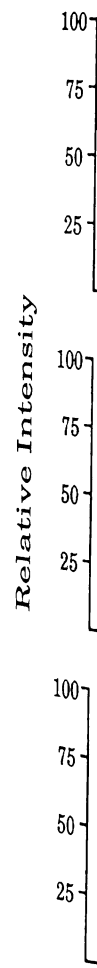
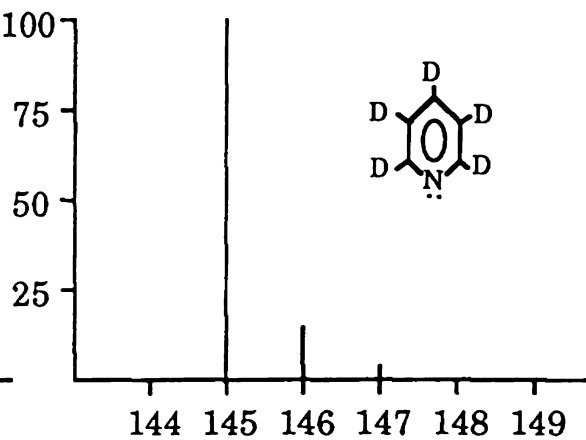
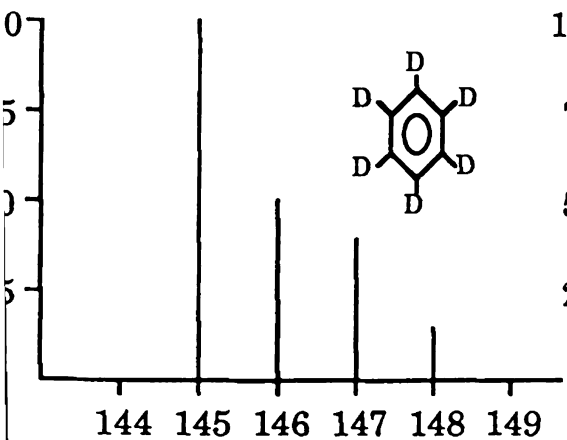
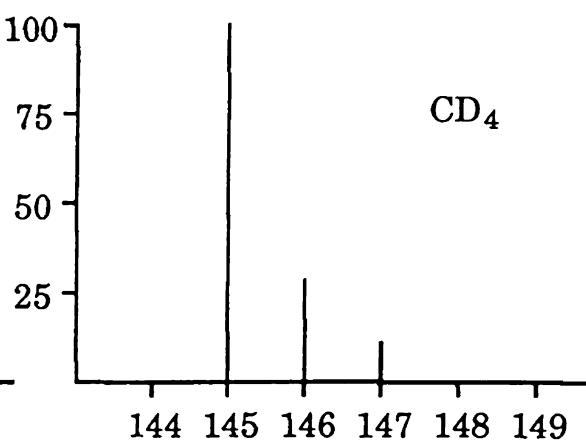
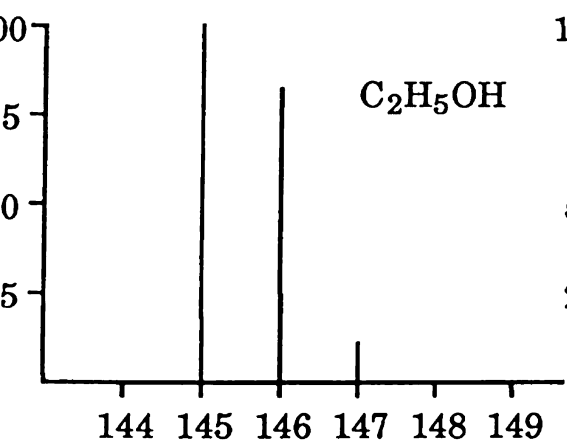
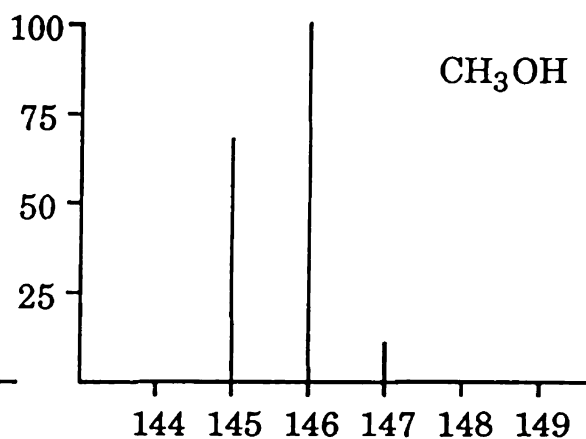
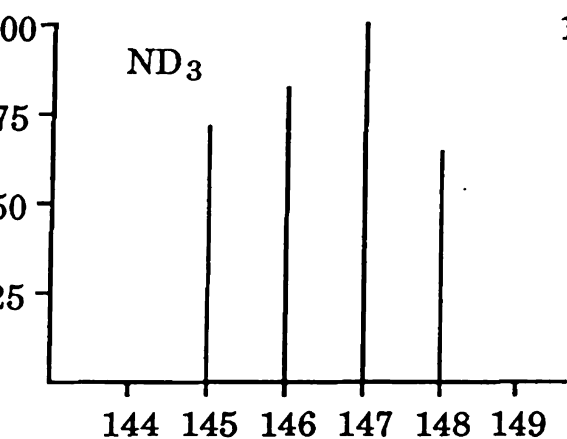
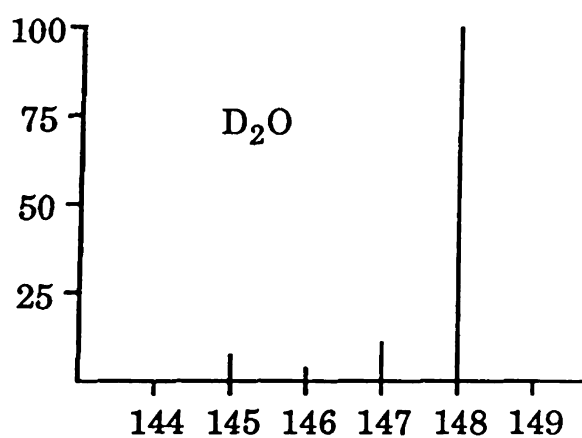


Figure 2-4
b
c
c



m/z

4 Product mass spectra obtained from H/D exchange reactions between the $[M-1]^-$ of o-dichlorobenzene (m/z 145) and different deuterated reagents. The reagents that do not produce any observable H/D exchange peaks are not shown in the figure.

optimized
expected t
instrumen
for the ex
for all the
varies sub
the collision
while the
pressure se
5.0, 4.5 an
setting dif
gauge from
for the diff
one anothe
other reage
its somewh
[M-1] of o
hydrogens,
well be the
reactivities
application

ized because the optimum collision pressure setting for the reagent is
ted to be well beyond the highest collision pressure allowable by the
ment. The results clearly show that D₂O is the most effective reagent
e exchange reactions. Although the optimum collision offset setting
l the reagents is at about 3.0 V, the optimum collision pressure setting
s substantially depending on types of reagents used. From optimizing
ollision pressure settings of the different reagents, it is found that
the optimum pressure setting for D₂O is at 4.0 mtorr, the optimum
ure settings for CH₃OD, C₂H₅OD, CD₄, C₆D₆ and C₅D₅N are at 2.5, 1.5,
5 and 2.0 mtorr, respectively. It is quite possible that these pressure
g differences are due to biases in pressure calibrations for the ion
from one compound to another. In other words, the real pressures
e different readings of the different reagents may actually be closer to
another than indicated. In addition to D₂O and ND₃, C₆D₆ is the only
reagent to allow the production of the D₃-substituted product despite
newhat bulky structure. Since H/D exchanges between C₆D₆ and the
of o-dichlorobenzene involve only aromatic deuteriums and aromatic
gens, the chemical similarity between the two exchanging atoms may
e the main contributing factor for the unusual reactivity of C₆D₆. The
ivities of the other reagents are too low to be useful for analytical
ations.

C. H/D Ex

Chloro

Deu

exchangin

dichlorobe

differentia

in the nex

hydrogen

substituti

functional

functionali

deprotonat

chlorobenz

are explore

The

were chos

donating p

selected su

these hydr

aromatic r

reactant i

substituen

reactions

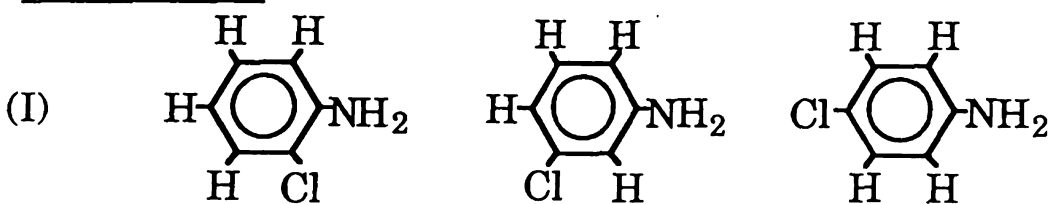
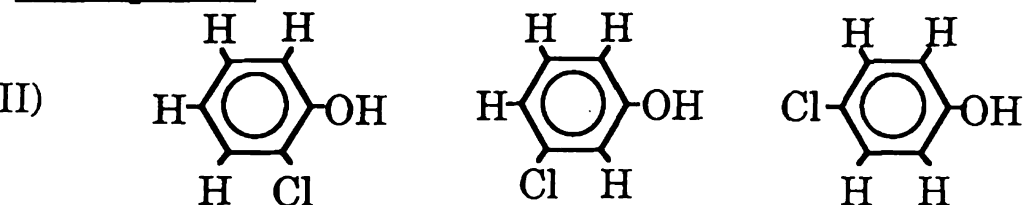
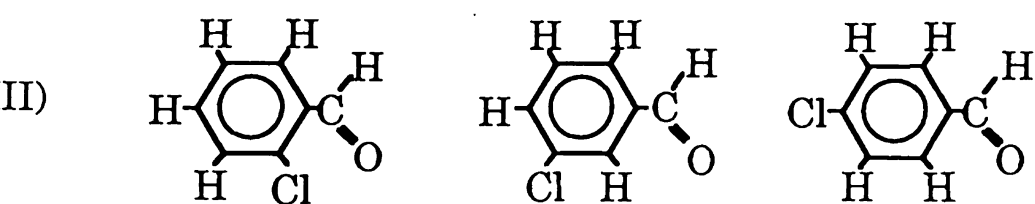
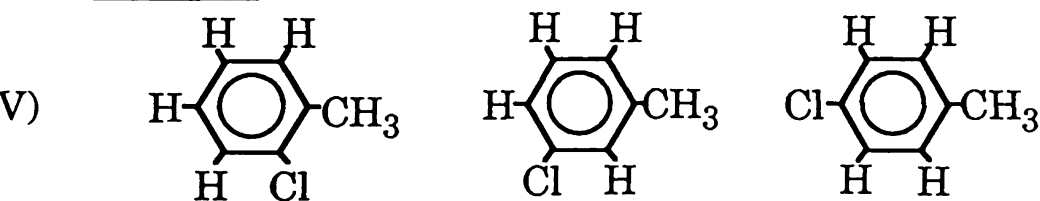
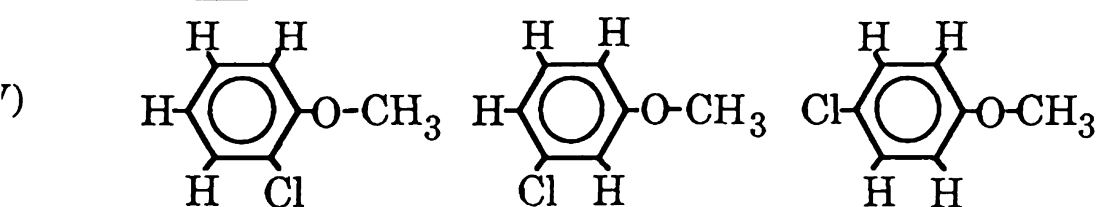
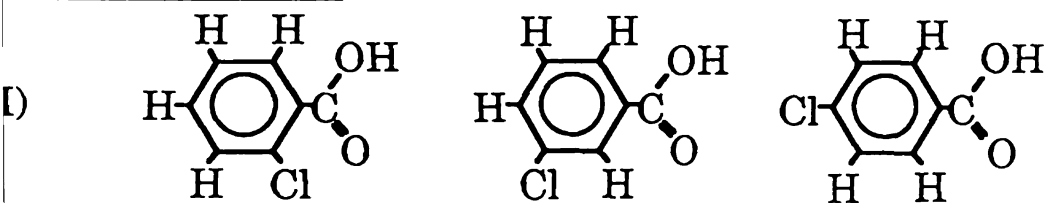
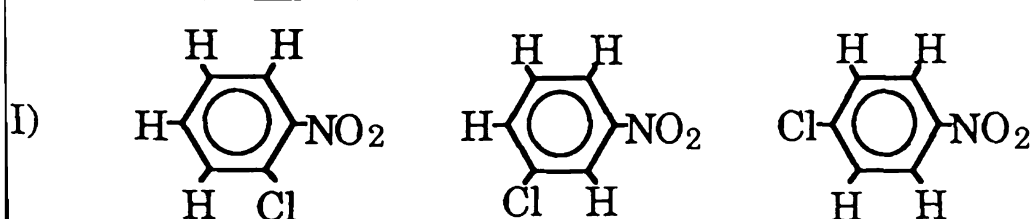
through F

exchanges

H/D Exchange Reaction for the [M-1]⁻ of Isomers of Substituted Chlorobenzenes with D₂O

Deuterated water has been found to be a powerful reagent for exchanging deuterium for the hydrogen atoms of the [M-1]⁻ ion from o-chlorobenzene. Successful applications of the exchange reactions for differentiating isomers of chlorinated benzenes will be discussed in detail in the next chapter. Because the characteristic chemistry of a specific substituent depends on the chemical environment of its parent molecule, substituting one of the two chlorine atoms with other chemical functionalities may alter the reactivity of its [M-1]⁻ with D₂O. If the functionalities also contain hydrogen atoms, [M-1]⁻ may be formed from the deprotonation of one of these hydrogens. In this section, the [M-1]⁻ ions of chlorobenzene isomers substituted with different chemical functionalities are explored for H/D exchange reactions with D₂O.

The isomers selected for this study are listed in Figure 2-5. They were chosen originally for their electron-withdrawing and electron-releasing properties towards the benzene rings. Except for NO₂, all the substituted substituents also contain one or more hydrogens. Because most of these hydrogens are expected to be more acidic than the hydrogens on the aromatic ring, it is conceivable that for most of the isomers, the [M-1]⁻ ions are formed by direct or indirect deprotonation of the substituent instead of the benzene ring. The results of H/D exchange reactions between the [M-1]⁻ ions and D₂O are shown in Figures 2-6 through Figure 2-12. The product ions derived from successful H/D exchanges are represented by peaks having one or more m/z units above the

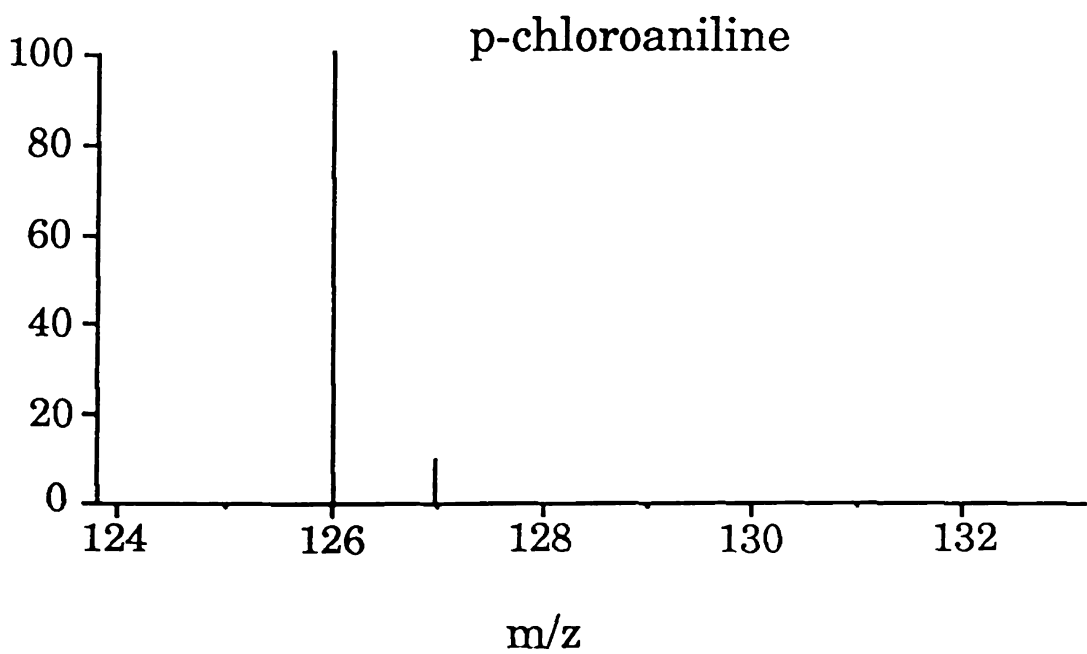
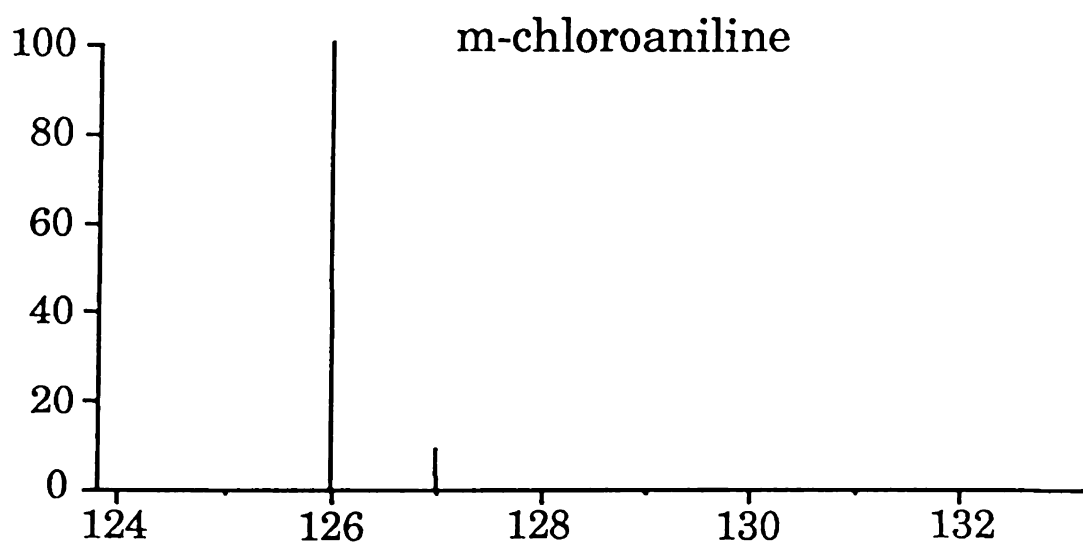
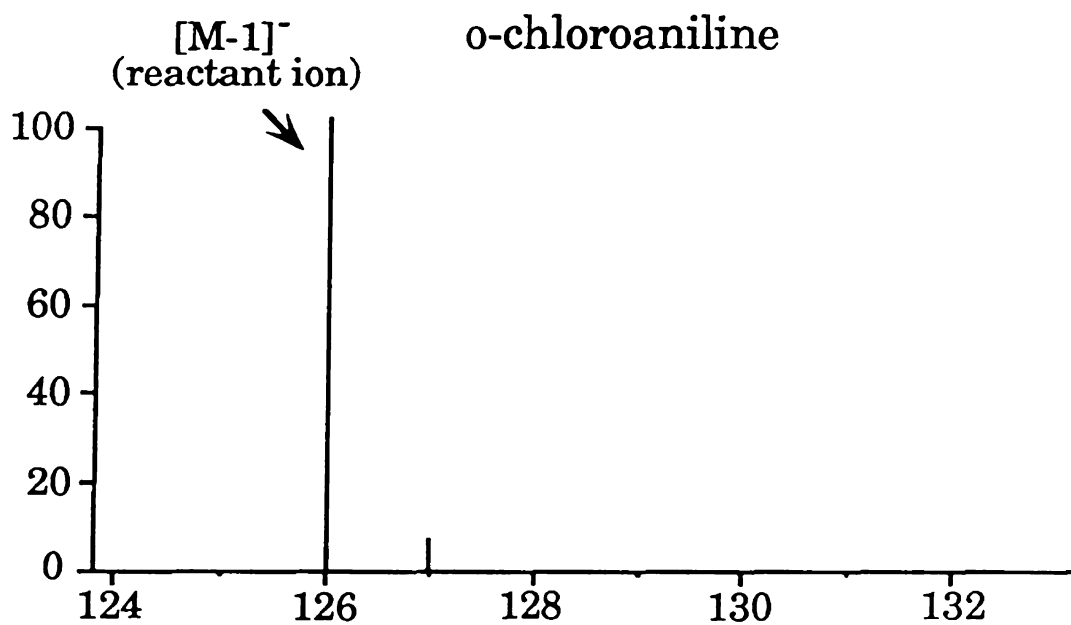
chloroanilinechlorophenolchlorobenzaldehydechlorotoluenechloroanisolechlorobenzoic acidchloronitrobenzeneFigure 2-5 Selected isomers for H/D exchange reactions with D₂O

10
8
6
4
2

Relative Intensity
10
8
6
4
2

10
8
6
4
2
0

Figure 2-6

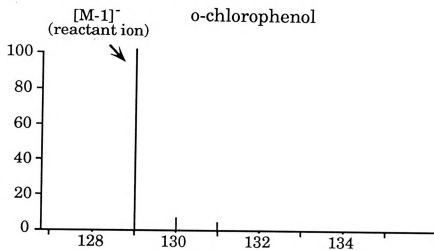


2-6 Product mass spectra for the [M-1]⁻ ion of the isomers of chloroaniline upon H/D exchange reactions with D₂O.

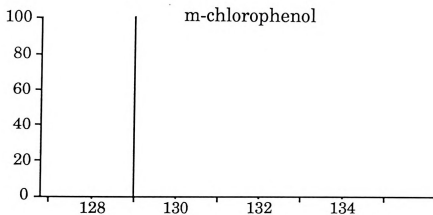
Relative Intensity

Figure

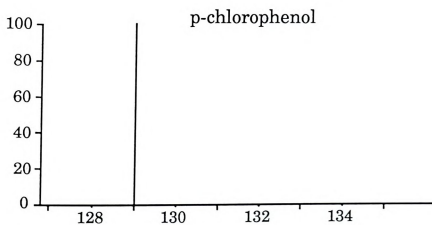
o-chlorophenol



m-chlorophenol



p-chlorophenol



m/z

Figure 2-7 Product mass spectra for the [M-1]⁻ ion of the isomers of chlorophenol upon H/D exchange reactions with D₂O.

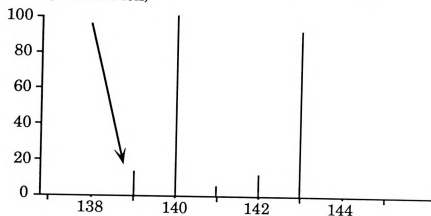
Relative Intensity

1
0
4
2
10
8
6
4
2
0
100
80
60
40
20
0

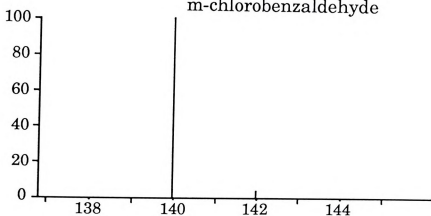
Figure 2

$[M-1]^-$
(reactant ion)

o-chlorobenzaldehyde



m-chlorobenzaldehyde



p-chlorobenzaldehyde

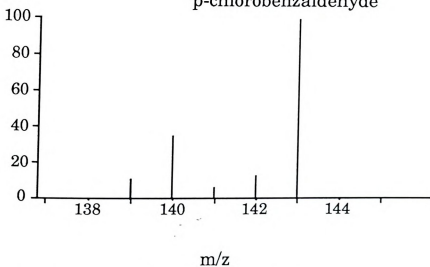


Figure 2-8 Product mass spectra for the $[M-1]^-$ ion of the isomers of chlorobenzaldehyde upon H/D exchange reactions with D_2O .

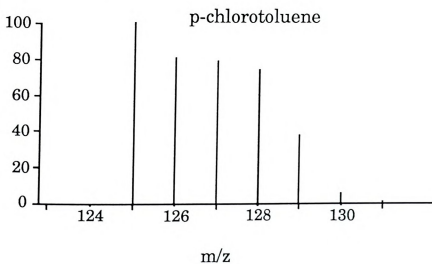
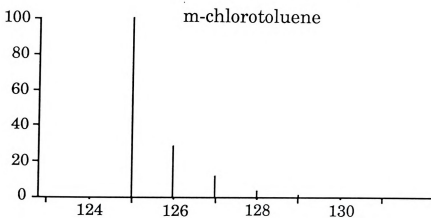
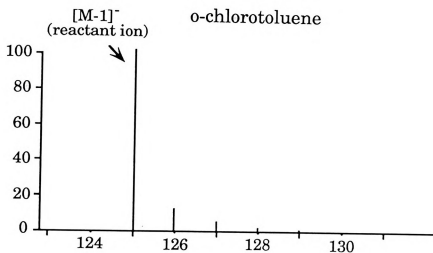
10
8
6
4
2
0

Relative Intensity

10
8
6
4
2
0

100
80
60
40
20
0

Figure 2-9



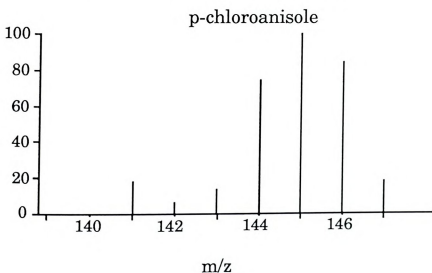
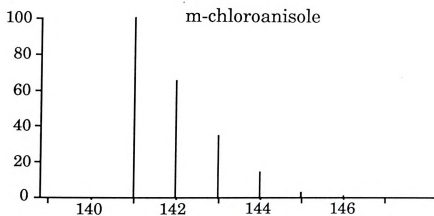
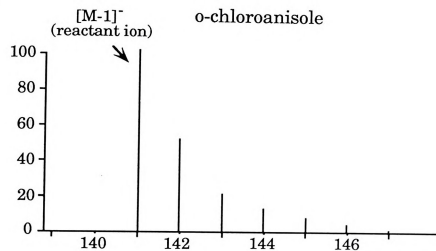
2-9 Product mass spectra for the [M-1]⁻ ion of the isomers of chlorotoluene upon H/D exchange reactions with D₂O.

10
8
6
4
2

Relative Intensity
10
8
6
4
2
0

10
8
6
4
2
0

Figure 2-1



2-10 Product mass spectra for the [M-1]⁻ ion of the isomers of chloroanisole upon H/D exchange reactions with D₂O.

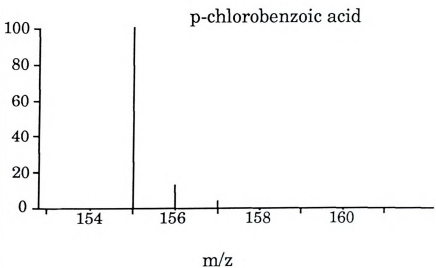
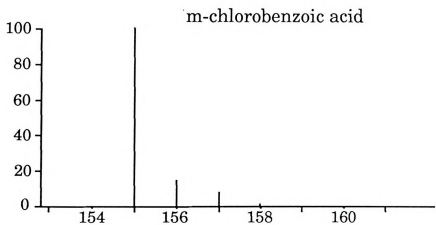
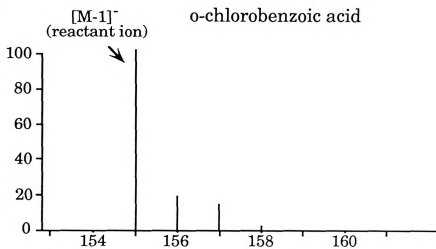
10
8
6
4
2
0

Relative Intensity

100
80
60
40
20
0

100
80
60
40
20
0

Figure 2-1



2-11 Product mass spectra for the [M-1]⁻ ion of the isomers of chlorobenzoic acid upon H/D exchange reactions with D₂O.

10

8

6

4

2

Relative Intensity

10

8

6

4

2

10

8

6

4

2

Figure 2-

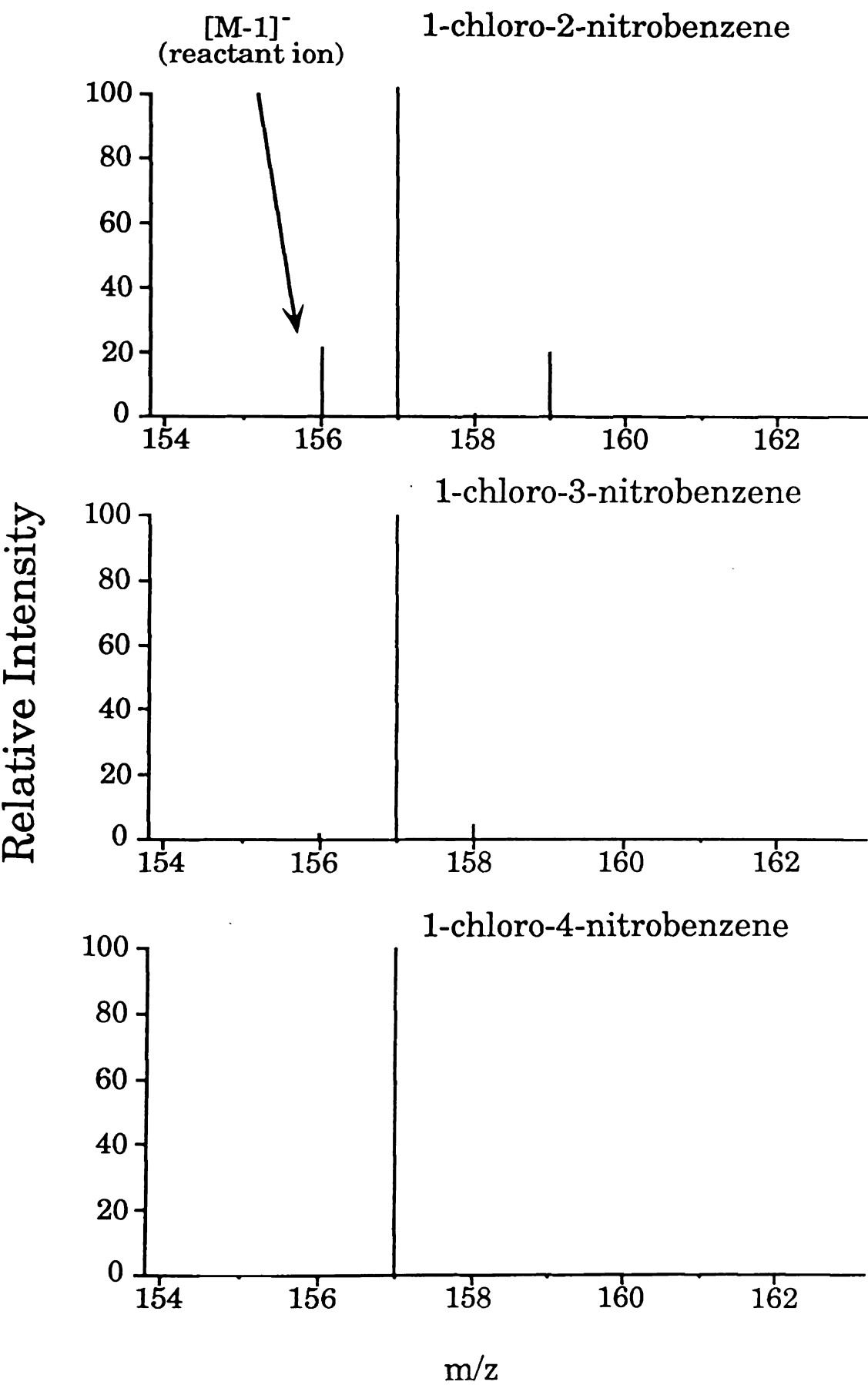


Figure 2-12 Product mass spectra for the [M-1]⁺ ion of the isomers of chloronitrobenzene upon H/D exchange reactions with D₂O.

m/z of the
atoms with
the [M-1]
three isom
hydrogen
reactions
interestin
minimal.

For
are observ
that whil
chlorophe
deuterium
and chloro
demonstre
addition t
these thr
compared
in reactiv
chloroani
chloroben
substitute
chloroben
deuterium
chloroben
differentia

m/z of the reactant. It is clear that substituting one of the two chlorine atoms with the selected substituents substantially reduces the reactivity of the $[M-1]^-$ ion with D_2O . Figure 2-6 shows that the product spectra of all three isomers of chloroaniline are essentially identical. Only one of the five hydrogens of $[M-1]^-$ from the chloroaniline isomers is exchangeable upon reactions with D_2O . Although the results suggest that there may be some interesting chemistry involved, the analytical value of the reactions is minimal.

For the other substituted chlorobenzenes, some spectral differences are observed for the different isomers. In Figure 2-7, the spectra indicate that while no H/D exchange product is observed for either p- or m-chlorophenol, o-chlorophenol gives product spectra indicative of two deuterium substitutions. For isomers of chlorobenzaldehyde, chlorotoluene and chloroanisole, the results presented in Figure 2-8 - Figure 2-10 clearly demonstrate that hydrogens on the substituents are also exchangeable, in addition to the aromatic hydrogens. The reactivities of the para isomers of these three substituted chlorobenzenes are consistently the highest compared to those of the meta and ortho isomers. Although the difference in reactivity for the ortho and meta isomers of chlorotoluene and chloroanisole is small, the reactivity of the meta isomer of chlorobenzaldehyde is very different from that of ortho isomer. While ions substituted with four deuteriums are major products for the anions of o-chlorobenzaldehyde, a small peak representing a maximum of only three deuterium substitutions is observed for the anions of m-chlorobenzaldehyde. Nevertheless, individually these isomers can still be differentiated on the basis of their differences in H/D exchange efficiencies

with D₂O
D₃-subst
Product i
observed

An
substitute
former.
indirect c
molecule
chloronitr
the [M-1
substituen
shown in
predomin
exchange
found to
maximum
and para
[M-1] of d
three H/
chloronitr
dichlorob
its [M-1]-
exchange
the three

with D_2O . For the isomers of chlorobenzoic acid, Figure 2-11 shows that the D_3 -substituted products are observed for both the meta and ortho isomers. Product ions associated with a maximum of only two H/D exchanges are observed for the para isomers.

An important difference between chloronitrobenzene and the other substituted chlorobenzenes is the absence of non-aromatic hydrogens in the former. A chloronitrobenzene $[M-1]^-$ ion must be formed by direct or indirect deprotonation of one of the three aromatic hydrogen of a neutral molecule. This means that while the initial reaction site of a chloronitrobenzene $[M-1]^-$ ion is on the aromatic ring, the equivalent site of the $[M-1]^-$ of the other substituted chlorobenzenes may be on the substituents. The product spectra for the isomers of chloronitrobenzene are shown in Figure 2-12. Although ions having only one H/D exchange are the predominant products for all the isomers, the observed maximum H/D exchanges are different for different isomers. Only the ortho isomer is found to allow all three hydrogens of its anion to be exchanged; a maximum of two and one hydrogens exchanged is observed for the meta and para isomers, respectively. Compared to the same reactions with the $[M-1]^-$ of dichlorobenzene, the relative yields for the formation of the two and three H/D exchange products are significantly lower in the case of chloronitrobenzene. Clearly, substituting one of the two chlorines of a dichlorobenzene molecule with NO_2 substantially reduces the reactivity of its $[M-1]^-$ ion towards the formation of the products of higher order H/D exchanges. Nevertheless, the reactions are still useful for differentiating the three isomers.

Conclusi

In
transmit
collision
increased
optimum
exchange
2.8 eV and
observed
energies
react with
for H/D e

In
chloroben
and NC
dichlorob
reduced
chloroben
the [M-1
deuterium
of chloro
For the [D
deuterium
functiona

Conclusions

In the TSQ-70B triple quadrupole system, the efficiency of transmitting the $[M-1]^-$ of *o*-dichlorobenzene from the ion source into the collision chamber is a strong function of collision offset voltage, but is not increased beyond a collision offset potential voltage of around 3.0 V. The optimum collision offset energy and collision pressure setting for the H/D exchange reactions between the $[M-1]^-$ of *o*-dichlorobenzene and D_2O are at 1.8 eV and 4.0 mtorr, respectively. No H/D exchange reaction products are observed for measured collision pressures below 0.3 mtorr or collision energies above 5.0 eV. Among the many deuterated reagents selected to react with the $[M-1]^-$ of *o*-dichlorobenzene, D_2O is the most effective reagent for H/D exchange.

In the study of H/D exchange reactions between D_2O and the $[M-1]^-$ of chlorobenzene isomers substituted with NH_2 , OH, CHO, CH_3 , OCH_3 , COOH and NO_2 functionalities, it was found that replacing a Cl of a chlorobenzene molecule with one of the functionalities substantially reduced the reactivity of the $[M-1]^-$. While the para isomers of chlorobenzaldehyde, chlorotoluene and chloroanisole allow all hydrogens of the $[M-1]^-$ ions to be substituted with deuteriums, no more than two deuterium substitutions are observed for the $[M-1]^-$ ions of the para isomers chloroaniline, chlorophenol, chlorobenzoic acid and chloronitrobenzene. For the $[M-1]^-$ ions of chlorobenzaldehyde, chlorotoluene and chloroanisole, deuterium substitutions clearly occur on hydrogens connecting to the functionalities as well as the aromatic hydrogens. The reactivity of the $[M-$

1] ions o
produce
that som
exchangi

Reference

1. Hu
45:
2. Hu
3. Fr
19'
4. Ch
5. Sc
19'
6. Sc
49:
7. De

[M-1]⁻ ions of chlorobenzoic acid, chlorophenol and chloroaniline are too low to produce useful information for isomeric differentiation. It is very likely that some other deuterated reagents may be more suitable than D₂O for exchanging hydrogens of substituted chlorobenzene [M-1]⁻ ions.

References

1. Hunt, D. F.; McEwen, C. N.; Upham, R. A., *Tetrahedron Lett.* **1971**, 4539.
2. Hunt, D. F.; Sethi, S. K., *J. Am. Chem. Soc.* **1980**, 102, 6953.
3. Freiser, B. S.; Woodin, R. L.; Beauchamp, J. L., *J. Am. Chem. Soc.* **1975**, 97, 6893.
4. Chakel, J. A., Ph.D dissertation, Michigan State University, 1982.
5. Schmit, J. P.; Dawson, P. H.; Beaulieu, N., *Org. Mass Spectrom.* **1985**, 20, 269
6. Schmit, J. P.; Beaudet, S.; Brisson, A., *Org. Mass Spectrom.* **1986**, 21, 493.
7. DePuy, C. H.; Bierbaum, V. M., *Acc. Chem. Res.* **1981**, 14, 146.

MECHA
IONS

Introduc

Ma

reactions

studies o

have dem

Presuma

H_3^+ , D_3^+ ,

(6,7) first

under ch

Active hy

reactions

reagents.

or MeOD

exchange

allowed t

Exchange

using ion

ions (9).

condition

CHAPTER 3

MECHANISTIC STUDY OF H/D EXCHANGE BETWEEN [M-1]- IONS OF CHLORINATED BENZENES AND DEUTERATED WATER OR DEUTERATED AMMONIA

Introduction

Mass spectrometric studies on hydrogen-deuterium (H/D) exchange reactions in solution have been used for structure elucidation (1,2). Kinetic studies on isotopic methane-hydrogen and methane-deuterium systems have demonstrated the feasibility of H/D exchanges in the gas phase (3,4,5). Presumably, the reactant ions involved for the exchange reactions include H_3^+ , D_3^+ , CH_3^+ , CD_3^+ , CH_4^+ , CD_4^+ , CH_5^+ and CD_5^+ . Hunt and co-workers (6,7) first reported H/D exchanges for organic compounds in the gas phase under chemical ionization (CI) conditions with deuterium oxide reagent. Active hydrogens in organic compounds were determined by H/D exchange reactions between neutral organic molecules and ionic deuterated reagents. Isotopic exchange for amines was observed when either ND_3 (7) or MeOD (8) was used as the CI reagent. Differences in the number of exchanges observed between ND_4^+ or $MeOD_2^+$ and amine molecules allowed the differentiation of primary, secondary and tertiary amines. Exchange of aromatic hydrogens was first reported by Beauchamp et al. using ion cyclotron resonance (ICR) spectroscopy for protonated benzene ions (9). This study suggested that ring protonation was a necessary condition for exchanging aromatic hydrogens of a cation. Further studies

by Marti
confirmed
than on th

Deu
compound
conditions
observed
afterglow
EtOD and
afterglow
general ru
an excha
significan
positional
Chakel (15

In t
exchange
compound
benzenes
confirm th

by Martinsen and Buttrill (10) on a variety of substituted benzenes confirmed that when protonation occurred on the substituent groups rather than on the aromatic rings, H/D exchange products were not observed.

Deuterium exchanges for the $[M-1]^-$ ions of a number of organic compounds were first shown by Stewart et al. under flowing afterglow conditions, using D_2O as the reagent (11). Exchange reactions were also observed for similar types of compounds under both CI and flowing afterglow conditions, using other deuterated reagents such as ND_3 , MeOD, EtOD and CF_3CD_2OD (12,13). Based on the results obtained from a flowing afterglow instrument, Depuy and Bierbaum (14) have concluded that, as a general rule, H/D exchange can usually be observed between an anion and an exchange reagent which is as much as 20 kcal less acidic. The significance of using H/D exchange reactions for the differentiation of positional isomers of aromatic compounds was then demonstrated by Chakel (15).

In this work, we postulate a reaction mechanism for the H/D exchange reaction between the hydrogen on the $[M-1]^-$ ions of aromatic compounds and molecules of D_2O and ND_3 . Isomers of chlorinated benzenes were the model compounds chosen for this study. The results confirm that the reaction is potentially useful for isomeric differentiation.

Experiments

Two
experiments
the experi
mass spec
reagent w
instrumen
instrumen
quadrupole
Finnigan m

For
instrument
insertion p
source. Fo
rates were
reservoir a
rate was
experimen
were intro
chromatogr
SE-54 phas
injection po
A transfer
Helium wa
temperatur

Experimental

Two types of tandem quadrupole instruments were used for all experiments. In the cases where ND_3 was used as the deuterated reagent, the experiments were performed on a Finnigan TSQ-70B triple quadrupole mass spectrometer. Experiments involving the use of D_2O as a deuterated reagent were later performed on a Finnigan TSQ-700 tandem quadrupole instrument. The configuration and the components used for both the instruments are essentially identical, with the exception that the second quadrupole in the Finnigan TSQ-70B instrument is an octopole device in the Finnigan model TSQ-700.

For the experiments performed on the Finnigan TSQ-70B instrument, samples were introduced into the ion source by either a direct insertion probe or from an external glass reservoir connected to the ion source. For the samples in the external glass reservoir, the sample flow rates were controlled by two adjustable leak valves installed between the reservoir and the ion source. As far as possible, a steady-state sample flow rate was maintained during each individual experiment. For the experiments performed on the Finnigan TSQ-700 instrument, samples were introduced into the ion source through the Varian 3400 gas chromatograph (GC). A capillary column was used (30 m, 0.25 mm i.d., SE-54 phase with 0.25 μm film thickness) for component separation. The injection port of the GC was set at 250 °C under a splitless injection mode. A transfer line set at 275 °C directed the column effluent into the ion source. Helium was used as the carrier gas at a pressure of 15 psi. The temperature of the GC was programmed from 80 °C to 200 °C at 10 °C/min.

The GC to
emerging
isomers of
the sample

The
source at
extracted f
of the ta
quadrupole
were intro
ion produc
(according
throughout
source was
were main
indicated o
consistency
in terms of
Duplicate
same. The
average of t

All c
from Ultra
compounds
Milwaukee,

The GC temperature program was set such that all the selected compounds emerging from the GC column were at least base-line separated. The isomers of o-dichlorobenzene were injected into the GC as mixtures. All the samples were dissolved in hexane to a concentration of about 10 ppm.

The $[M-1]^-$ ions of the test compounds were generated by CI in the ion source at 150 °C using NH_3 as a reagent. In general, the reactant ions extracted from the source were mass-selected by the first quadrupole of one of the tandem quadrupole instruments for reaction in the second quadrupole (Q2) or the octopole device (O2) where the deuterated reagents were introduced. The last quadrupole was set to scan for the spectra of the ion products of the reactions in Q2 or O2. A collision energy at 2.8 eV (according to the Q2 or O2 offset voltage reading of the instrument) was used throughout all the experiments. The pressure of the reagent gas in the ion source was maintained at 1.5 torr. The collision pressures for ND_3 and D_2O were maintained at approximately 7 and 4 mtorr, respectively, except when indicated otherwise. All the experiments were performed twice to test for consistency in the results. The replicates were compared for discrepancies in terms of relative peak ratios and the absence or presence of stray peaks. Duplicate runs consistently gave spectra that were approximately the same. The data shown come from one set of results rather than the average of the replicates.

All chlorinated isomers used in the experiments were purchased from Ultra Scientific, North Kingston, RI. All other halogenated compounds were purchased from Aldrich Chemical Company, Inc., Milwaukee, WI. Deuterated ammonia (99.5 atom %D) was obtained from

MSD Isot
purchased
chemicals

Results and

A. Mechanism

Low
dichlorobenzene
exchange
observed for
abundance
dichlorobenzene
selected reagent
substitution
reagent is
reactant ion
peaks at m/z
ions with a
by peaks at
indistinguishable
the [M-1]⁺
isomers, or
corresponding
deuterium

MSD Isotopes, Montreal, Canada. Deuterated water (99+% grade) was purchased from Cambridge Isotopes Laboratory, Woburn, MA. All the chemicals were used without further purification.

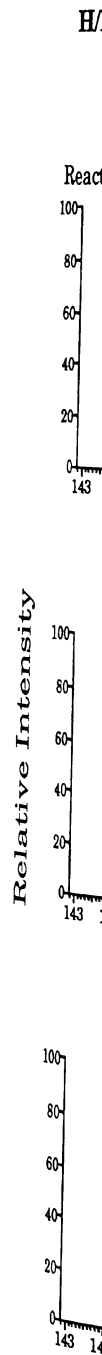
Results and Discussion

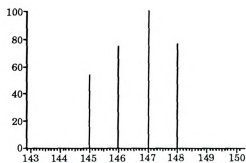
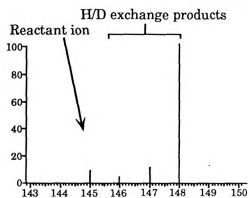
A. Mechanistic Analysis

Low-energy collision between $[M-1]^-$ ions of all the isomers of dichlorobenzene and deuterated water or deuterated ammonia produce H/D exchange products. For each isomer, the same exchange products are observed for either D_2O or ND_3 reagent, though not in the same relative abundance. The product mass spectra of the three isomers of dichlorobenzene are shown in Figure 3-1 for both D_2O and ND_3 . The selected reactant ions at m/z 145 contain only the ^{35}Cl isotope. Each substitution of a deuterium from an exchange reaction with the deuterated reagent is indicated by the gain of one mass unit from the mass of the reactant ions. Sequential H/D exchanges of the same ions are indicated by peaks at more than one m/z unit above the reactant ion mass, thus product ions with all three hydrogens substituted with deuteriums are represented by peaks at m/z 148. Although these isomers are known to produce nearly indistinguishable EI mass spectra, the pattern of H/D exchange products of the $[M-1]^-$ ion of each isomer is quite distinctive. For the anions of these isomers, only o-dichlorobenzene gives a predominant peak at m/z 148 which corresponds to ion products with all the three hydrogens exchanged with deuteriums; the predominant products for m-dichlorobenzene and p-

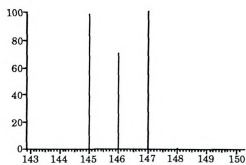
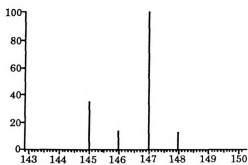
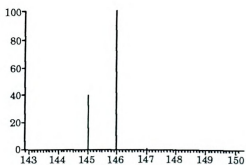
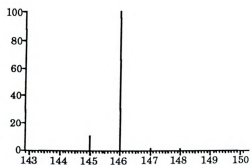


Figure 3-1 Product spectra obtained from the H/D exchange reactions between the [M-1]⁻ ions of the individual isomers of dichlorobenzene and deuterated water and deuterated ammonia. The reactant ions are at m/z 145. Peaks at higher mass units are due to one or more H/D exchange reactions.



H/D Exchanges with D₂OH/D Exchanges with ND₃o-dichlorobenzenem-dichlorobenzene

Relative Intensity

p-dichlorobenzene

m/z

dichlorob
respective
indicate th
ring affec
exchange

Since
are essent
believe th
essentially
Scheme I
mechanism
between th
formation o
molecule or
hydrogen).
hydrogen a
complex. A
the interme
removes the
one carbon
Further H/
until no mo
with three
which, acco
reactant ion
adjacent to t

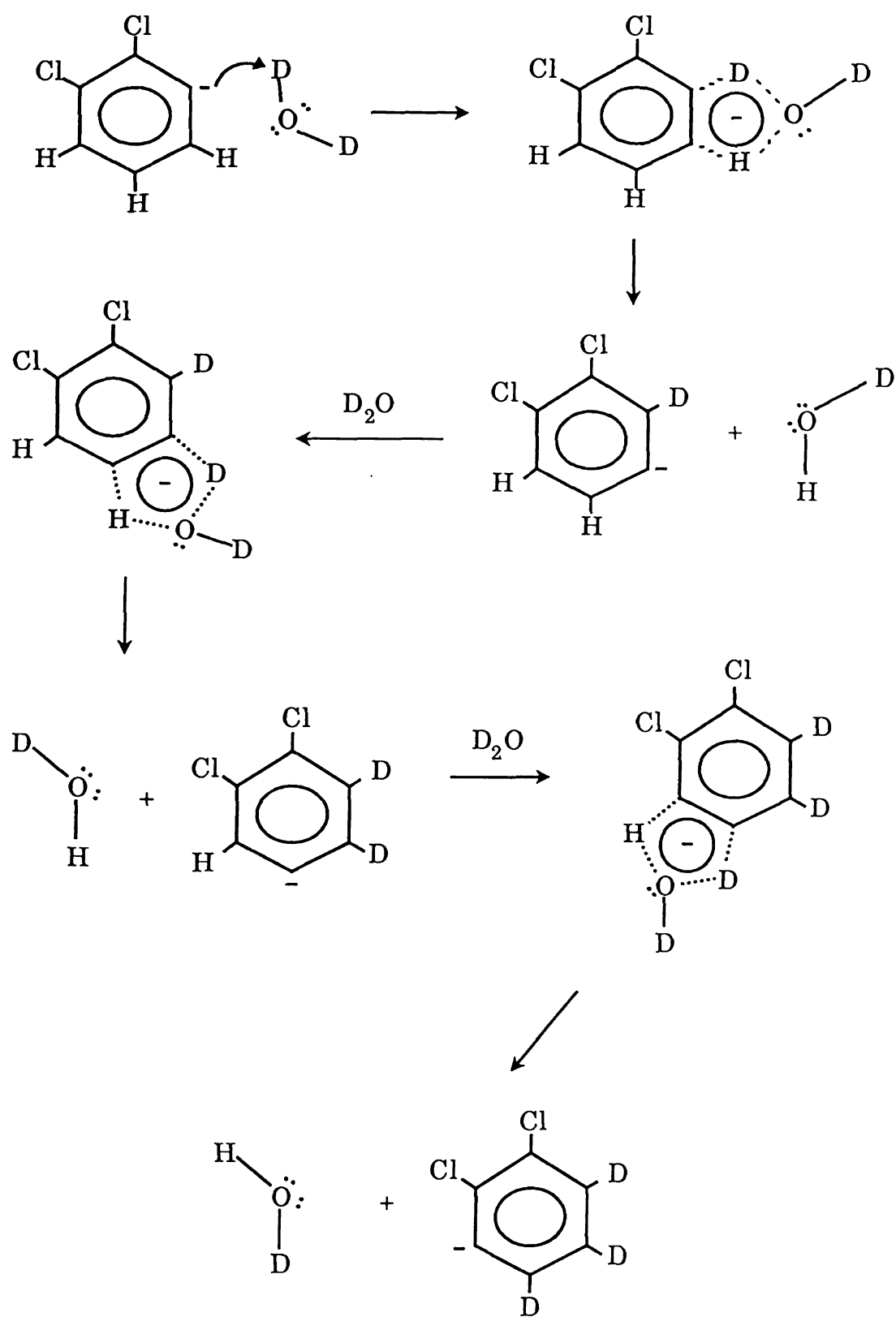
dichlorobenzene are ions substituted with two and one deuteriums, respectively. The dramatic differences in the product patterns observed indicate that the relative positions of the chlorine atoms on the aromatic ring affects the ability of certain ring hydrogens to undergo the H/D exchange reaction.

Since the reaction products observed with both D_2O and ND_3 reagents are essentially the same (though in differing relative abundances), we believe that the basic reaction mechanisms for the two species are essentially the same. We postulate the reaction mechanism shown in Scheme I for ortho dichlorobenzene $[M-1]^-$ ion and D_2O . In this mechanism, a five-membered-ring reaction intermediate is formed between the $[M-1]^-$ ion and the reagent molecule (either D_2O or ND_3). The formation of this intermediate is initiated by the attack of the deuterated molecule on the charge site (localized at the carbon atom with the missing hydrogen). An electron pair on the neutral reagent molecule reacts with a hydrogen atom adjacent to the charge site to form the intermediate complex. A successful H/D exchange occurs only if the decomplexation of the intermediate complex leaves a D atom at the initial charge site and removes the adjacent H atom. The charge site in the product ion is shifted one carbon atom around the ring from its position in the reactant ion. Further H/D exchange reactions can continue by the same mechanism until no more adjacent aromatic hydrogens remain. Products substituted with three deuteriums are the result of three successful H/D exchanges which, according to the proposed mechanism, requires that the initial reactant ion contain three aromatic hydrogens adjacent or sequentially adjacent to the initial charge site.

Cl

H





Scheme I

The
initial re
positions
charge sit
The chlor
anions all
intermedi
three diffe
aromatic l
of two arc
the charg
atoms is s
the five-m
deuterium
predomina
formed wit
the locati
hydrogens
intermedia
reactant p
those of t
reactant io
anions, the
hydrogens
that the ch
other two h
an ionic c

The number of adjacent (or sequentially adjacent) hydrogens in the initial reactant ion depends on the location of the charge and the relative positions of the chlorine atoms on the aromatic ring. All the possible charge sites for the three dichlorobenzene isomers are listed in Figure 3-2. The chlorine positions and the charge locations of the ortho-substituted anions allow sequential deuterium substitution, via the five-membered-ring intermediate, of all three hydrogens. For the meta-substituted anions, three different charge sites are possible. Both structure III and IV contain aromatic hydrogens adjacent to the charge site. These sites allow exchange of two aromatic hydrogens which are adjacent or sequentially adjacent to the charge sites. The third hydrogen located between the two chlorine atoms is separated from the charge sites and can not be exchanged through the five-membered-ring intermediate. Reactant ions substituted with two deuteriums are shown in the product spectra of m-dichlorobenzene as the predominant products. Structure V shows a meta-substituted anion formed with a charge site sandwiched between two chlorine atoms. Since the location of this charge site is remote from the three aromatic hydrogens, deuterium substitution through the five-membered-ring intermediate is not possible for this reactant ion. The relatively larger reactant peak in the product spectrum of m-dichlorobenzene compared to those of the other dichlorobenzene isomers suggests that some of the reactant ions have the structure V configuration. For the para-substituted anions, there is only one possible charge site because all four aromatic hydrogens in the original molecule are equivalent. Structure VI shows that the charge site is adjacent to only one hydrogen and separated from the other two hydrogens by a chlorine atom. By the proposed mechanism, such an ionic configuration allows only one hydrogen of the anion to be

Ortho-

- Bot
exc

Meta-

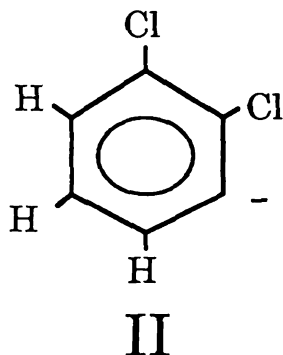
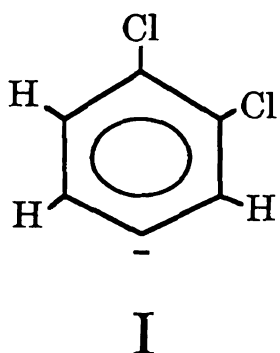
Figure 3-2 The possible charge sites for the $[M-1]^-$ ions of dichlorobenzene isomers and the consequent location and number of exchangeable hydrogens according to the proposed reaction mechanism.



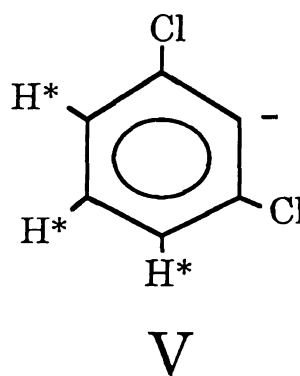
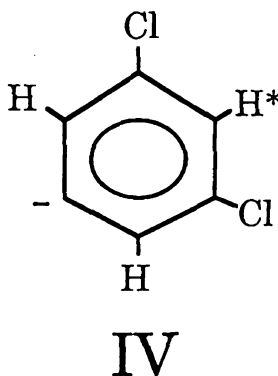
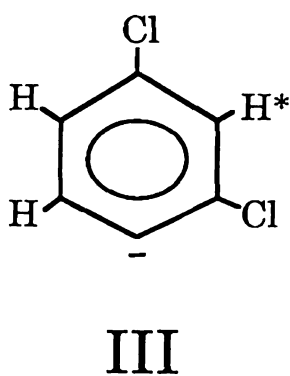
- Stru
- Stru
to be

Para-s

- Stru

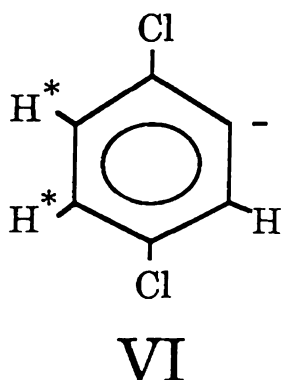
Ortho-substituted anions

- Both structure I & II allow all three hydrogens to be exchanged

Meta-substituted anions

* Non-exchangeable hydrogens

- Structure III and IV will exchange up to 2 H's
- Structure V will not react with D_2O , but may be isomerized to become II inside the ion source.

Para-substituted anion

* Non-exchangeable hydrogens

- Structure VI allows only one hydrogen to be exchanged

exchange

dichlorob

Ove

mechanis

than the

in each di

of a D₃-s

dichlorobe

dichlorobe

any D₃-su

wrong, or

which is o

the D₃-sul

can breach

remaining

of m-dichl

likelihood

about the

substantia

dichlorobe

explanation

anions of

dichlorobe

m-dichlorob

exchanged. The predominant ions in the product spectrum of p-dichlorobenzene are substituted with only one deuterium.

Overall, the observed results correlate well with the proposed mechanism. The predominant deuterium exchange observed is one less than the maximum number of hydrogen atoms between the chlorine atoms in each dichlorobenzene isomer. However, a peak representing about 12% of a D₃-substituted product is found in the product spectrum of m-dichlorobenzene, in reactions with the D₂O reagent. For the [M-1]⁻ of m-dichlorobenzene, the proposed mechanism would not allow the formation of any D₃-substituted product. Thus, either the proposed mechanism is wrong, or there is an additional process, specific to the m-dichlorobenzene, which is occurring. Two possible additional processes that could result in the D₃-substituted product are : a different substitution mechanism that can breach the intervening Cl atom located between the charge site and the remaining aromatic hydrogen, and a possible isomerization of structure V of m-dichlorobenzene to structure II of o-dichlorobenzene. Since the likelihood of the success of a Cl-breaching mechanism is expected to be about the same for both the anions of m- and p-dichlorobenzene, the substantially smaller D₃-substituted product peak observed for the p-dichlorobenzene favors the latter explanation. If the isomerization explanation is true, it appears that the degree of isomerization for the anions of p-dichlorobenzene is substantially lower than that of m-dichlorobenzene. Of all the anionic structures, the structure V anions of m-dichlorobenzene may be the most susceptible to isomerization.

B. Collis

The
resident i
pressure
deuterate
sequentia
the yield o
dichlorobe
minimum
deuterate
ions may r
required n
with D₂O,
sequential
highest de
with lowe
substituted
pressures.
replace the
high collis
substituted
involves the

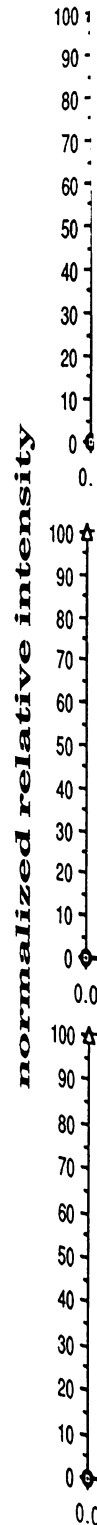
For
dependence
collision pr

B. Collision Pressure Dependence on Products of H/D Exchanges

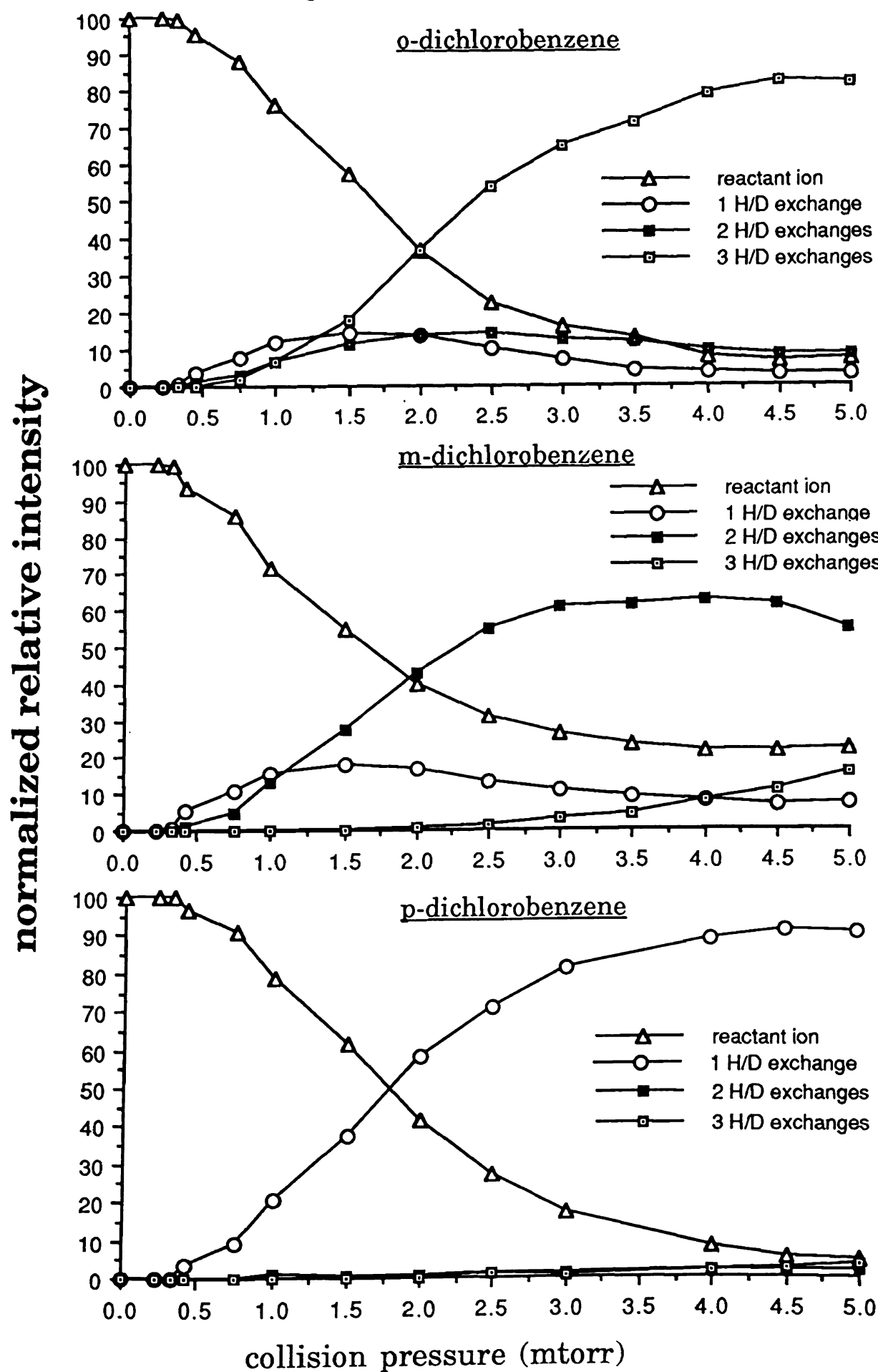
The number of collisions of an anion with a deuterated reagent while resident in Q2 is affected by the reagent gas pressure in Q2. A higher gas pressure allows a reactant ion to have a higher collision frequency with the deuterated reagent molecules. For ion products derived from a step-wise sequential process, increasing the total number of collisions can enhance the yield of the more highly substituted ion products. For the [M-1]⁻ ion of o-dichlorobenzene, the formation of D₃-substituted products requires a minimum of three reactive collisions of the initial reactant ion with deuterated molecules. At low collision pressures, D₃-substituted product ions may not be observed because the reactant ions may leave Q2 before the required number of ion-molecule collisions can occur. For H/D exchanges with D₂O, the collision pressure study shown in Figure 3-3 supports the sequential process depicted in our proposed mechanism. Products with the highest degree of deuterium substitution are not observed until products with lower degrees of deuterium substitution are formed. The D₁-substituted ions are the predominant products at very low collision pressures. As the collision pressure increases, higher substituted ions replace the less substituted ions as predominant products. At a sufficiently high collision pressure, most the anions of o-dichlorobenzene are fully substituted before they leave Q2. These data support a mechanism that involves the substitution of only one deuterium per reactive collision.

For the reactant ions from m-dichlorobenzene, the pressure-dependence plot shown in Figure 3-3 indicates that following an increase in collision pressure, the relative intensity of the reactant ions decreases; but

Figure 3-3 Plots for normalized relative product intensity vs collision pressure for H/D exchange reactions between the [M-1]⁻ ions of dichlorobenzene isomers and D₂O molecules.



Exchanges with deuterated water



the decre
Thereafter
total ion
result sug
reactant i
pressure c
proposed m
which the
contribution
about 20%
of all meta
anions iden
likely occur
a slow isom
also possible

The p
indicates th
formation of
the D₁-subst
substituted v
reactions be
relatively sm
dichlorobenz
likely to und
At the collisi

the decrease of the reactant ions levels off beginning at about 3.5 mtorr. Thereafter, the contribution of the reactant ions remains at about 25% of the total ion intensity, despite further increases in collision pressure. This result suggests that in the case of *m*-dichlorobenzene, about 25% of all reactant ions are unreactive with D_2O molecules under any collision pressure conditions. This lack of reactivity can be accounted for within our proposed mechanism, if about 25% of the reactant ions have structure V, in which the charge site is not adjacent to any aromatic hydrogens. Since the contribution of the D_3 -substituted products in the *m*-dichlorobenzene plot is about 20% at the collision pressure of 5.0 mtorr, we believe that at least 20% of all meta-substituted reactant ions undergo isomerization to reactant anions identical to those from *o*-dichlorobenzene. This isomerization most likely occurs in the source, possibly as part of the ionization process, though a slow isomerization of the ion, continuing through the ion lifetime in Q2 is also possible.

The pressure-dependence plot for *p*-dichlorobenzene (Figure 3-3) indicates that an increase in collision pressure enhances primarily the formation of the D_1 -substituted product. Even at a high collision pressure, the D_1 -substituted product remains predominant. This means that ions substituted with only one deuterium are generally the terminal products for reactions between D_2O and the *p*-dichlorobenzene $[M-1]^-$ ions. The relatively small contribution of the D_2 - and D_3 -substituted products in the *p*-dichlorobenzene plot suggests that the *p*-dichlorobenzene anions are less likely to undergo isomerization than are the anions of *m*-dichlorobenzene. At the collision pressure of 4.5 mtorr, over 90% of the *p*-dichlorobenzene

anions a
products.

Col

ND_3 reag

involving

formation

for both D

reagents

dichlorobe

H/D excha

ND_3 than

the H/D ex

than that

product for

similar exc

Altho

between dic

does not o

exchange m

3-3 & 3-4 b

reactant ion

proposed me

the percent

pressure as

product. A

anions are converted into the expected predominant D₁-substituted products.

Collision pressure studies were also performed on reactions with ND₃ reagent. The pressure-dependence plots for H/D exchange reactions involving ND₃ reagent are shown in Figure 3-4. The trends for the formation of different H/D exchange products for each isomer are the same for both D₂O and ND₃ reagents. The major difference between the two reagents are their relative reactivities towards the anions of the dichlorobenzene isomers for H/D exchange reactions. To achieve a specific H/D exchange product yield, the required collision pressure is higher for ND₃ than for D₂O. A comparison between Figures 3-3 and 3-4 suggests that the H/D exchange efficiency of D₂O molecules is about three times better than that of ND₃ molecules. The similarity in the trends of H/D exchange product formation for the two deuterated reagents supports the notion that similar exchange mechanism are followed by both reagents.

Although H/D exchange products are observed upon collision between dichlorobenzene anions and D₂O or ND₃ reagent, reaction probably does not occur on every single collision. Based on our proposed H/D exchange mechanism, we have generated plots similar to those of Figures 3-3 & 3-4 by computer simulation of H/D exchange reactions initiated by reactant ions of all the structures shown in Figure 3-2 and following our proposed mechanism. In these simulations, the number of collisions times the percent of collisions that are reactive are used instead of the collision pressure as the parameter to calculate the relative intensities for each ion product. A simulated collision-dependence plot for o-dichlorobenzene

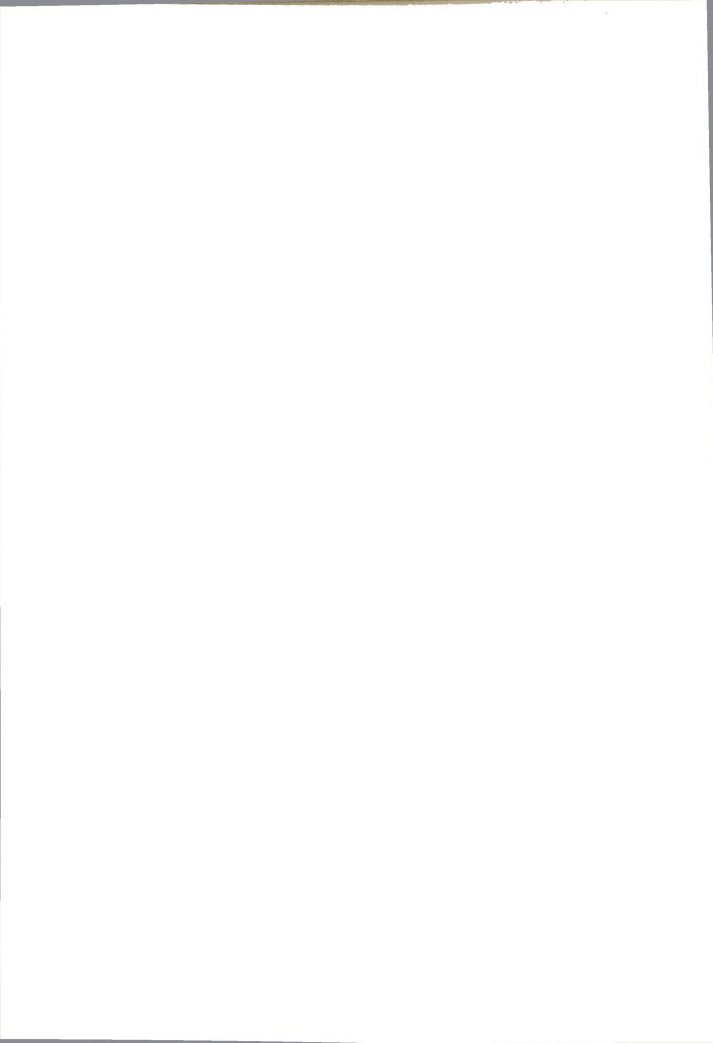
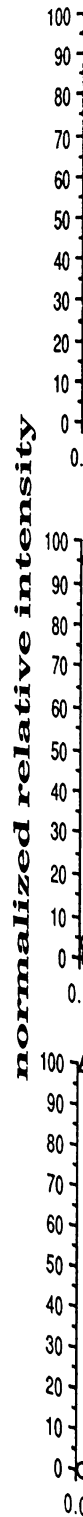
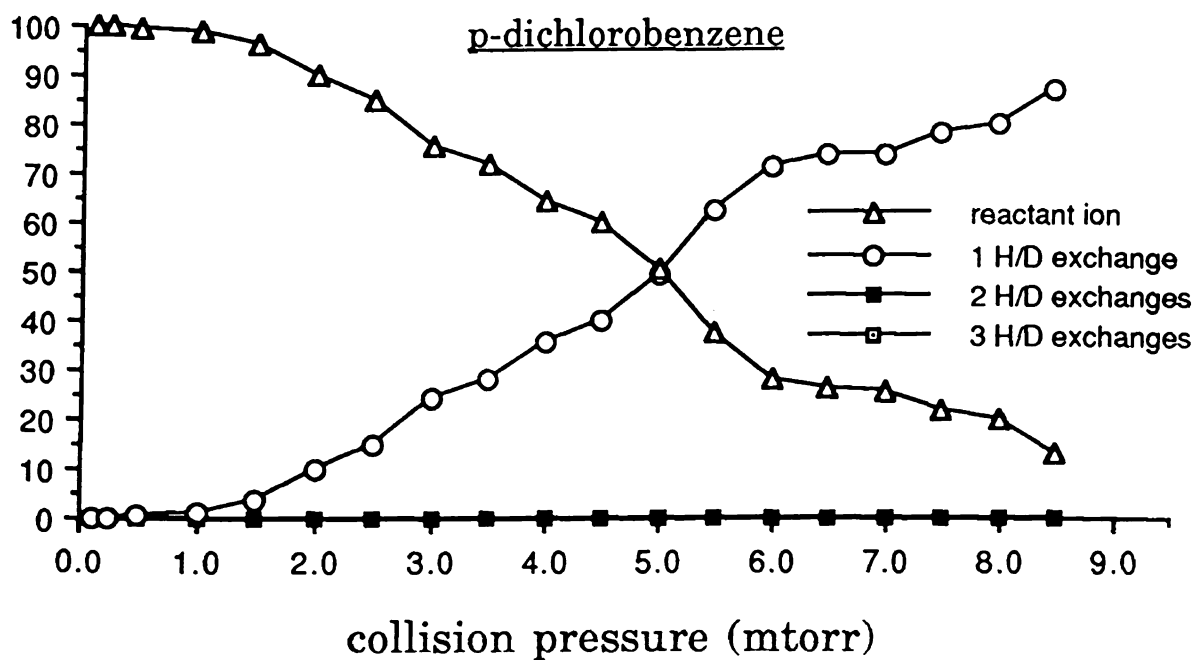
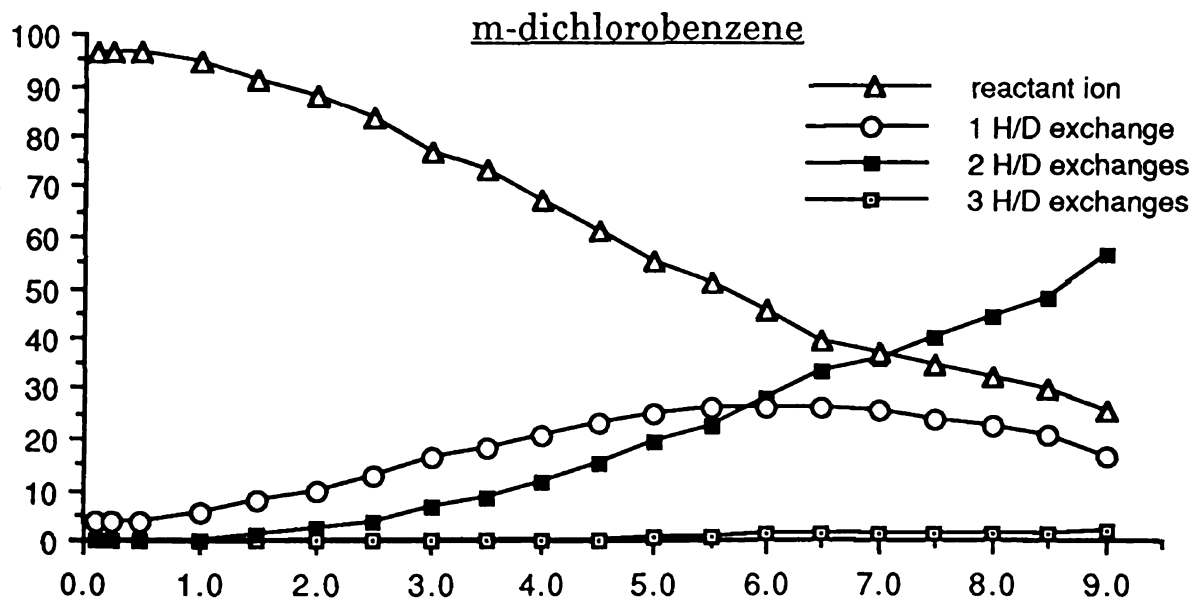
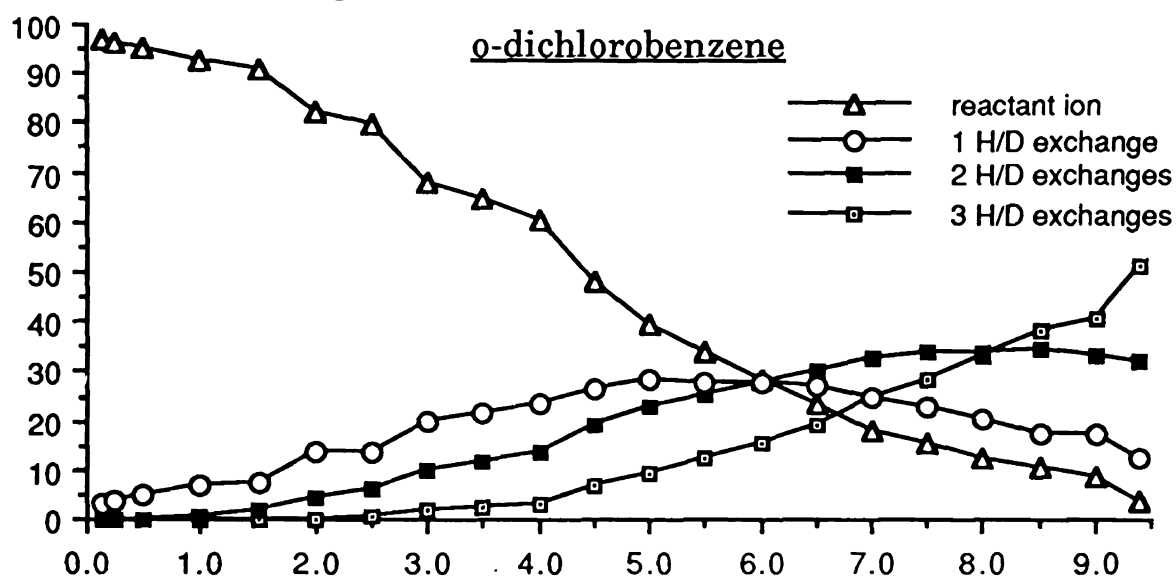


Figure 3-4 Plots for normalized relative product intensity vs collision pressure for H/D exchange reactions between the [M-1]⁻ ions of dichlorobenzene isomers and ND₃ molecules.



Exchanges with deuterated ammonia



anions h
reaction
structure
either a
assume
exchange
1 shown
is the sa
abundant
the num
no new r
is also as
for all io
Figure 3-
(top) reve
product-r
Continue
equivalen
of the de
reaction
number c
"average"

Fig
I anions
reactive
pathway

anions having the structure II configuration is shown in Figure 3-5. The reaction pathway used for the simulation is shown in Figure 3-6 for the structure II reactant ions. In this study, a reactive collision is defined as either a successful H/D exchange or D/D exchange. In our calculations, we assume that there is an equal chance for an ion to undergo either a H/D exchange or a D/D exchange where both are possible. For example, for ion 1 shown in Figure 3-6, the chance of its conversion into either ion 1' or ion 2 is the same. The collision-dependence plot of Figure 3-5 shows the relative abundance of the reactant and various product ion masses as a function of the number of reactive collisions. In making this plot, it was assumed that no new reactant was added, nor products removed over the time shown. It is also assumed that the percent of collisions that are reactive is the same for all ion structures. A comparison of the collision dependence plot of Figure 3-5 with the experimental pressure-dependence plot of Figure 3-3 (top) reveals that the zero input and output flux assumption made in the product-ratio calculations is not valid under our experimental conditions. Continued influx of reactant ions extends its high abundance into the equivalent of higher collision numbers and reduces the relative abundance of the deuterium-exchanged product ions. Departure of ions from the reaction chamber before they have actually undergone the "average" number of collisions yields finite values for their abundance seen at high "average" collision numbers.

Figure 3-7 shows a simulated collision-dependence plot for structure I anions of o-dichlorobenzene. These reactant ions require at least four reactive collisions to form the D₃-substituted products. The reaction pathway used for calculating the relative product intensity of the structure

Figure 3-5 A simulated collision-dependence plot that represents a composite of individual collision-product plots for different percentages of reactive collision. The simulation is based on the proposed H/D exchange reaction mechanism between the structure II of o-dichlorobenzene and D_2O or ND_3 molecules.

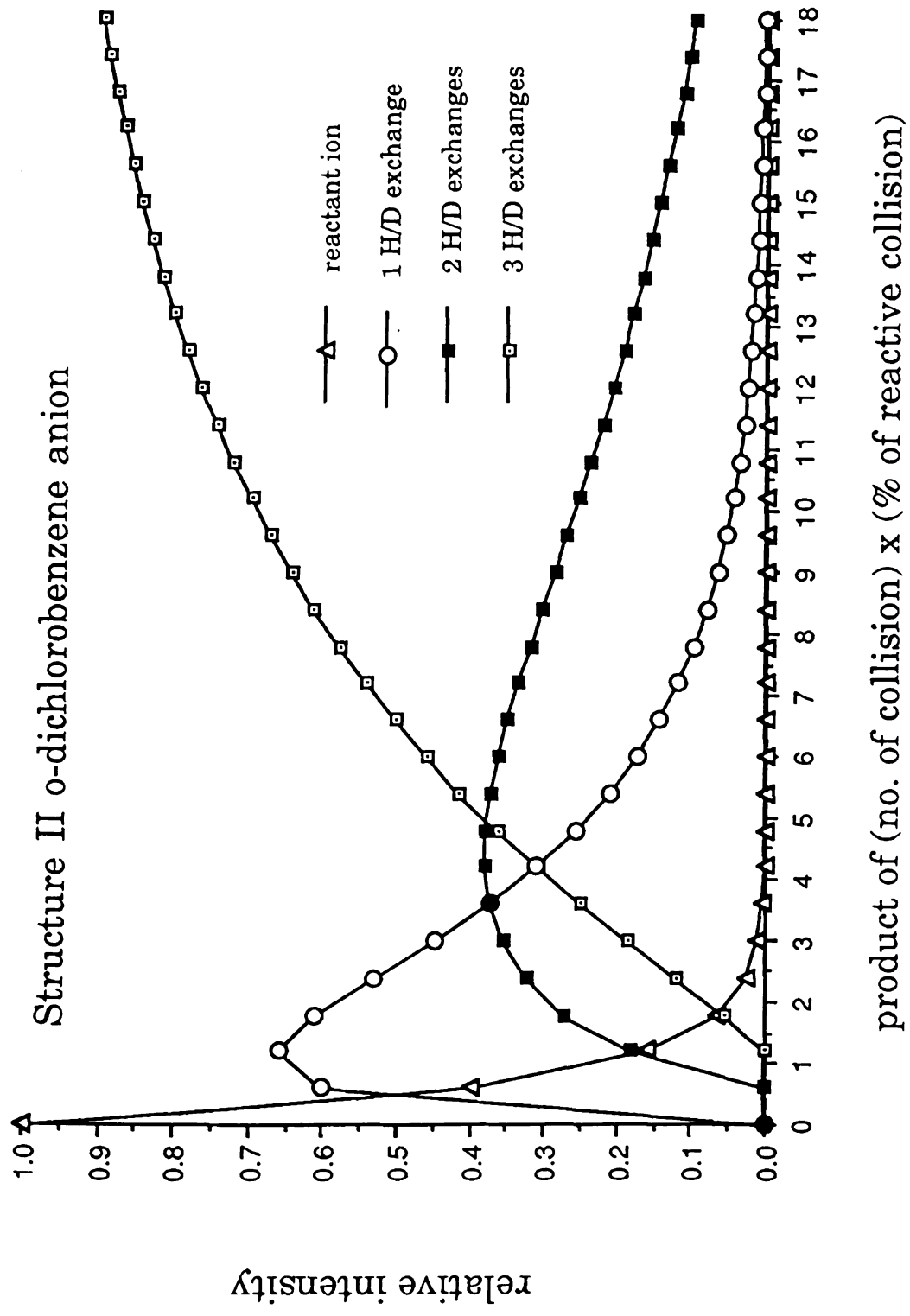




Figure 3-6 The reaction pathway for the structure II anions of o-dichlorobenzene upon reactive collisions with D_2O or ND_3 molecules.

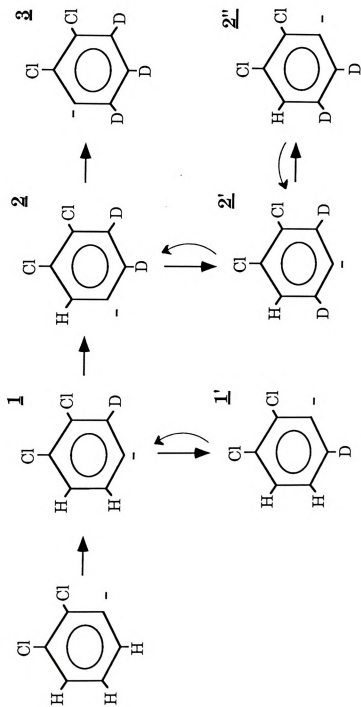
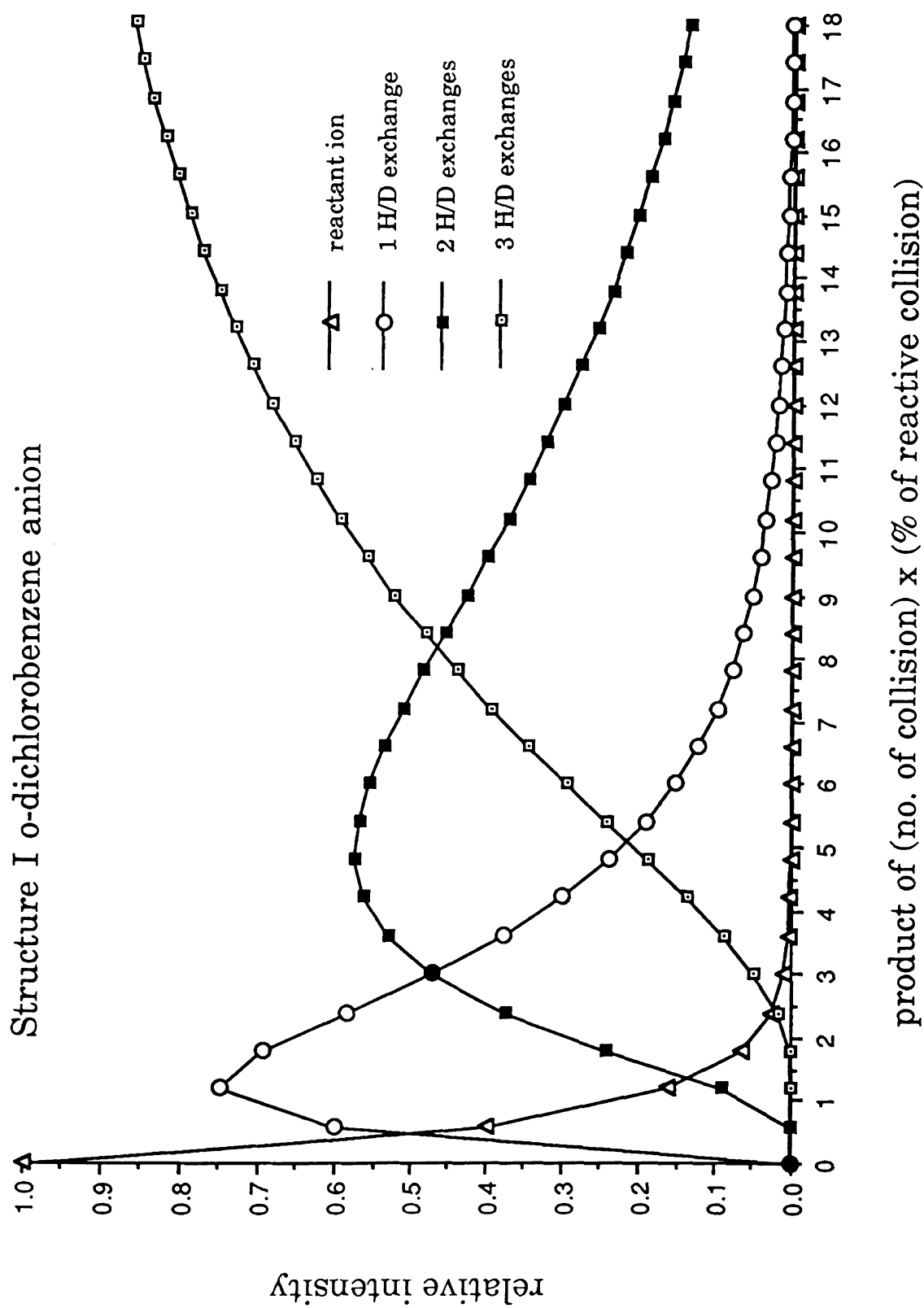


Figure 3-7 A simulated collision-dependence plot that represents a composite of individual collision-product plots for different percentages of reactive collision. The simulation is based on the proposed H/D exchange reaction mechanism between the structure I anions of o-dichlorobenzene and D₂O or ND₃ molecules.



I anion
structu
differen
the coll
and II
pressur
betwee
differen
clear pr

F
the th
contrib
V. The
structu
match
ions wi
50/50 r
reaction
to isom
simula
initiate
structu
shown
trends
in the
further

I anions is shown in Figure 3-8. Comparisons between plots obtained from structure I reactant ions and those with structure II show marked differences in the relative abundances of product ions at many points along the collision number axis. Ideally, one could choose between structures I and II based on the comparison of the collision-dependence plots with the pressure-dependence plot. Unfortunately, the differences in conditions between the experimental and simulated data are greater than the differences between the structure I and II simulations thus precluding a clear preference for either one.

For the anions of *m*-dichlorobenzene, our simulations assume that of the three meta-substituted ionic structures shown in Figure 3-2, the contribution of structure III is insignificant compared to structures IV and V. The reaction pathways for the formation of various products for both structure III and structure VI anions are shown in Figure 3-9. In order to match the experimental results, we further assume that the number of ions with structures IV and V are initially formed in the ion source in a 50/50 ratio. Before the anions enter the collision chamber for H/D exchange reactions, 50% of the initially formed structure V anions are also assumed to isomerize to become structure II anions. As such, the collisional simulations of the anions of *m*-dichlorobenzene are based on collisions initiated by a mixture of anions with three different structures (50% structure IV, 25% structure V and 25% structure II). The results are shown in Figure 3-10 as a collision-dependence plot. The product formation trends represented in this plot compare well with the similar trends shown in the experimental pressure-dependence plot of Figure 3-3 (middle). This further supports the isomerization explanation and the existence of the

Figure 3-8 The reaction pathway for the structure I anions of o-dichlorobenzene upon reactive collision with D_2O or ND_3 molecules.

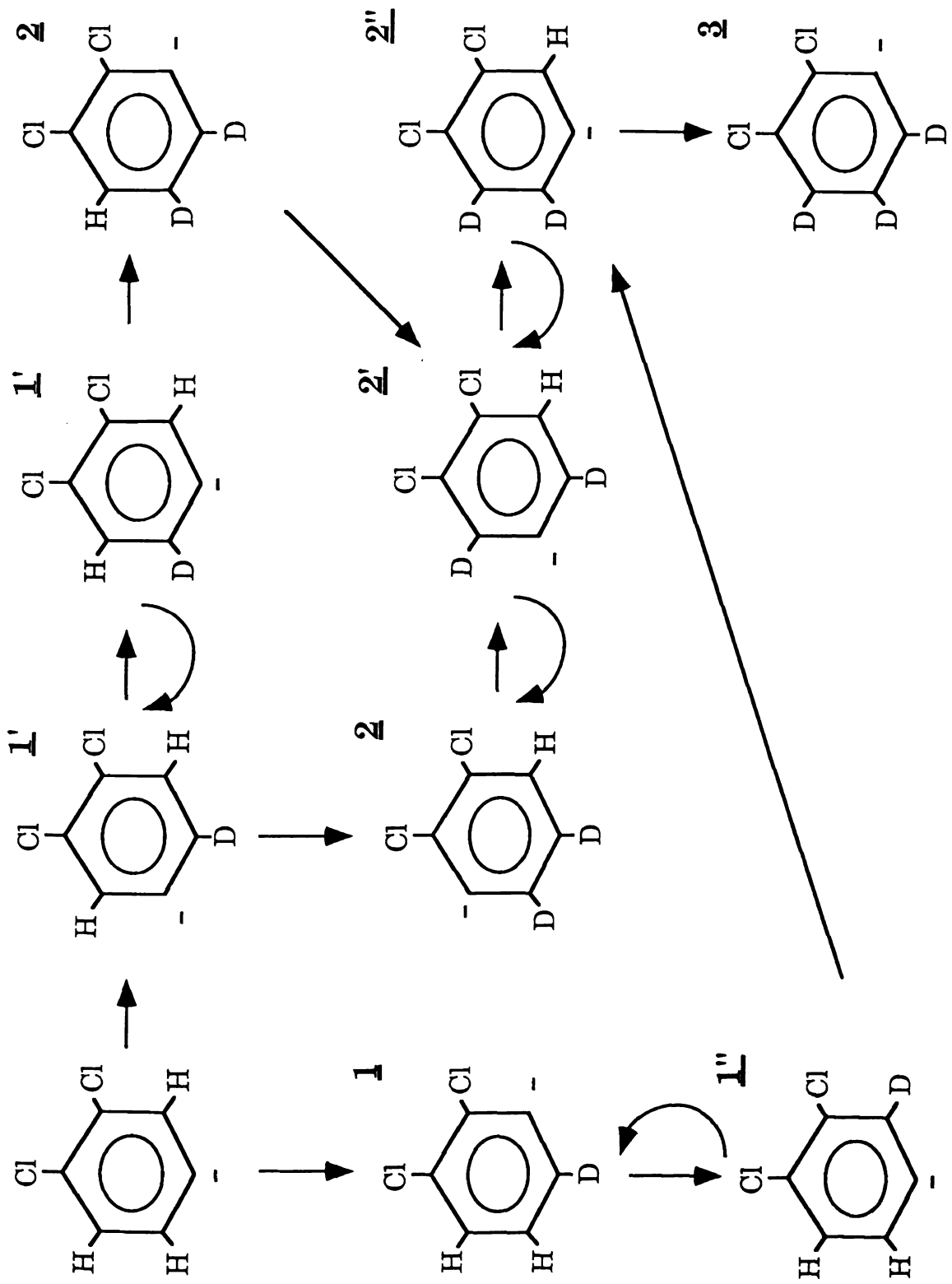




Figure 3-9 The reaction pathway for the structure III (top) and structure IV (bottom) anions of o-dichlorobenzene upon reactive collisions with D₂O or ND₃ molecules.

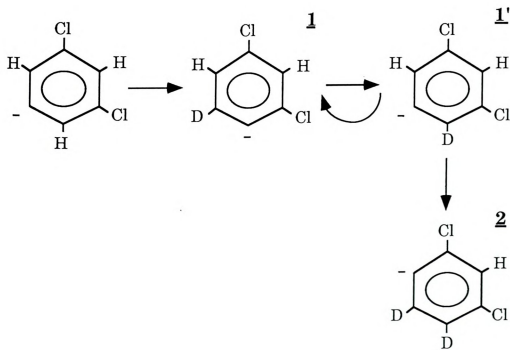
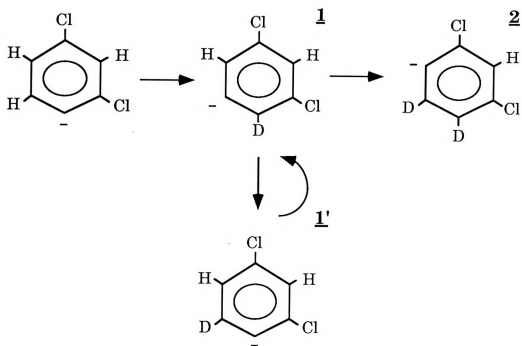


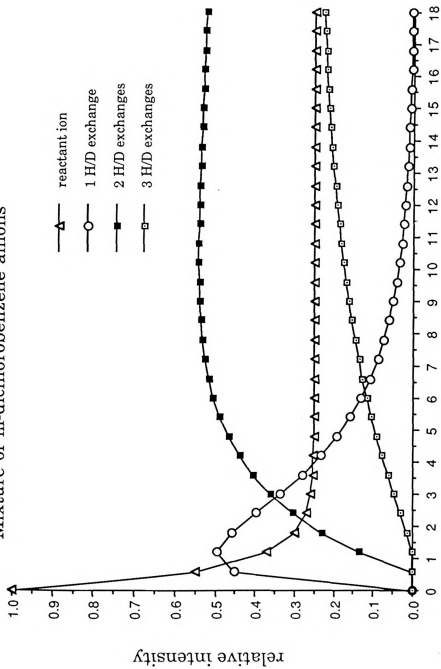


Figure 3-10 A simulated collision-dependence plot that represents a composite of individual collision-product plots for different percentages of reactive collision. The simulation is based on the proposed H/D exchange reaction mechanism between a mixture of different m-dichlorobenzene anions and D₂O or ND₃ molecules. The mixture of anions is assumed to contain 50% structure IV, 25% structure V and 25% structure II.

Mixture of m-dichlorobenzene anions

1.0
0.9

Mixture of m-dichlorobenzene anions



product of (no. of collision) x (% of reactive collision)

unreactive
individual
dichlorob

The
relatively
formation
collision-
reactant
the forma
comparab
plot of F
abundanc
different
the gener
obtained
data .

C. Reaction

We
proposed
anion to u
hydrogen
derived fr
tetrachlor

unreactive structure for the m-dichlorobenzene anions. (Simulated individual collision-product plots for the different ionic structures of dichlorobenzenes are shown in the Appendix.)

The collision simulations of the anions of p-dichlorobenzene are relatively simple because of the simplicity of the reaction pathway for the formation of the expected predominant products. Figure 3-11 shows the collision-dependence plot for the anions of p-dichlorobenzene, based on reactant ions with structure VI configuration. In this case, the trends for the formation of the predicted product shown in the simulated plot are comparable to those represented in the experimental pressure-dependence plot of Figure 3-3 (bottom). Overall, although the relative product abundances represented in all the simulated collision-dependence plots are different from those shown in the experimental pressure-dependence plots, the general trends for the formation of various H/D exchange products obtained from the simulated results are consistent with the experimental data .

C. Reactions with Other Aromatic Isomers

We have also used isomers of other chlorinated benzenes to test the proposed mechanism. According to the mechanism, in order for a [M-1]⁻ anion to undergo an H/D exchange, there must be at least one aromatic hydrogen adjacent to the charge site on the anion. For the [M-1]⁻ ions derived from 1,3,5-trichlorobenzene, 1,2,4,5-tetrachlorobenzene and 1,2,3,5-tetrachlorobenzene, none of the possible charge sites have any adjacent

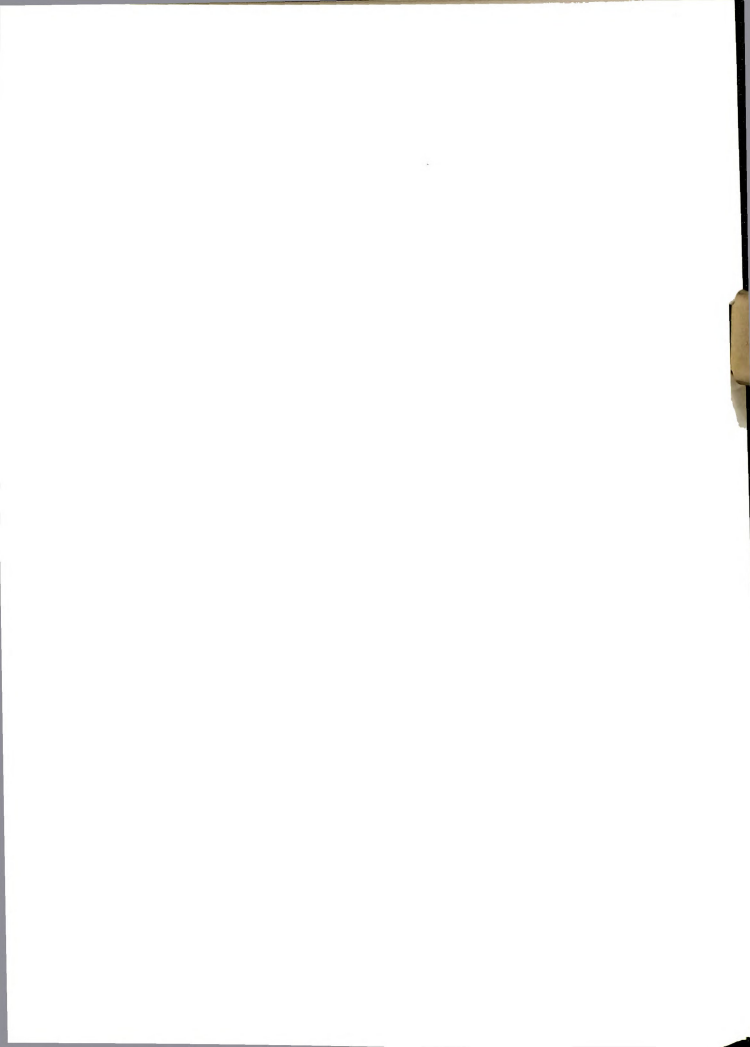
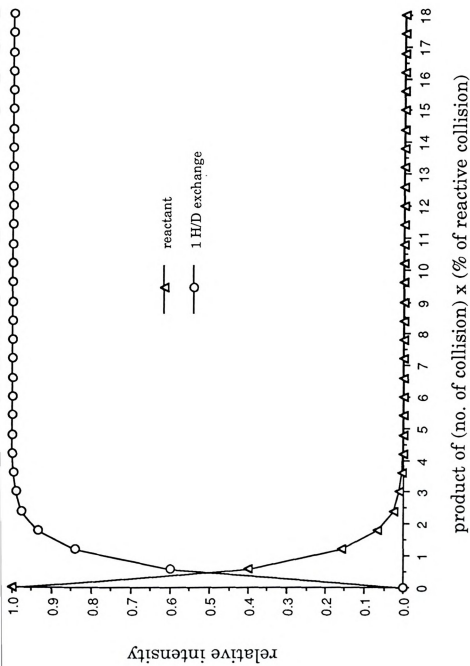


Figure 3-11 A simulated collision-dependence plot that represents a composite of individual collision-product plots for different percentages of reactive collision. The simulation is based on the proposed H/D exchange reaction mechanism between p-dichlorobenzene anions (structure VI) and D_2O or ND_3 molecules.



aron

reac

1,2,

tetra

pred

to th

shou

neut

chlo

1,2,3

the

with

mec

1,2,

desc

with

mos

diff

reac

be c

dem

ND,

exce

of t

diff

sam

aromatic hydrogens and no products resulting from the H/D exchange reactions are observed. The product spectra derived from the reaction of 1,2,3-trichlorobenzene, 1,2,4-trichlorobenzene and 1,2,3,4-tetrachlorobenzene anions with D_2O , shown in Figure 3-12, exhibit predominant exchanges of 2, 1 and 1 deuteriums, respectively. According to the proposed mechanism, reactant ions substituted with two deuteriums should be the predominant products for 1,2,3-trichlorobenzene because its neutral configuration contains three sequential hydrogens between the chlorine atoms. The original molecules of both 1,2,4-trichlorobenzene and 1,2,3,4-tetrachlorobenzene contain only two sequential hydrogens between the chlorine atoms, the predominant products should be ions substituted with only one deuterium. All the results are consistent with the proposed mechanism. The small D_2 -substituted peak in the product spectrum of 1,2,4-trichlorobenzene could be due to isomerization of the reactant ions as described earlier. Similar results are also observed for the same reactions with ND_3 reagent. The dramatic differences in the product patterns for most of the isomers studied suggest that these reactions are useful for differentiating isomers of chlorinated benzenes. The results of the reactions are summarized in Table 3-1. Since the number of chlorines can be determined from the masses of different $[M-1]^-$ ions, our studies clearly demonstrate that tandem MS along with H/D exchange reactions using ND_3 or D_2O as a reagent can positively identify all the chlorinated benzenes except two of the tetrachlorinated isomers. Product spectra similar to those of the dichlorobenzene isomers are also obtained for the isomers of difluorobenzene and bromochlorobenzene. This strongly suggests that the same mechanism is operating on all halogenated benzenes.



Figure 3-12 Product spectra for the tetra and trichlorobenzene isomers that produce H/D exchange ion products. The H/D exchange products are due to reactions between the $[M-1]^-$ ions of the isomers indicated and D_2O molecules. No H/D exchange products are observed for the other tetra and trichlorobenzene isomers.

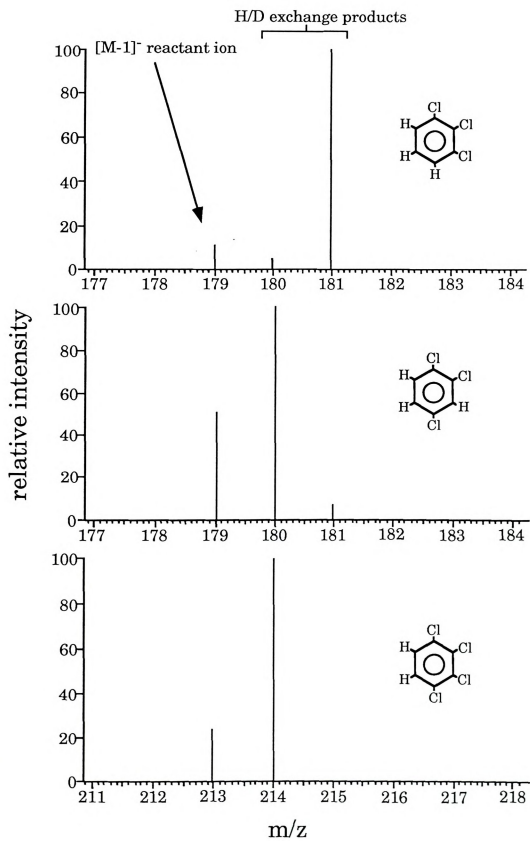


Table 3-1. Maximum number of H/D exchanges for the [M-1]⁻ ions of isomers of chlorinated benzenes (in cases of no isomerization).

type of Cl substitution	position of Cl on an aromatic ring	max. # of D substitution
mono	(no isomers)	
di	1,2	3
	1,3	2
	1,4	1
tri	1,2,3	2
	1,2,4	1
	1,3,5	0
tetra	1,2,3,4	1
	1,2,3,5	0
	1,2,4,5	0
penta	(no isomers)	

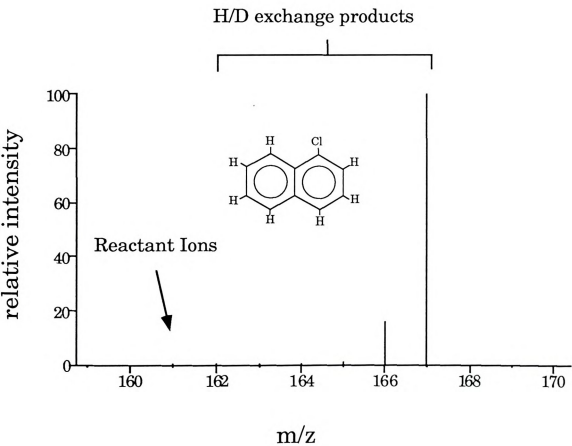
We have begun studies on larger chlorinated aromatic compounds. For a molecule made up of fused benzene rings, the initial negative charge site of an $[M-1]^-$ ion may be on a different ring than the exchanging aromatic hydrogens. For example, sequential H/D exchanges for aromatic hydrogens on different rings of a chlorinated naphthalene molecule require the formation of a six-membered-ring intermediate for relocation of the charge site from one ring to another assuming a similar mechanism is also operating. The product spectrum of 1-chloronaphthalene shown in Figure 3-13 indicates that reactant ions with all five hydrogens substituted with deuteriums are the predominant products. For the $[M-1]^-$ anion of 1-chloronaphthalene, substituting more than three hydrogens requires a mechanism of relocating the charge site from one ring to the other. In this case, the mechanism should involve the formation of a six-membered-ring intermediate, as shown in Scheme II. It is quite possible that the same mechanism may also apply to chlorinated compounds with more than two adjacent rings.

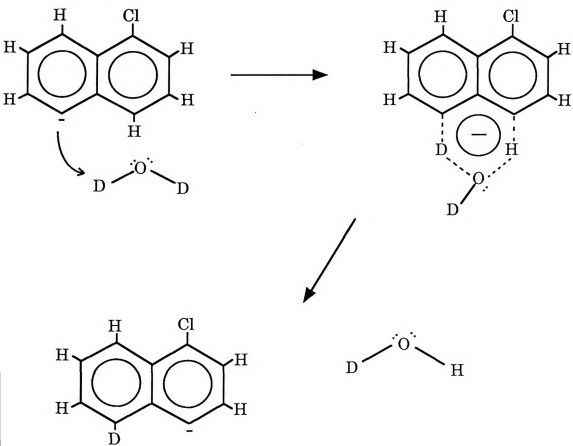
Conclusions

Using ND_3 or D_2O as a reagent, H/D exchange reactions are found to occur between the reagents and the $[M-1]^-$ ions of halogenated benzenes originating from molecules with two or more sequential aromatic hydrogens. The reactivity of D_2O is about three times that of ND_3 in the exchange reactions. A mechanism involving the formation of a five-membered-ring intermediate is consistent with the results derived from the



Figure 3-13 A product spectrum for H/D exchange reactions between the [M-1]⁻ ions of 1-chloronaphthalene and D₂O molecules. Reactant ions having five hydrogens substituted with deuteriums are the predominant products.





Scheme II

isomers of all the chlorinated benzenes in this study. The results obtained from the isomers of fluorinated and brominated benzenes strongly suggest that the same mechanism is also applicable to all halogenated benzenes. The number of deuterium substitutions for the predominant H/D exchange products is one less than the number of sequential aromatic hydrogens in the original molecules of chlorobenzene. It is possible that a mechanism involving a six-membered-ring intermediate is used for exchanging hydrogens across two or more fused benzene rings.

Computer simulations based on the proposed mechanism are also consistent with the product formation trends derived from the experimental results. The anions of *m*-dichlorobenzene are more susceptible to isomerization than the anions of *o*- and *p*-dichlorobenzene. A comparison among the experimental pressure-dependence plots suggests the existence of an unreactive structure for the anions of *m*-dichlorobenzene which is predicted by our proposed mechanism. For most chlorinated benzenes, we have demonstrated the potential of using H/D exchange reactions for isomeric differentiation.

References

1. Biemann, K, "Mass Spectrometry", McGraw-Hill, New York, 1962, Chapter 5.
2. Budzikiewicz, H.; Djerassi, C.; Williams, D. H. "Structure Elucidation of Natural Products by Mass Spectrometry", Vol 1, Holden-Day, San Francisco, CA, 1964, Chapter 2.
3. Harrison, A. G.; Heyer, B. G., *Can. J. Chem.* **1973**, *51*, 1265.
4. Inoue, M.; Wexler, S., *J. Am. Chem. Soc.* **1969**, *91*, 5730.

5. Bowers, M. T.; Elleman, D. D., *J. Am. Chem. Soc.* **1970**, *92*, 1847.
6. Hunt, D. F.; McEwen, C. N.; Upham, R. A., *Anal. Chem.* **1972**, *44*, 1292.
7. Hunt, D. F.; McEwen, C. N.; Upham, R. A., *Tetrahedron Lett.* **1971**, 4539.
8. Blum, W.; Schlumpf, E.; Liehr J. G.; Richter, W. J., *Tetrahedron Lett.* **1976**, 565.
9. Frieser, B. S.; Woodin, R. L.; Beauchamp, J. L., *J. Am. Chem. Soc.* **1975**, *97*, 6893.
10. Martinson, D. P.; Buttrill, S. E. Jr., *Org. Mass Spectrom.* **1976**, *11*, 762.
11. Stewart, J. H.; Shapiro, R. H.; DePuy, C. H.; Bierbaum, V. M., *J. Am. Chem. Soc.* **1977**, *99*, 7650.
12. Depuy, C. H.; Bierbaum, V. M.; King, G. K.; Shapiro, R. H., *J. Am. Chem. Soc.* **1978**, *100*, 2921.
13. Hunt, D. F.; Sethi, S. K. J., *Am. Chem. Soc.* **1980**, *102*, 6953.
14. DePuy, C. H.; Bierbaum, V. M., *Acc. Chem. Res.* **1981**, *14*, 146.
15. Chakel, J. A., Ph.D Dissertation, Michigan State University, East Lansing, MI, 1982.

CHAPTER 4

EXPLORATION OF ION-MOLECULE REACTIONS IN TANDEM MASS SPECTROMETRY FOR DISTINGUISHING ISOMERS OF POLYCHLORODIBENZO-P-DIOXINS

Introduction

Polychlorodibenzo-p-dioxins (PCDDs) are well known for the great concern over their occurrence in the environment. With the exception of the octachloro-congeners, all the very toxic PCDD congeners have chlorine substitution at the 2, 3, 7, and 8 positions (1). In particular, the extreme toxicity of 2,3,7,8-tetrachlorodibenzo-p-dioxin (TCDD) has attracted much attention. For many years, GC/MS has been a standard method for analyzing TCDDs in environmental samples. However, isomers of TCDD often give identical or similar spectra when traditional mass spectrometric techniques are used. Although the use of oxygen negative chemical ionization (NCI) has been shown to provide distinct mass spectra for 1,2,3,4-TCDD and 2,3,7,8-TCDD (2), there is no experimental evidence that the technique is capable of differentiating among 2:2 substituted TCDD isomers (3).

Chemical interferences are the major concerns in analyzing environmental samples for 2,3,7,8-TCDD. Prior to the mass spectrometric analysis of a sample, extensive chemical cleanup and high resolution gas chromatography (HRGC) are necessary in order to reduce interferences to

a reasonable level. Even so, high resolution mass spectrometry (HRMS) with resolving power of over 10,000 is needed to resolve TCDDs from many common chemical interferences (4,5). However, for modern double-focusing mass spectrometers, achievement of the requisite resolving power results in a substantial loss of instrument sensitivity. Tandem mass spectrometry (MS/MS) was first described by Chess and Gross (6) as a rapid-screening method for analyzing TCDD. The loss of COCL by the metastable decomposition of the molecular ion of TCDD was monitored for the analysis. Despite the fact that this technique offers speed and reduced interferences from PCBs, its overall specificity and sensitivity are significantly worse than GC/HRMS. Since then, a number of workers have explored the use of MS/MS coupled with GC or HRGC for analyzing TCDD (7-20). In most cases, the increased specificity of MS/MS was found to greatly reduce chemical interferences, which were seen in HRMS when real samples with complex matrices were analyzed (5,9,10,14,15,17,19,20).

Since the MS/MS techniques mentioned above monitor only the loss of COCL by collisionally induced dissociation (CID) of $[M]^+$, they are not isomer-specific for 2,3,7,8-TCDD. From analyzing fly ash samples, Buser and Rapper (21) found a complex isomeric mixture of at least 17 TCDDs. It was estimated that 2,3,7,8-TCDD was present at only 1% of the total TCDD amount in the samples. Although isomer-specific chromatographic methods have been developed for analyzing 2,3,7,8-TCDD (22-24), lengthy separations are still required. Kostianinen and Auriola (25,26) have recently employed the reaction between the $[M]^+$ of TCDDs and O_2 in the collision cell of a triple quadrupole system to distinguish 1,2,3,4-, 1,2,3,6/1,2,3,7,- and 2,3,7,8-TCDD isomers.

In this work, we have further explored the use of reactions between the $[M-1]$ ions of PCDDs and different neutral molecules for distinguishing the more toxic PCDDs from the less toxic ones.

Experimental

All the experiments were performed on the Finnigan TSQ-70B triple quadrupole mass spectrometer (TQMS). Samples were introduced into the Varian 3400 gas chromatograph (GC) which is directly interfaced with the TQMS. A capillary column was used (30 m, 0.25 mm i.d., SE-54 phase with 0.25 μm film thickness) to ensure the high purity of the PCDD samples entering the TQMS. The injection port of the GC was set at 250 °C under a splitless injection mode. The temperature was programmed from 150 °C to 300 °C at 15 °C/min. A transfer line directs the column into the ion source of the TQMS and was set at 275 °C. Helium was used as the carrier gas at a pressure of 15 psi. Each injection contained 1-2 μL of sample. The ion source temperature was held at 150 °C, the electron ionization at 70 eV, and the electron current at 200 μA . During ammonia chemical ionization (CI), a pressure of 1.5 torr was maintained throughout the experiments. During the MS/MS operations, ions extracted from the source were selected by the first quadrupole (Q1) of the TQMS to enter the second quadrupole (Q2) where neutral molecules were introduced for ion-molecule reactions. Product ions emerging from Q3 were then mass scanned to obtain the product mass spectra. A somewhat better than unit resolution was tuned for Q1 in order to ensure the purity of the selected parent ions, whereas Q3 was maintained at unit resolution. A collision energy of 3 eV (laboratory

energy as determined by the Q2 offset voltage) was used for all the experiments involving ion-molecule reactions. All the experiments were performed twice to test for consistency in the results. The replicates were compared for discrepancies in terms of relative peak ratios and the absence or presence of stray peaks. Duplicate runs consistently gave spectra that were approximately the same. The data shown come from one set of results rather than the average of the replicates.

All the PCDD congeners were purchased from AccuStandard, New Haven, CT, except for 1,3,6,8-TCDD and congeners with six chlorines or more, which were purchased from UltraScientific, North Kingstown, RI, and Cambridge Isotope Laboratories (CIL), Woburn, MA, respectively. All the congeners were obtained in toluene solution. All alcohols were obtained from Aldrich Chemical Company Inc., Milwaukee, WI. Deuterated water (99.5+% grade) was also purchased from CIL. Deuterated ammonia (99.5 atom %D) was obtained from MSD Isotopes, Montreal, Canada. All the chemicals were used without further purification.

Results and Discussion

A. Generation of Reactant Ions

A mixture of $\text{CH}_4/\text{N}_2\text{O}$ was used by Oehme and Kirschmer as a reagent to obtain the negative chemical ionization (NCI) mass spectra of TCDD isomers (27). Most of the isomers were found to form predominantly the $[\text{M}-1]^-$ ion due to direct or indirect deprotonation by OH^- . In our

experiments, NH_3 was used as the NCI reagent and is found to produce a higher $[\text{M}-1]^-$ yield than the previous study with $\text{CH}_4/\text{N}_2\text{O}$. The abundance of the $[\text{M}-1]^-$ relative to $[\text{M}]^-$ is related to the acidity of the $[\text{M}]^-$ ion which, in turn is affected by the positions of the chlorines. The NCI spectra obtained from the five TCDD isomers (Figure 4-1) in this study indicate that 2,3,7,8-TCDD has the highest acidity and therefore the highest relative abundance of $[\text{M}-1]^-$. The acidity of 1,2,3,4-TCDD is shown to be the lowest among the isomers by having only a very small peak at m/z 319. This is primarily due to the lack of electron-withdrawing Cl adjacent to H in 1,2,3,4-TCDD. For the rest of the TCDD isomers, the acidity is directly related to the number of hydrogens at the 1, 4, 6 and 9 positions. The lower acidity of 1,3,6,8-TCDD compared to 1,2,7,8-TCDD and 1,3,7,8-TCDD is the result of having only two hydrogens at the 1, 4, 6 and 9 positions instead of three. The trends observed in our study (summarized in Table 4-1) matches well with the results obtained by Oehme et al. (27) using $\text{CH}_4/\text{N}_2\text{O}$ as reagents. A similar trend is also observed for the lower chlorinated PCDD congeners. However, congeners containing five chlorines or more do not produce any $[\text{M}-1]^-$ ions under our CI conditions because of their relatively low acidity. For these higher chlorinated congeners, the predominant NCI product is $[\text{M}]^-$ (see examples in Figure 4-2), which is mainly due to the capture of a thermal electron inside the CI source.

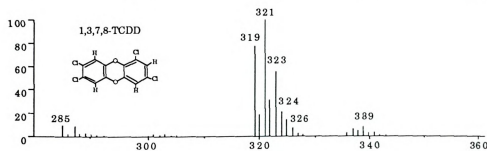
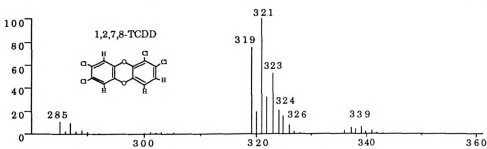
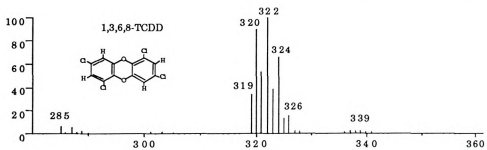
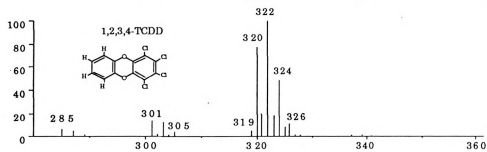
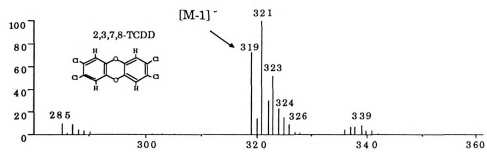
B. Reactions with D_2O

Hydrogen/deuterium (H/D) exchange reactions between the $[\text{M}-1]^-$ ions of chlorinated benzenes and D_2O were found to be distinctive for the three dichlorinated isomers as well as the others (28,29). Upon low energy



Figure 4-1 Mass spectra of TCDD isomers derived from negative chemical ionization (NCI) using ammonia as a reagent.

relative intensity



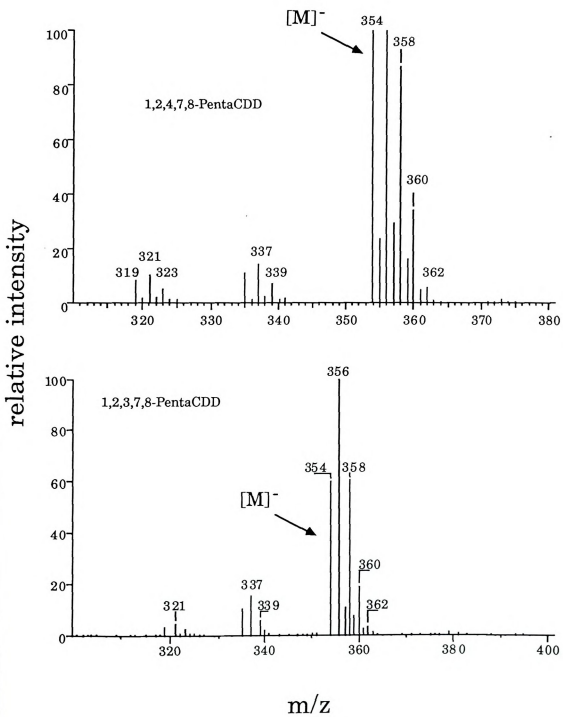
m/z

Table 4-1 Ion intensity ratios for m/z 319 and m/z 320 derived from the ammonia NCI mass spectra of the selected TCDD isomers.

<u>TCDD isomers</u>	<u>319/320</u>	<u># of Hs at the 1,4,6,9 positions</u>
2378	100/ 20	4
1278	100/ 27	3
1378	100/ 25	3
1368	100/ 210	2
1234	100/1700	2



Figure 4-2 Mass spectra of 1,2,4,7,8- and 1,2,3,7,8-pentachlorodibenzo-p-dioxin derived from negative chemical ionization (NCI) using ammonia as a reagent.



collisions with D_2O the $[M-1]^-$ ions of most PCDD congeners undergo H/D exchange reactions. The product mass spectra for the five TCDD isomers selected for this study are shown in Figure 4-3. The exact mass for TCDD was used to select the $[M-1]^-$ reactant ions by Q1. The $[M-1]^-$ ions selected contain only the ^{35}Cl and ^{12}C isotopes that corresponds to m/z 318.9 in the mass spectra. Product ions with deuterium substitutions are shown by peaks with one or more m/z units above those for the reactant ions. Only product ions indicative of one deuterium exchange are observed for 2,3,7,8-TCDD. This product pattern is unique among the five TCDD isomers. For both 1,2,7,8- and 1,3,7,8-TCDD, up to two hydrogens are found to be exchanged. No H/D exchange product was observed for 1,3,6,8-TCDD. However, product ions associated with exchange of three hydrogens in the anions of 1,2,3,4-TCDD are found.

In this study, the reactivity of the 1,2,3,4-TCDD anions is found to be significantly higher than the anions of the other selected isomers. In addition, there is also a strong tendency for 1,2,3,4-TCDD to form a $[M-1+D_2O]^-$ adduct which is completely absent from the spectra of the other isomers. Although the mechanism of the exchange reactions is not known at this point, we propose that the H/D exchange reaction is initiated by attack of the negative charge site on the $[M-1]^-$ ions of TCDD isomers to one of the two deuteriums of a D_2O molecule. Multiple deuterium substitutions on the reactant ion are then formed by sequential H/D exchange reactions with different D_2O molecules. Clearly, the number of exchangeable hydrogens of a TCDD $[M-1]^-$ ion depends on the positions of the chlorines. The formation of $[M-1+D_2O]^-$ and the relatively high H/D exchange reactivity for the anions of 1,2,3,4-TCDD are probably due to the absence of

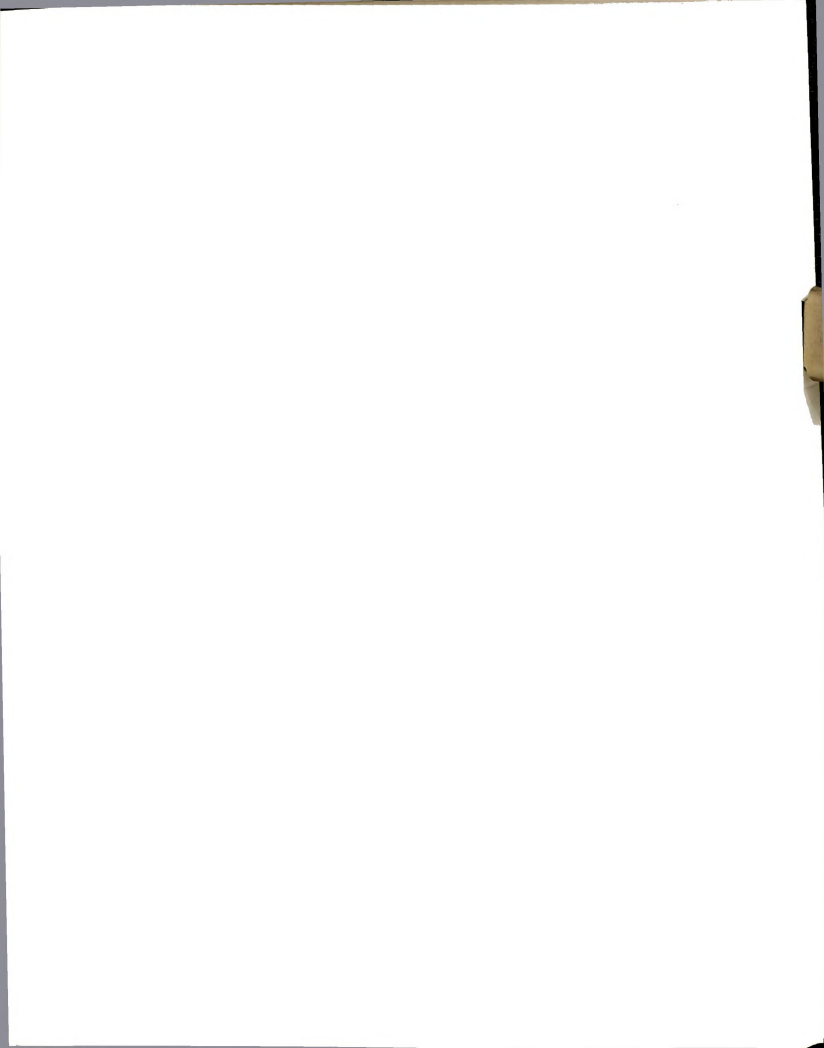
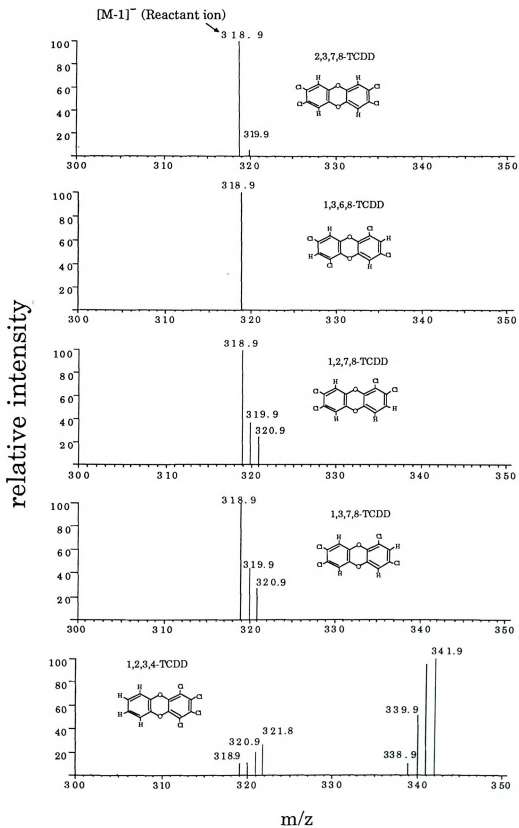


Figure 4-3 Product mass spectra of [M-1]⁻ ions derived from TCDD isomers upon hydrogen/deuterium (H/D) exchange reactions with D₂O. The exchange products are indicated by peaks at one or more m/z units above the reactant ions.



hindrance of Cls on the benzene ring where the charge is located. A complete understanding of the specificity of the H/D exchange reactions may not be known until a more comprehensive study involving all possible isomers is done. Nevertheless, this preliminary study has demonstrated that the H/D exchange reactions allow 2,3,7,8-TCDD to be differentiated from 1,2,7,8-, 1,3,7,8-, 1,3,6,8- and 1,2,3,4-TCDD. An attempt to observe H/D exchange reactions between D₂O and the [M]⁻ ions of PCDD's was unsuccessful; no exchange products were observed. Since the [M]⁻ ion is an odd-electron species, we conclude that the lone-pair electrons on the [M-1]⁻ ions are critical for the initiation of a fruitful H/D exchange reaction.

C. Reactions with Alcohols

When the [M-1]⁻ ions of PCDDs react with simple alcohols, ion-molecule adduct complexes, [M-1+alcohol]⁻, are formed. Under our experimental conditions, the reactivities of the TCDD isomers are found to be dependent on the positions of the Cls. The alcohols selected for this study, in ascending order of acidity, are methanol, ethanol, isopropanol and isobutanol. The abundances of the adducts formed for various combinations of alcohol and TCDD isomers are tabulated in Table 4-2.

The reactivity of 2,3,7,8-TCDD is shown to be consistently the lowest among the isomers studied. According to our NCI experiment and others (27), the acidity of 2,3,7,8-TCDD is the highest among all the TCDDs. This means that the [M-1]⁻ of 2,3,7,8-TCDD is the weakest base of all the anions of TCDDs. For 2,3,7,8-TCDD, there is only one possible site for the negative charge of the [M-1]⁻ ion because the positions of all four hydrogens on the

Table 4-2 Percentages of the [M-1+alcohol]- adducts based on 100% of the [M-1]- reactants.

	TCDD isomers	methanol	ethanol	isopropanol	isobutanol
2378	7	17	42	0.5	
1368	20	29	50	2.0	
1278	34	55	73	2.5	
1378	46	74	100	2.7	
1234	410	450	6600	3.0	

molecule are equivalent. It is conceivable that adduct complexes are formed by interactions between the lone-pair electrons on the charge site and the H of the OH functional group of the alcohol molecules. This explanation is supported by a significant isotopic effect observed when alcohols with an OD functionality are used. The charge site on the $[M-1]^-$ of 2,3,7,8-TCDD is less likely to attack a proton because of its weaker basicity. The reactions with alcohols were also extended to the $[M-1]^-$ ions of 2,3- and 2,7-dichlorodibenzo-p-dioxin (DCDD). Overall, the reactivities of 2,3-DCDD are also consistently lower than those of 2,7-DCDD. In the case of reactions with methanol, the ratio of $[M-1+alcohol]^- : [M-1]^-$ for 2,7-DCDD is found to be about 10 times that of 2,3-TCDD. The differences in reactivities for the two isomers coincide with the fact that while the structure of 2,7-DCDD allows four hydrogens to be adjacent to the chlorines, only the two hydrogens at the 1 and 4 positions of 2,3-DCDD are adjacent to the chlorines. This means that most of the $[M-1]^-$ ions of 2,3-DCDD would have a charge site at the location identical to that of a 2,3,7,8-TCDD $[M-1]^-$ ion. The results from these two DCDD isomers appear to substantiate the above explanation on the differences in TCDD reactivities with the alcohol molecules.

For the alcohol reagents, an increase in reactivity is observed when the acidity of the alcohol is increased from that of methanol to that of isopropanol. This is exactly what is expected for an acid/base reaction. The dramatic decrease in reactivity for isobutanol is probably due to the steric hindrance of its structure. For the higher chlorinated PCDD congeners, reactions between the $[M]^-$ ions and alcohol molecules do not produce any

products. The lack of the lone-pair electrons on the $[M]^-$ ions apparently do not allow the formation of the complexes.

D. Reactions with O_2

Oxygen molecules were also used as a reagent to react with the $[M]^-$ ions of PCDDs. At a collision pressure of 0.8 mtorr and collision offset energy of 2.8 eV, reactions between the $[M]^-$ of 1,2,3,4-TCDD and O_2 produce $[M-Cl+O]^-$ ions from oxygen/chlorine (O/Cl) exchanges. Although the ratio of $[M-Cl+O]^- : [M]^-$ for 1,2,3,4-TCDD is found to be about 3:1, the O/Cl exchange product is not observed for the $[M]^-$ ions from 2,3,7,8-, 1,3,6,8-, 1,2,7,8- and 1,3,7,8-TCDD under our experimental conditions. It is necessary to point out that the $[M]^-$ ions selected for the 2:2 substituted TCDD isomers also include the ^{13}C isotope of the $[M-1]^-$ ions, which could not be separated by the first quadrupole mass filter. However, this should have little or no effect on the formation of any product ions resulted from the $[M]^-$ ions because no reaction was observed when the $[M-1]^-$ ions of PCDDs were reacted with O_2 . The $[M-Cl+O]^-$ ions are obtained from the $[M]^-$ ions of the penta-, hexa- and hepta-chlorinated PCDD congeners. Although others (25,26) have demonstrated the potential of using O_2 as a reagent to differentiate 2,3,7,8-TCDD from 1:3 substituted TCDD isomers, we could not produce experimental evidence to support the potential usefulness of using O_2 to differentiate 2,3,7,8-TCDD from the other 2:2 substituted TCDD isomers. More experiments are needed in order to determine the mechanism of the O/Cl exchange on the $[M]^-$ ions of PCDDs, and thus the reason for the apparent lack of reactivity of the 2:2 substituted TCDDs.

Conclusions

Ion-molecule reactions occurring in the center stage of a triple quadrupole mass spectrometer are feasible options for distinguishing the more toxic isomers of PCDDs from the less toxic ones. For reactions involving the formation of $[M-1+\text{alcohol}]^-$ adducts, the reactivity of the $[M-1]^-$ of 2,3,7,8-TCDD is consistently the lowest among the five TCDD isomers studied. Of the four simple alcohols selected for these reactions, methanol appears to allow 2,3,7,8-TCDD to be differentiated to a greater degree from the other less toxic isomers. The H/D exchange product patterns obtained from reactions between the $[M-1]^-$ ions of TCDD isomers and D_2O permit 2,3,7,8-TCDD to be differentiated from 1,3,6,8-, 1,2,7,8-, 1,3,7,8- and 1,2,3,4-TCDD. At this stage, it is not known whether the H/D exchange reactions are useful to differentiate 2,3,7,8-TCDD from all other TCDD isomers. A more comprehensive study involving all possible TCDD isomers is needed in order to gain additional insight into the mechanism of these reactions, and verify their applicability as analytical techniques.

The unique negative charge location on the $[M-1]^-$ of 2,3,7,8-TCDD may be further utilized for a continuous search of ion-molecule reactions which are truly specific for 2,3,7,8-TCDD. With the selectivity of MS/MS, the added specificity provided by ion-molecule reactions may reduce sample cleanup and shorten GC separation time for 2,3,7,8-TCDD analysis.

References

1. Clement, R. E.; Tosine, H. M., *Mass Spectrom. Rev.* **1988**, 7, 593.
2. Hass, J. R.; Friesen, M. D.; Hoffman, M. K., *Org. Mass Spectrom.* **1979**, 14, 9.
3. Mitchum, R. K.; Korfmacher, W. A.; Moler, G. F.; Stalling, D. L., *Anal. Chem.* **1982**, 54, 719.
4. Tondeur, Y.; Beckert, W. F.; Billets, S.; Mitchum, R. K., *Chemosphere* **1989**, 18, 119.
5. Tondeur, Y.; Niederhut, W. E.; Campana, J. E.; Missler, S. R., *Biomed. Environ. Mass Spectrom.* **1987**, 14, 443.
6. Chess, E. K.; Gross, M. L., *Anal. Chem.* **1980**, 52, 2057.
7. Shushan, B.; Fulford, J. E.; Thomson, B. A.; Davidson, W. R.; Danlewych, L. M.; Ngo, A.; Nacson, S.; Taner, S. D., *Int. J. Mass Spectrom. Ion Physics* **1983**, 46, 225.
8. Shushan, B.; Tanner, S. D.; Clement, R. E.; Bobbie, B., *Chemosphere* **1985**, 14, 843.
9. Clement, R. E.; Bobbie, B.; Taguchi, V., *Chemosphere* **1986**, 15, 1147.
10. Charles, M. J.; Green, B.; Tondeur, Y.; Hass, J. R., *Chemosphere* **1989**, 19, 51.
11. McCurvin, D. M. A.; Schellenberg, D. H.; Clement, R. E.; Taguchi, V. Y., *Chemosphere* **1989**, 19, 201.
12. McCurvin, D. M. A.; Clement, R. E.; Taguchi, V. Y.; Reiner, E. J.; Schellenberg, D. H.; Bobbie, B. A., *Chemosphere* **1989**, 19, 205.

13. Fraisse, D.; Gonnord, M. F.; Becchi, M., *Rapid Commun. Mass Spectrom.* **1989**, 3(3), 79.
14. De Jong, A. P. J. M.; Liem, A. K. D.; Den Boer, A. C.; Van Der Heeft, E.; Marsman, J. A.; Van De Werken, G.; Wegman, R. C. C., *Chemosphere* **1989**, 19, 59.
15. Moore, C.; Moncur, J.; Jones, D.; Wright, B., *Rapid Commun. Mass Spectrom.* **1990**, 4(10), 418.
16. Reiner, E. J.; Schellenberg, D. H. Taguchi, V. Y.; Mercer, R. S.; Townsend, J. A.; Thompson, T. S.; Clement, R. E., *Chemosphere* **1990**, 20, 1385.
17. Charles, M. J.; Tondeur, Y., *Environ. Sci. Technol.* **1990**, 24, 1856.
18. Charles, M. J.; Marbury, G. D., *Anal. Chem.* **1991**, 63, 713.
19. Iida, J.; Takeda, T.; Takasuga, T.; Moncur, J.; Ireland, P.; Wright, B., *J. High Res. Chromatogr.* **1991**, 14(2) 103.
20. Reiner, E. J.; Schellenberg, D. H.; Taguchi, V. Y., *Environ. Sci. Technol.* **1991**, 25, 110.
21. Buser, H. R.; Rappe, C., *Anal. Chem.* **1980**, 52, 2257.
22. O'Keefe, P. W.; Smith, R.; Meyer, C.; Hilker, D.; Aldous, K.; Jelus-Tyror, B., *J. Chromatogr.* **1982**, 242, 305.
- (23) Naikwadi, K. P.; Karasek, F. W., *Chemosphere* **1990**, 20, 1379.
24. Tiernan, T. O.; Garrett, J. H.; Solch, J. G.; Harden, L. A.; Lautamo, R. M.; Freeman, R. R., *Chemosphere* **1990**, 20, 1371.
25. Kostiainen, R.; Auriola, S., *Rapid Commun. Mass Spectrom.* **1988**, 2, 135.

26. Kostiainen, R.; Auriola, S., *Org. Mass Spectrom.* **1990**, 25, 255.
27. Oehme, M.; Kirschmer, P., *Anal. Chem.* **1984**, 56, 2754.
28. Chakel, J. A., Ph.D Dissertation, Michigan State University 1982.
29. Chan, S.; Enke, C. G., paper submitted for publication.

CHAPTER 5

IMPROVEMENT TO THE DETECTION OF LOW-ENERGY ION PRODUCTS IN A TRIPLE QUADRUPOLE MASS SPECTROMETER - A THEORETICAL CONSIDERATION

Introduction

Ion-molecule reactions occurring at thermal or near thermal energies are often very sensitive to structural differences. Ion products formed by these reactions possess little or no kinetic energy. Unfortunately, the lack of kinetic energy of the ion products creates a challenge for their detection. In a triple quadrupole mass spectrometer (TQMS), the detection of these ions in the second quadrupole collision chamber (Q2) depends on the ability of the ions to reach the detector. Without a guiding field, many of these ions would eventually be lost from the reaction chamber in directions other than towards the detector. In order to increase the detection efficiency of these ions, a standard technique uses a withdrawing potential applied between Q2 and the third quadrupole (Q3) to extract the low-energy and thermalized ions from Q2 for mass analysis by Q3. However, for thermalized ions, ion currents are limited by the rate of diffusion along the axis of Q2 from the point where their axial kinetic energy becomes zero until they reach the drawout potential field that extends only a short distance into the reaction chamber. This chapter will describe novel designs of the second quadrupole for facilitating the movement of low-energy ion products towards the detector.

Where the study of the thermochemistry of ion-molecule reactions is not the main goal, relatively high collision pressures (≈ 4 mtorr) of neutral molecules can be introduced into Q2 in order to assure an abundance of neutral molecules for reactions. Under high pressure conditions, ions transmitted into the reaction chamber may have multiple collisions with the neutral molecules before reaching the exit of Q2. Such reaction conditions increase the rate of ion-molecule reactions and thus the yield of products. Furthermore, multiple collision conditions have a stabilization effect on products and intermediates that would otherwise be unstable and undetectable under single collision conditions (1). A novel ion trapping technique (2,3) has been developed at Michigan State University by Dr. Watson's and Dr. Enke's research groups for enhancing multiple collision conditions even at low collision pressures. The detection of reaction products is improved essentially by a net gain of product signals due to the presence of more product ions.

The novel ion trapping technique requires no hardware modification to a traditional TQMS instrument. The so-called trap-and-pulse mode of this technique involves the use of an extraction lens (EL) that is placed between Q2 and Q3 as an ion trapping and pulsing device. Usually, +100V is applied to the extraction lens for trapping positive ions and -100V for negative ions. In this method, parent ions of a selected mass are continuously transmitted into Q2 for ion-molecule reactions while the trapping potential is applied to EL. After a certain length of time, a pulsing potential, which is opposite in polarity to the trapping potential, is applied to extract a fraction of the trapped ions from Q2 for detection. Ion trapping time can be varied to maximize ion signals. Normally, 90% of the

maximum intensity can be obtained within 100 ms of trapping time. This method is necessarily limited to collecting ions of a single nominal mass-to-charge value per pulse because the millisecond duration of the ion pulse is too short for full range Q3 mass scanning. Nevertheless, significant improvements in signal-to-noise ratios have been obtained over those in the conventional data collection method. The greater residence time of ions in Q2 made possible by extending the trap time revealed some reaction products not observed by continuous product extraction.

Designs for the Second Quadrupole Collision Chamber of a TQMS Instrument

The extraction lens used in both the standard and the trap-and-pulse methods can only extract ions that are very near the exit of Q2. A high percentage of the thermalized ions still stay in Q2 without being detected as products. Figure 5-1 shows a potential contour diagram for the standard ion extraction design based on calculations using SIMION (4), a computer program for ion optics calculations. This diagram indicates that the 100 V extraction potential applied to the lens at the end of the collision chamber can only penetrate a very short distance into Q2. Most ion products formed in Q2 are not directly affected by the extraction potential. An idea to assist the thermalized ions to move towards the exit of Q2 is to create a longitudinal electric field along the path of the ions towards that region. In this way, ions can experience a continuous pushing force in the direction of the Q2 exit. This is particularly important for ions that are heavily surrounded by neutral molecules under high collision pressure conditions.

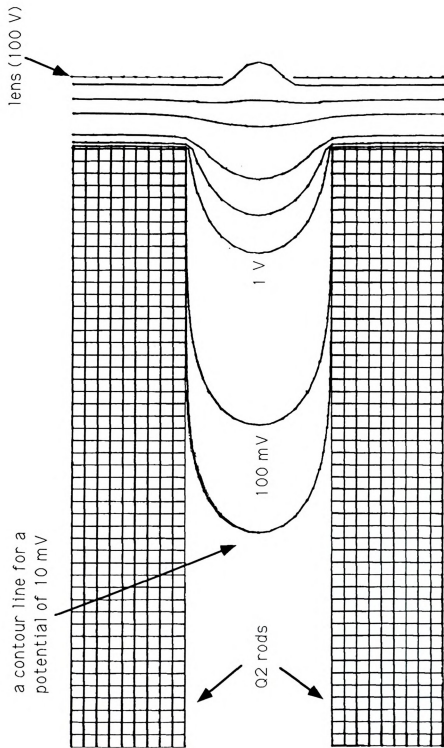


Figure 5-1 A potential contour diagram for the extraction lens design.

The first idea for creating such a longitudinal electric field is to modify the design of the Q2 rods in such a way that the rods are made of stainless steel segments which are separated by thin layers of non-conductive Teflon (Figure 5-2). Resistors are connected to each segment to divide the total voltage along the rod into equal steps for each segment. If a potential difference is applied to the ends of each rod, a potential field gradient is created in space along the ion path of Q2. Theoretically, for a true smooth continuous potential field gradient, an infinite number of infinitesimally thin segments are needed in each rod. If the rods are made of too few segments, the gradient created along the Q2 ion path would be in a step-jump fashion. Using SIMION calculations, the potential contour diagrams for the designs of 6-, 11-, 21-, 26- and 35-segmented Q2 rods have been generated. The configurations used for the calculations are shown in Figure 5-3 through Figure 5-7. In this case, all the calculations are based on a 5-V potential difference applied to the ends of a 20-cm Q2 assembly. Based on data extracted from the potential contour diagrams, plots of longitudinal potential as a function of spatial distance into Q2 for the 6-, 11-, 21-, 26- and 35-segmented designs are created and shown in Figure 5-8. The 6- and 11-segmented designs give distinct potential plateaus in the space along the ion path of Q2. At the region of a potential plateau, ions would experience only a very slight potential gradient. These ions may still stay in the collision chamber if the forward momenta of the ions are too small to allow their arrival to the next potential gradient regions. Since the potential gradient along the ion path of Q2 is related to the change of potential as a function of changing spatial distance inside Q2, plots that represent the 1st derivative of the results of Figure 5-8 would give a direct representation for the smoothness of the potential gradients for each

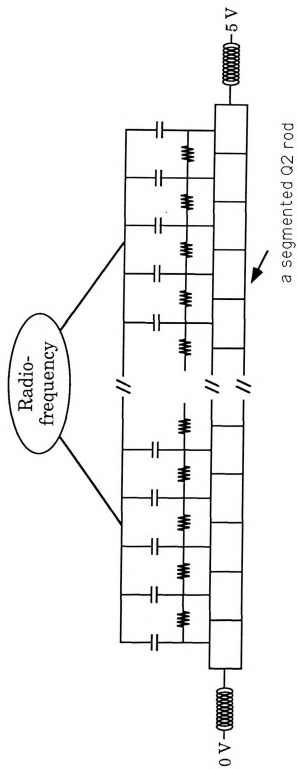


Figure 5-2 A design of segmenting the second quadrupole rods

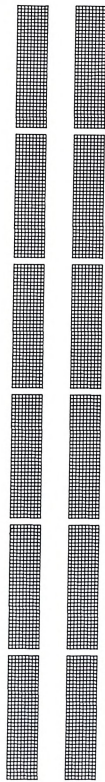


Figure 5-3 The configuration of a potential contour diagram for a Q2 made of 6-segmented rods with a 5-V potential applied.

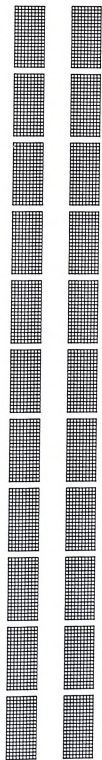


Figure 5-4 The configuration of a potential contour diagram for a Q2 made of 11-segmented rods with a 5-V potential applied.

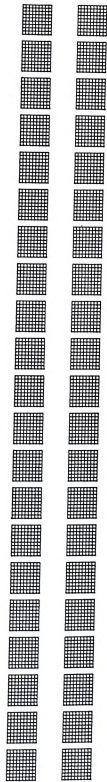


Figure 5-5 The configuration of a potential contour diagram for a Q2 made of 21-segmented rods with a 5-V potential applied.

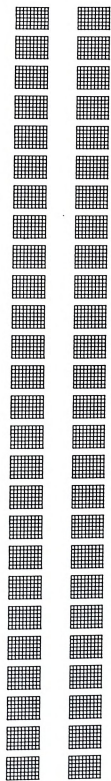


Figure 5-6 The configuration of a potential contour diagram for a Q2 made of 26-segmented rods with a 5-V potential applied.

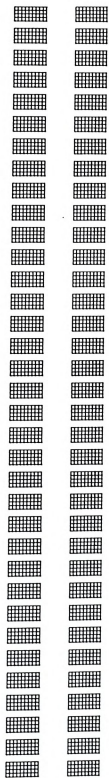
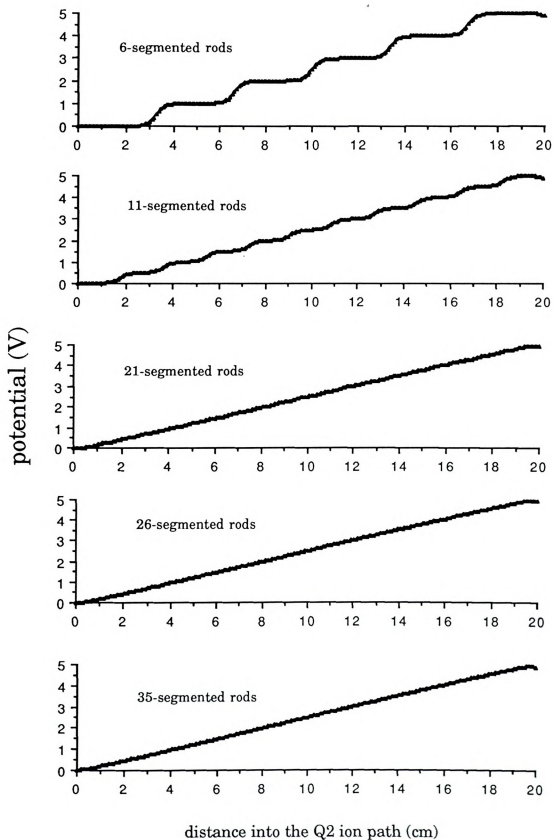


Figure 5-7 The configuration of a potential contour diagram for a Q2 made of 35-segmented rods with a 5-V potential applied.



Figure 5-8 Potentials along the ion path for the designs of Q2 made of different numbers of segments when a potential difference of 5-V is applied.



design. The potential gradient plots shown in Figure 5-9 indicate that increasing the number of segments for the Q2 rods allows a smoother potential gradient. With a 5-V potential applied to the 20-cm Q2 rods, an idea potential gradient throughout the entire Q2 ion path would be 0.25 V/cm. According to the potential gradient plots, the average potential gradient variations for the 21-, 26- and 35-segmented designs are approximately 40%, 20% and 5%, respectively from the idea 0.25 V/cm. For this application, an average variation in potential gradients should not be more than 10%. This means that at least 30 segments are needed for creating a reasonably smooth potential gradient along a 20-cm Q2 ion path. An extraction lens is still needed for the segmented designs because the calculations suggest that there is a negative potential gradient near the exit region of Q2. Nevertheless, the smoothness of the field gradient created is clearly a function of the number of segments used to make the Q2 rods. Mechanically, there is a limitation to the maximum number of segments possible for rods with a specific length. If the four rods of Q2 are each made of 50 segments, the fabrication of the device would be very labor-consuming and mechanically tedious.

Although the idea of a segmented Q2 quadrupole is theoretically feasible, the making of the device is very difficult. In the summer of 1988, after discussions with Dr. E. Strangas in the electrical engineering department and Dr. C. G. Enke, a new idea emerged for creating a smooth field gradient within Q2 without physically segmenting the quadrupole. In this novel idea, a resistance wire is wound around each Q2 rod to create the effect of a voltage divider. High resistance wires with resistivity up to 800 ohm/cm (or 1.38×10^{-6} ohm-meter) can be purchased from several

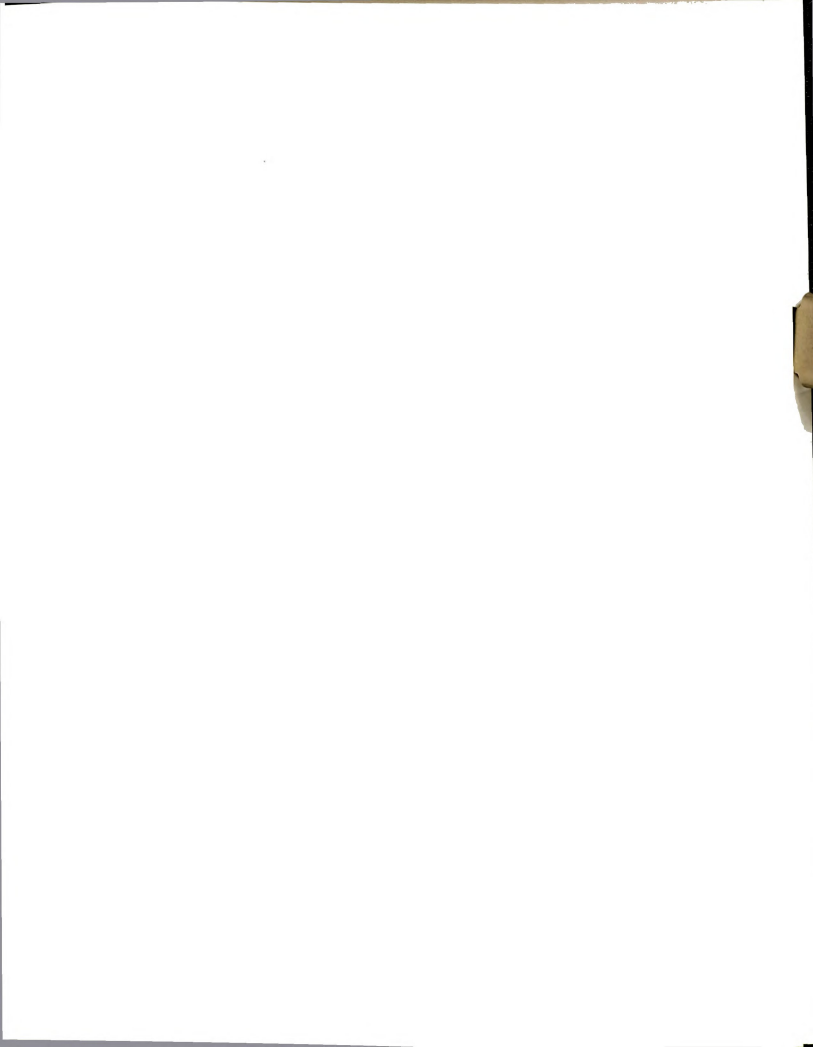
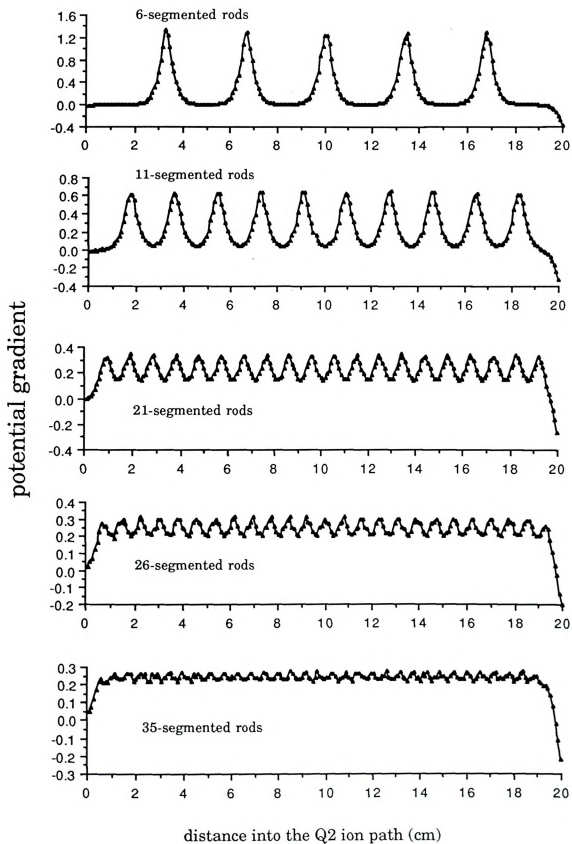


Figure 5-9 The 1st derivative plots representing potential gradient vs spatial distance into the Q2 ion path.



manufacturers. Winding the resistance wire by the conventional helical coil method will create an inductance that will make each rod an electro-magnet. It is certain that the magnetic field will have unwanted interactions with ions in Q2. The problem of inductance can be eliminated if wires are wound onto the rods by a non-circular zig-zag winding technique (Figure 5-10). In this winding technique, wire direction around the rod is reversed at a series of hooks installed on the back of each rod. Looking out from the inside of the quadrupole, this wire-winding design gives essentially the same physical features as the conventional circular coiling method except for the absence of inductance when an RF voltage is applied. Each winding turn of wires is equivalent to one segment of resistance. The maximum number of turns depends on the number of hooks on the rods. Clearly, winding 50 turns of wires on the rods of Q2 is a lot easier and more economical than making a Q2 quadrupole with 50 different segments. For a wire-winding design that gives an equivalence of 50 segments in each rod, ions entering Q2 should experience a very gentle longitudinal field gradient.

Because the purpose of using resistance wires for the Q2 modification is to create the effect of a voltage divider, rods that support these wires must not be conductors. Technically, a perfect insulator would be ideal for making the Q2 rods. Common metallic materials such as stainless steel and copper cannot be used to make rods in this case because of their high electrical conductivity. In order to evaluate the feasibility of this design, it is also necessary to obtain information about the resistance of the wires wound on Q2 as it is related to the amount of heat generated when a

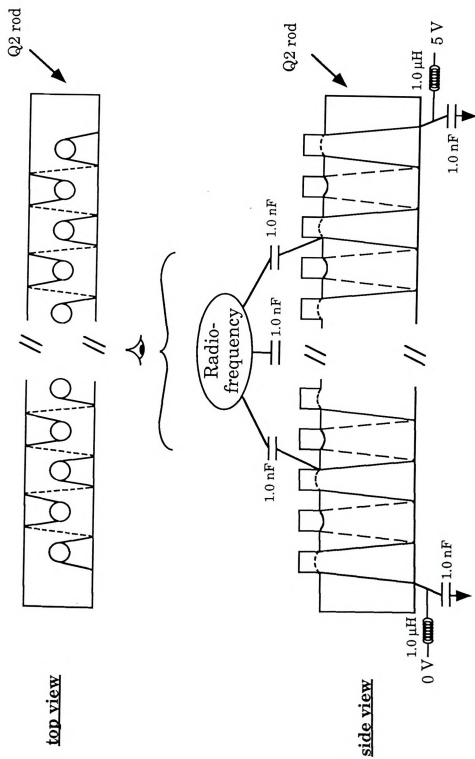


Figure 5-10 A design of modifying the second quadrupole using the non-circular zig-zag wire-winding technique. Dash lines represent wires wound on the back side of the rod.

potential gradient is applied. Generally, this can be calculated according to the following equation:

$$\text{resistance (R)} = \frac{\rho L}{A}$$

where ρ is the resistivity of the wire, L is the length of the wire, and A is the cross-section area of the wire. For a design that uses wires with resistivity of 800 ohm/cm² and a cross-section diameter of 0.5 mm, the resistance of a 50-turn wire wound on a 0.78 cm² x 20 cm rod is calculated to be about 11 ohm. This resistance will generate about 2.2 W of power when a 5-V potential difference is applied. The whole quadrupole wound with the resistance wires will generate close to 9 W of heat. For a system operated at high vacuum conditions, without the means of conduction, dissipation of such large amount of heat through radiation alone is too inefficient. The only efficient means for dissipating the heat would be by conduction through the rods. This imposes another restriction for the type of materials that can be used to make these rods. For this application, the four rods of Q2 must be made of a material that is both a good heat conductor and a good electrical insulator. This restriction excludes most available materials in the market. Upon an extensive library search, a ceramic material called beryllium oxide (BeO) (5) is found to be both an excellent heat conductor and electrical insulator. Figure 5-11 shows the room temperature thermal conductivity of BeO compared to various materials. In fact, the thermal conductivity of BeO is higher than most metallic materials. The Q2 design made of BeO can be fabricated by manufacturers for under \$1000.

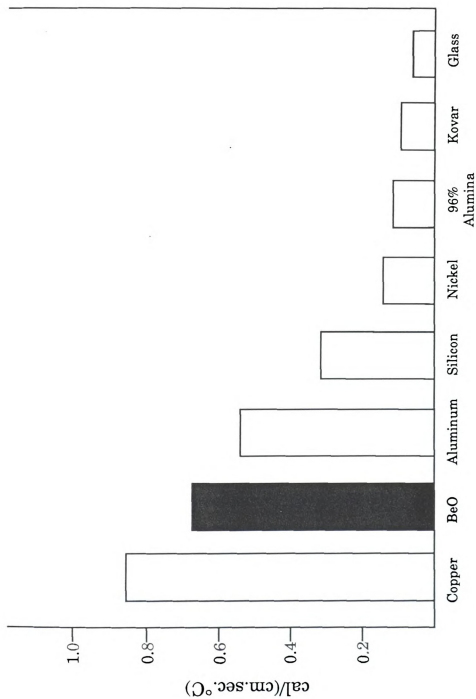


Figure 5-11 Room temperature thermal conductivity of BeO compared to various materials. (adapted from literature data compiled by Ceradyne, Inc., Costa Mesa, CA).

For the improvement of the trap-and-pulse technique described before, the wire-winding Q2 modification can be further refined. Instead of an extraction lens, the last 10 turns of the resistance wire of each rod can be used for a 10-step longitudinal field gradient either for trapping or pulsing of ions. This could provide an environment for a less abrupt potential field change at the Q2 exit region. Similarly, another 10-step longitudinal field gradient can be implemented near the entrance region of Q2 for a so-called inject-trap-and-pulse operation in which a large potential field applied at this region functions as an ion gate to allow only a packet of ions to enter the collision chamber for trapping and pulsing. The longitudinal potential field will be in "boat" and "chair" forms during ion trapping and pulsing, respectively.

Conclusions

The idea of facilitating the movement of low-energy ions in Q2 towards the detector could be accomplished by creating a longitudinal electric field gradient along the ion path inside Q2. This could be created by making Q2 rods behave as voltage dividers. This can be accomplished by either using segmented rods connected with resistors or rods wound with high resistance wires. Because the smoothness of a potential field gradient created within Q2 depends on the number of voltage-dividing segments on each rod, for creating rods with a high number of voltage-dividing segments, the design of using rods wound with resistance wires is mechanically more feasible than the other design. However, the wire-winding design requires the use of rods made of a material that is both a

good electrical insulator and a good heat conductor. Beryllium oxide would appear to be an ideal material for the application.

A smooth longitudinal potential field gradient created inside Q2 would allow the detector to sample low-energy product ions formed in every region of Q2. Product spectra obtained through the proposed method described in this chapter should represent the ion distribution in Q2 more closely than the traditional method.

References

1. White, E. L.; Tabet J. -C.; Bursley, M. M., *Org. Mass Spectrom.* **1987**, *22*, 132.
2. Dolnikowski, G. G.; Kristo, M. J.; Enke, C. G.; Watson, J. T., *Int. J. Mass Spectrom. Ion Phys.* **1988**, *82*, 1.
3. Kristo, M. J., Ph.D Dissertation, Michigan State University, 1987.
4. Dahl, D. A; Delmore, J. E., The SIMION PC/PS2 Users's Manual, Version 2; Informal Report EGG-CS-7233, Rev. 2, Idaho Falls National Engineering Laboratory, 1988.
5. National Beryllia Corporation: National Beryllia Technical Bulletin on Berlox Beo.

CHAPTER 6

CONCLUSIONS AND SUGGESTED FUTURE EXTENSIONS

The specificity of ion-molecule reactions has been well-demonstrated in this dissertation as a mean for distinguishing isomers of halogenated aromatic compounds. The unique features of a TQMS instrument offer enhanced selectivity for analytical applications of ion-molecule reactions. In particular, H/D exchange reactions are found to produce very distinct product spectra for the $[M-1]^-$ of halogenated benzene isomers. These allow the isomers to be differentiated when traditional mass spectrometric techniques fail. A series of studies of H/D exchange reactions using various deuterated reagents suggests that D_2O is among the most effective reagents for exchanging aromatic hydrogens of the $[M-1]^-$ ions of chlorobenzene isomers. When D_2O is used to react with the $[M-1]^-$ ions of tetrachlorodibenzo-p-dioxin (TCDD) isomers, 2,3,7,8-TCDD gives a unique H/D exchange product pattern which allows its differentiation from the other selected TCDD isomers. In addition, alcohol reagents are also found useful for differentiating 2,3,7,8-TCDD from the other less toxic TCDD isomers. The results described in this dissertation strongly demonstrate the great potential of applying ion-molecule reactions as analytical tools for differentiating organic isomers. A tandem quadrupole mass spectrometer is particularly well-suited for such applications.

Although studies of ion-molecule reactions have been extensive over the past three decades, the use of ion-molecule reactions for analytical

applications is largely unexplored. This dissertation has merely explored a very small aspect of the enormous potential of the reactions. Certainly, there is much work still to be done. The following are some suggestions.

I. Substituting one of the two chlorines of a dichlorobenzene molecule with other functionalities such as NH_2 , OH , CHO , CH_3 , OCH_3 , COOH or NO_2 is found to substantially reduce the reactivity of the $[\text{M}-1]^-$ ion for H/D exchange reactions with D_2O . The observed reduction in reactivity suggests that while D_2O is an excellent reagent for exchanging hydrogens of dichlorobenzene $[\text{M}-1]^-$ ions, different deuterated reagents are needed for effectively exchanging the hydrogens of the substituted chlorobenzene $[\text{M}-1]^-$ ions. The study of H/D exchange reactions on the substituted chlorobenzene $[\text{M}-1]^-$ ions should be continued by exploring the use of different deuterated reagents such as ND_3 , CD_4 , CH_3OD , CH_3COOD , etc.. The results of such a study may be important in establishing the effectiveness of using ion-molecule reactions for differentiating isomers of the substituted chlorobenzenes.

II. The proposed H/D exchange mechanism involving the formation of a five-membered-ring intermediate for reactions between the $[\text{M}-1]^-$ of chlorobenzene and D_2O is consistent with the results derived from all the isomers of chlorobenzenes. It is quite possible that a similar mechanism is also applicable to the $[\text{M}-1]^-$ of aromatic compounds containing two or more fused benzene rings. Our mechanistic study may be extended to compounds with multiple benzene rings. Isomers of chloronaphthalene are ideal candidates for initial studies. With a better understanding of the two-ring system, the investigation might then be continued on compounds

with three or more fused benzene rings. Information obtained from the mechanistic studies may be useful for developing better analytical strategies.

III. Although the ion-molecule reactions described in Chapter 4 are found useful to differentiate 2,3,7,8-TCDD from other less toxic isomers, the study was limited to only a few isomers. In order to investigate the usefulness of these reactions as analytical techniques, future studies should include all 22 TCDD isomers. Since the structures of polychlorodibenzofurans (PCDFs) are very similar to those of polychlorodibenzo-p-dioxins (PCDDs), the study of PCDDs may also be extended to include isomers of PCDF.

IV. Finally, the collision cell design described in Chapter 5 is expected to provide improvement in the detection of low-energy product ions formed inside the collision cell; the implementation of the proposed design would be an interesting project to explore.

APPENDIX

Appendix

Computer-simulated individual collision-product plots based on different percentages of reactive collision for the H/D exchange reactions derived from different structures of the [M-1]⁻ ions of dichlorobenzene isomers. The simulations are based on the proposed H/D exchange reaction mechanism described in Chapter 3.

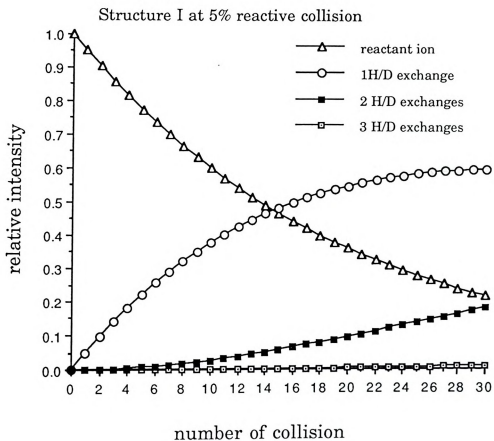


Figure A-1 A simulated collision-product plot for the structure I of o-dichlorobenzene based on an H/D exchange reactivity of 5% reactive collision.

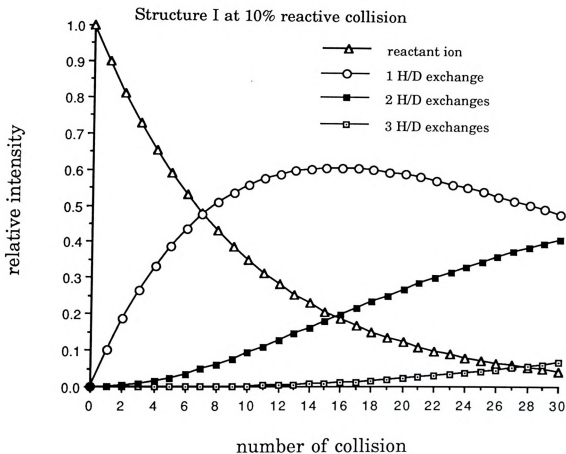


Figure A-2 A simulated collision-product plot for the structure I of *o*-dichlorobenzene based on an H/D exchange reactivity of 10% reactive collision.

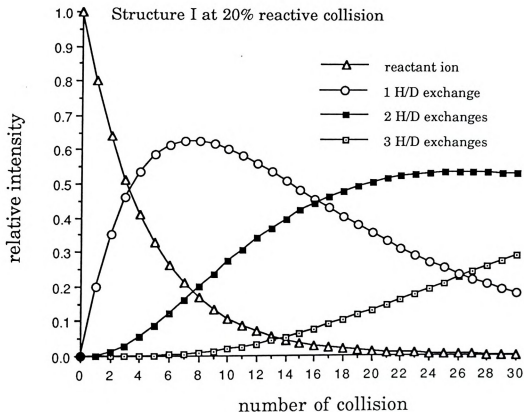


Figure A-3 A simulated collision-product plot for the structure I of o-dichlorobenzene based on an H/D exchange reactivity of 20% reactive collision.

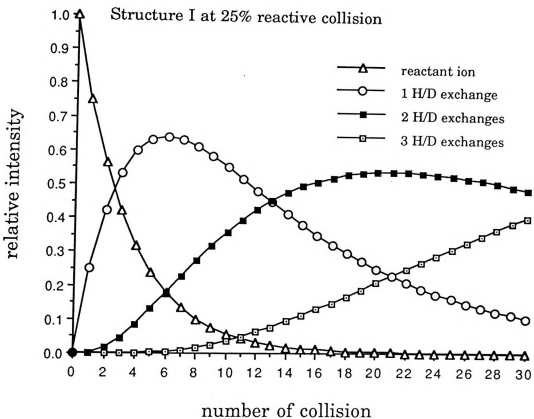


Figure A-4 A simulated collision-product plot for the structure I of *o*-dichlorobenzene based on an H/D exchange reactivity of 25% reactive collision.

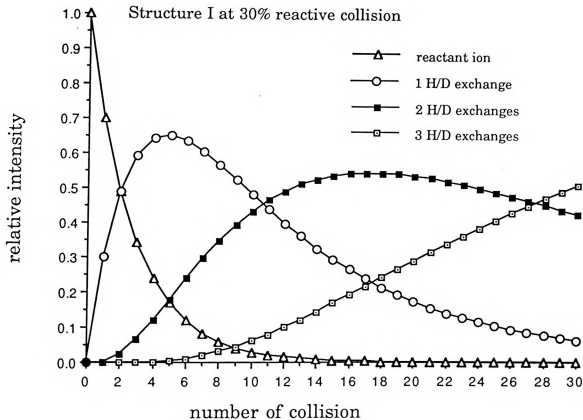


Figure A-5 A simulated collision-product plot for the structure I of o-dichlorobenzene based on an H/D exchange reactivity of 30% reactive collision.

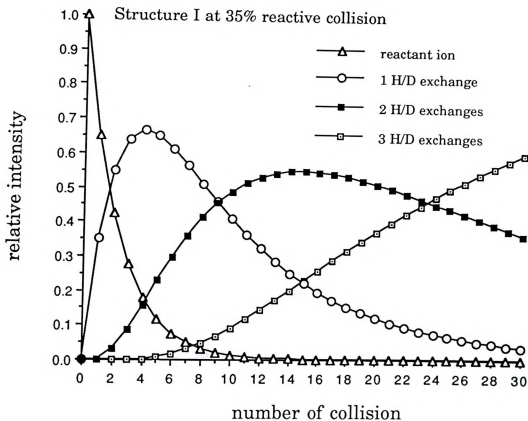


Figure A-6 A simulated collision-product plot for the structure I of *o*-dichlorobenzene based on an H/D exchange reactivity of 35% reactive collision.

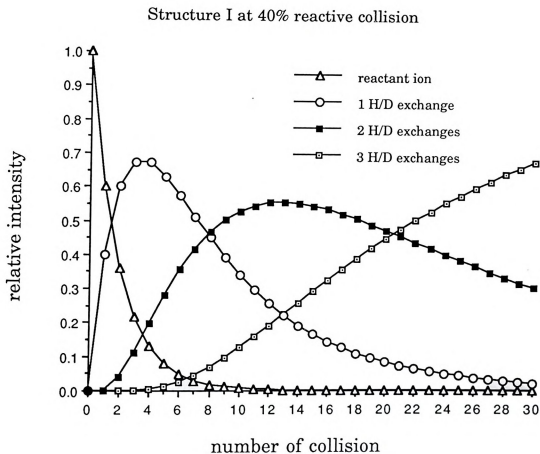


Figure A-7 A simulated collision-product plot for the structure I of o-dichlorobenzene based on an H/D exchange reactivity of 40% reactive collision.

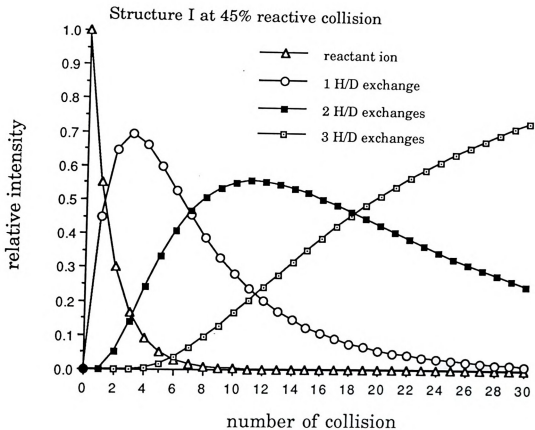


Figure A-8 A simulated collision-product plot for the structure I of *o*-dichlorobenzene based on an H/D exchange reactivity of 45% reactive collision.

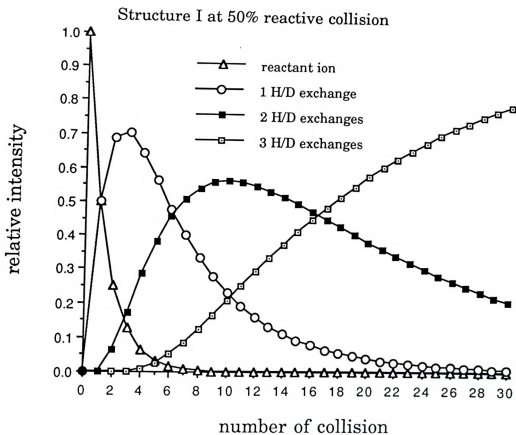


Figure A-9 A simulated collision-product plot for the structure I of o-dichlorobenzene based on an H/D exchange reactivity of 50% reactive collision.

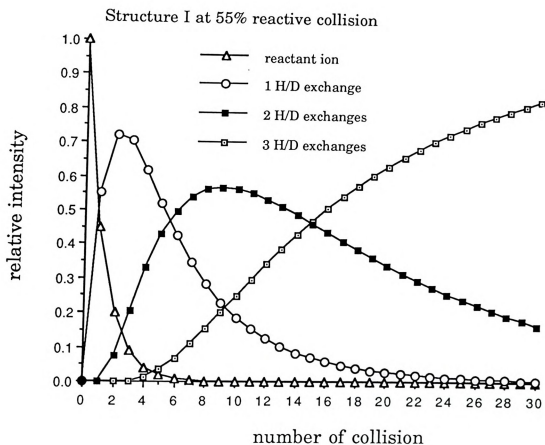


Figure A-10 A simulated collision-product plot for the structure I of *o*-dichlorobenzene based on an H/D exchange reactivity of 55% reactive collision.

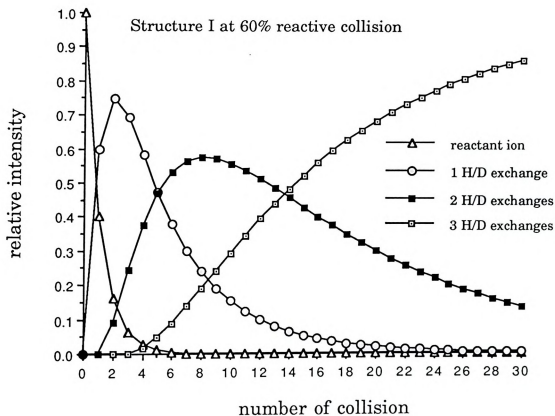


Figure A-11 A simulated collision-product plot for the structure I of *o*-dichlorobenzene based on an H/D exchange reactivity of 60% reactive collision.

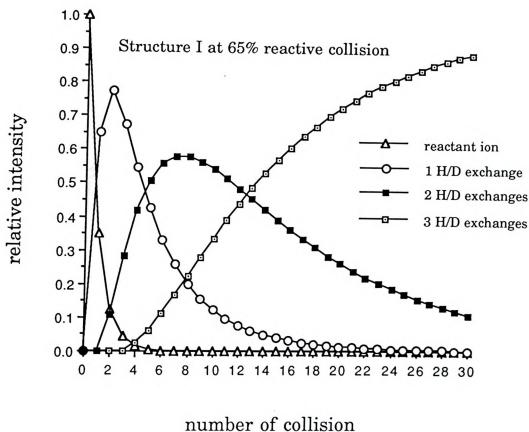


Figure A-12 A simulated collision-product plot for the structure I of o-dichlorobenzene based on an H/D exchange reactivity of 65% reactive collision.

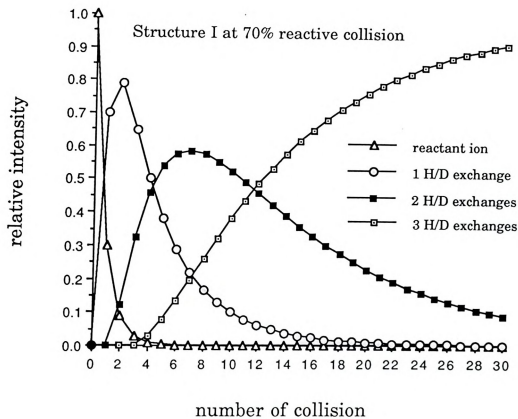
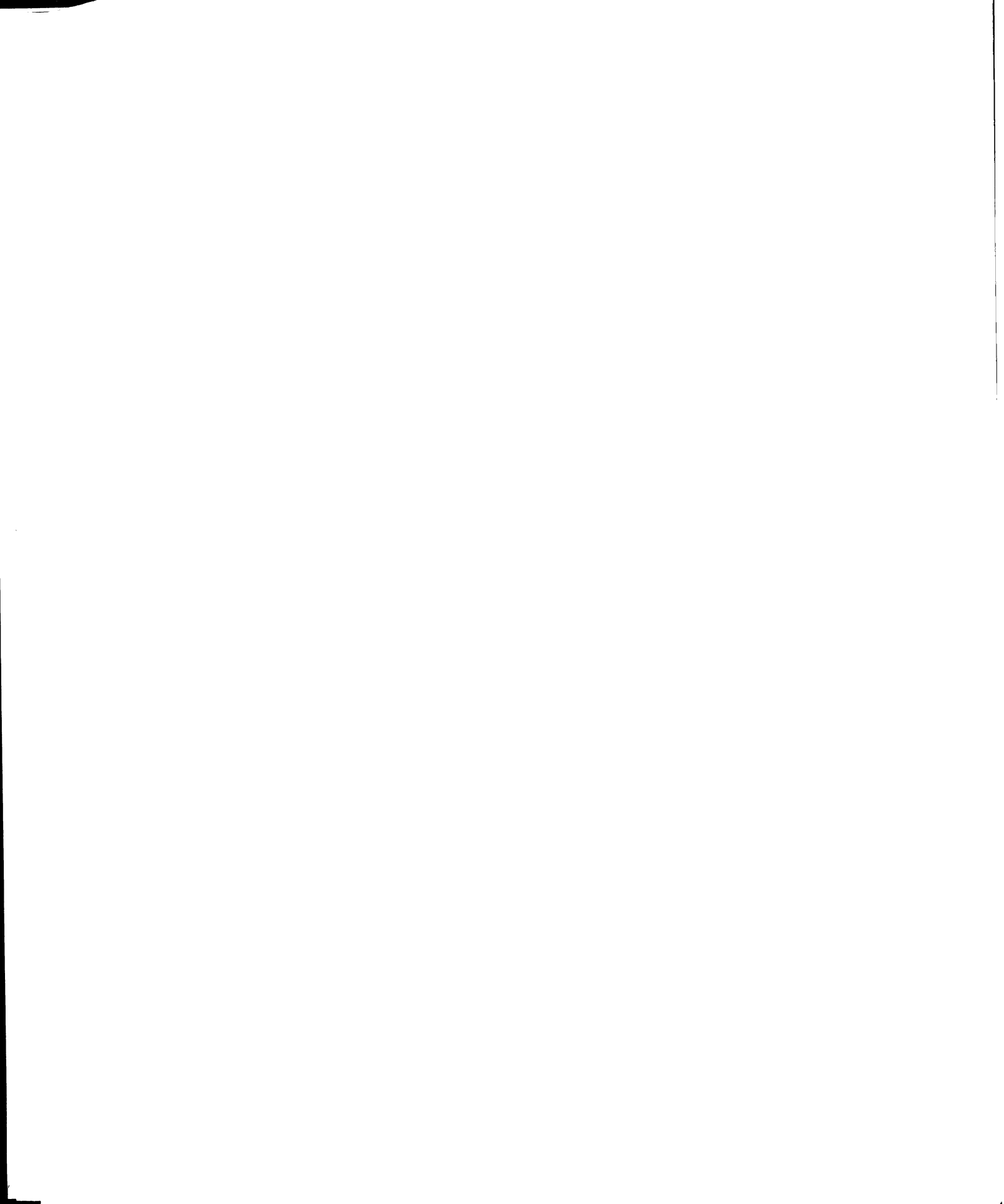


Figure A-13 A simulated collision-product plot for the structure I of o-dichlorobenzene based on an H/D exchange reactivity of 70% reactive collision.



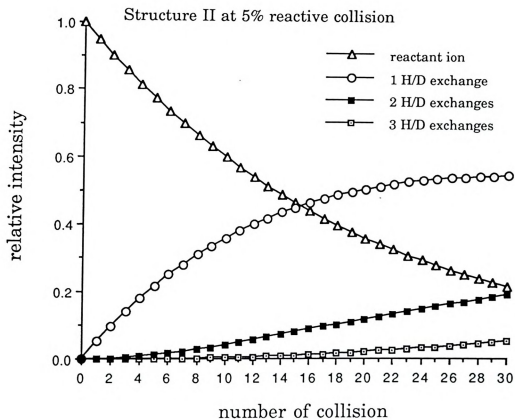


Figure A-14 A simulated collision-product plot for the structure II of o-dichlorobenzene based on an H/D exchange reactivity of 5% reactive collision.

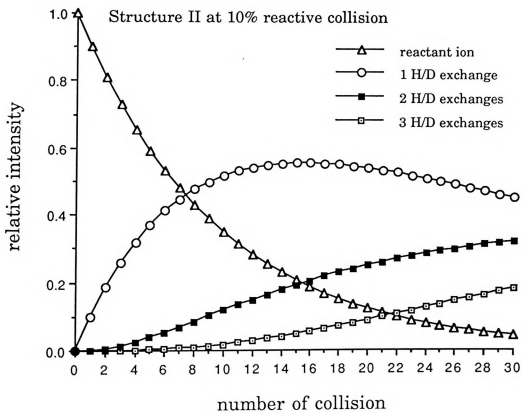


Figure A-15 A simulated collision-product plot for the structure II of *o*-dichlorobenzene based on an H/D exchange reactivity of 10% reactive collision.

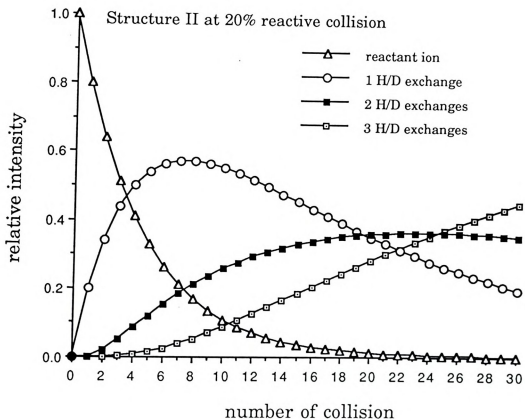


Figure A-16 A simulated collision-product plot for the structure II of *o*-dichlorobenzene based on an H/D exchange reactivity of 20% reactive collision.

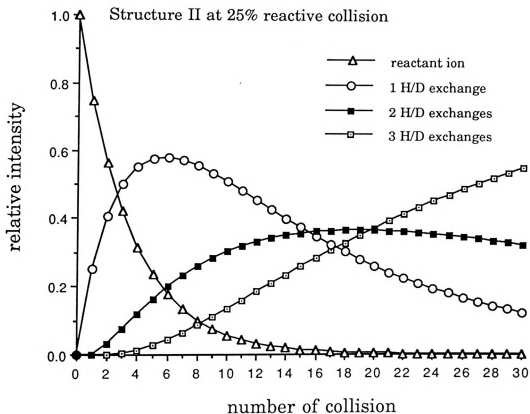


Figure A-17 A simulated collision-product plot for the structure II of *o*-dichlorobenzene based on an H/D exchange reactivity of 25% reactive collision.

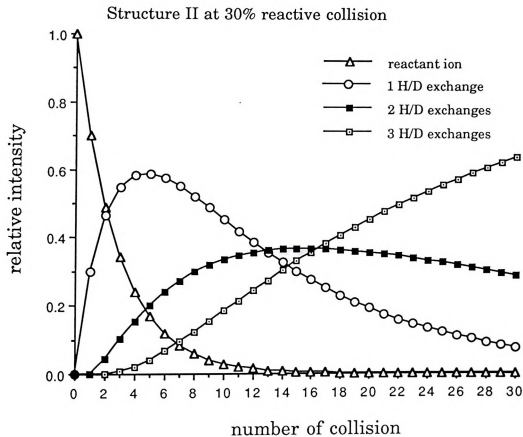


Figure A-18 A simulated collision-product plot for the structure II of o-dichlorobenzene based on an H/D exchange reactivity of 30% reactive collision.

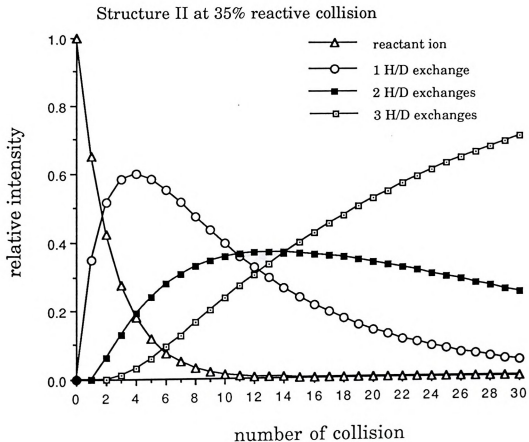


Figure A-19 A simulated collision-product plot for the structure II of *o*-dichlorobenzene based on an H/D exchange reactivity of 35% reactive collision.

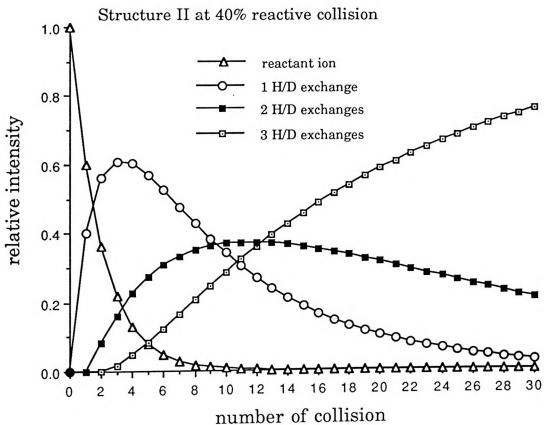


Figure A-20 A simulated collision-product plot for the structure II of *o*-dichlorobenzene based on an H/D exchange reactivity of 40% reactive collision.

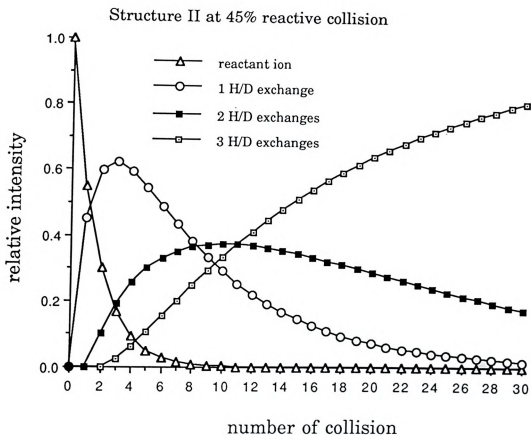


Figure A-21 A simulated collision-product plot for the structure II of o-dichlorobenzene based on an H/D exchange reactivity of 45% reactive collision.

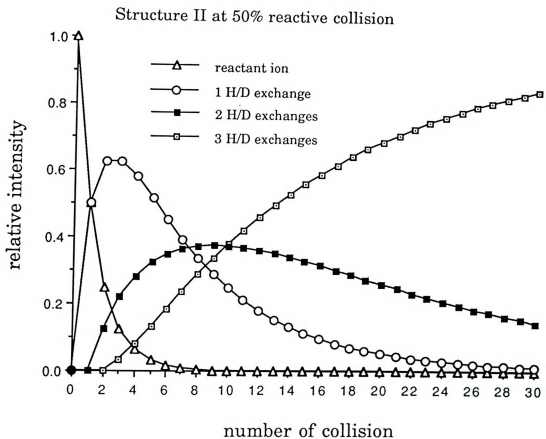


Figure A-22 A simulated collision-product plot for the structure II of o-dichlorobenzene based on an H/D exchange reactivity of 50% reactive collision.

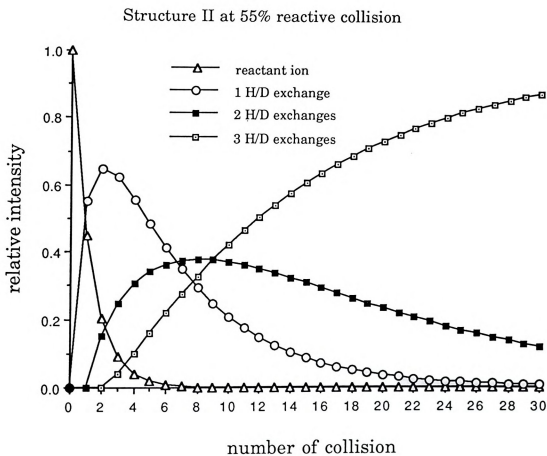


Figure A-23 A simulated collision-product plot for the structure II of o-dichlorobenzene based on an H/D exchange reactivity of 55% reactive collision.

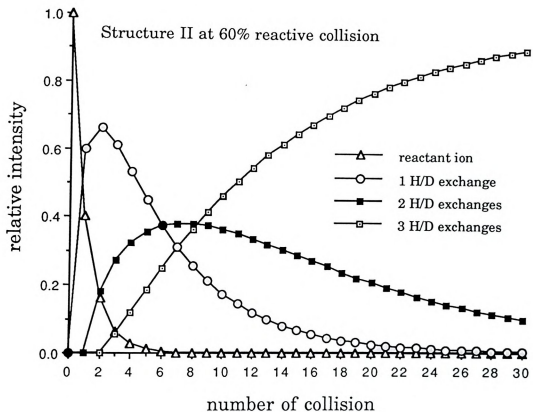


Figure A-24 A simulated collision-product plot for the structure II of o-dichlorobenzene based on an H/D exchange reactivity of 60% reactive collision.

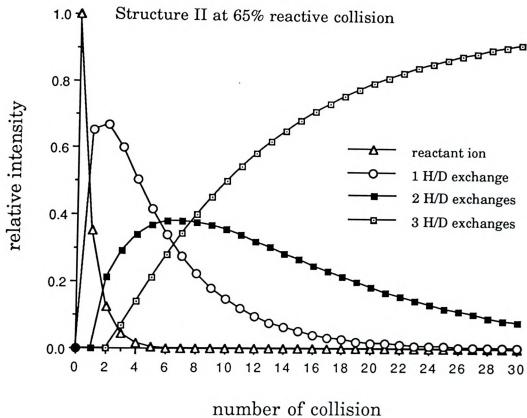


Figure A-25 A simulated collision-product plot for the structure II of o-dichlorobenzene based on an H/D exchange reactivity of 65% reactive collision.

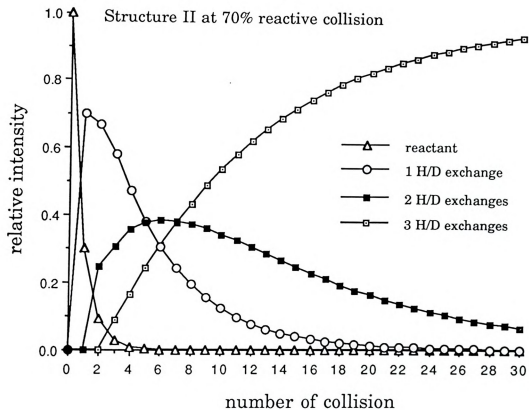


Figure A-26 A simulated collision-product plot for the structure II of *o*-dichlorobenzene based on an H/D exchange reactivity of 70% reactive collision.

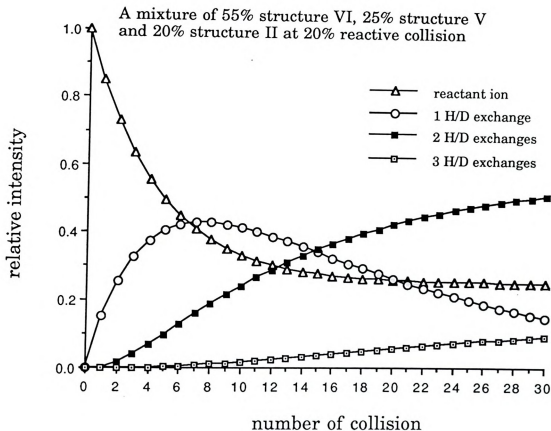


Figure A-27 A simulated collision-product plot for a mixture of dichlorobenzene anions originated from *m*-dichlorobenzene. The calculations are based on an H/D exchange reactivity of 20% reactive collision. The mixture contains anions of 55% structure VI, 25% structure V and 20% structure II.

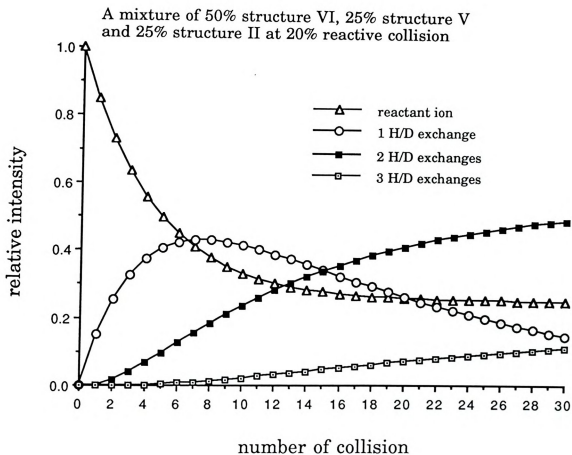


Figure A-28 A simulated collision-product plot for a mixture of dichlorobenzene anions originated from *m*-dichlorobenzene. The calculations are based on an H/D exchange reactivity of 20% reactive collision. The mixture contains anions of 50% structure VI, 25% structure V and 25% structure II.

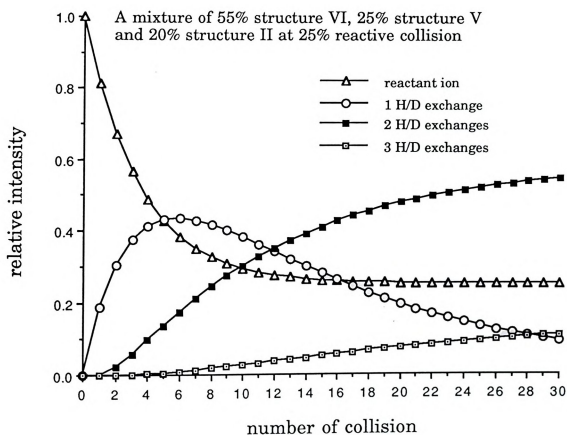


Figure A-29 A simulated collision-product plot for a mixture of dichlorobenzene anions originated from *m*-dichlorobenzene. The calculations are based on an H/D exchange reactivity of 25% reactive collision. The mixture contains anions of 55% structure VI, 25% structure V and 20% structure II.

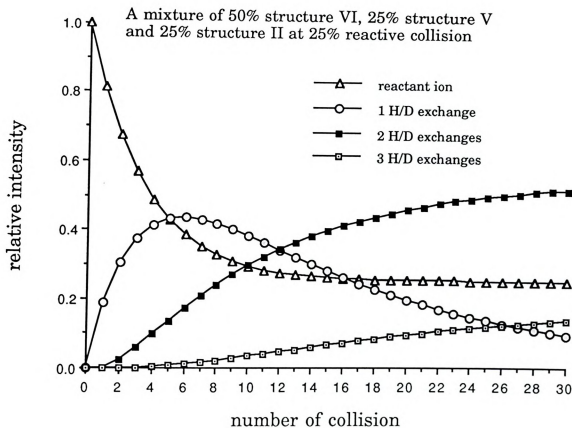


Figure A-30 A simulated collision-product plot for a mixture of dichlorobenzene anions originated from *m*-dichlorobenzene. The calculations are based on an H/D exchange reactivity of 25% reactive collision. The mixture contains anions of 50% structure VI, 25% structure V and 25% structure II.

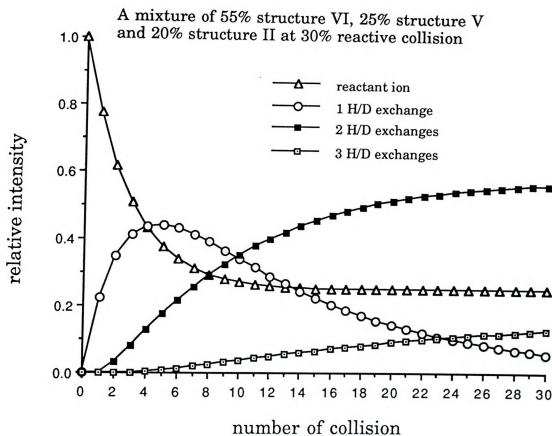


Figure A-31 A simulated collision-product plot for a mixture of dichlorobenzene anions originated from *m*-dichlorobenzene. The calculations are based on an H/D exchange reactivity of 30% reactive collision. The mixture contains anions of 55% structure VI, 25% structure V and 20% structure II.

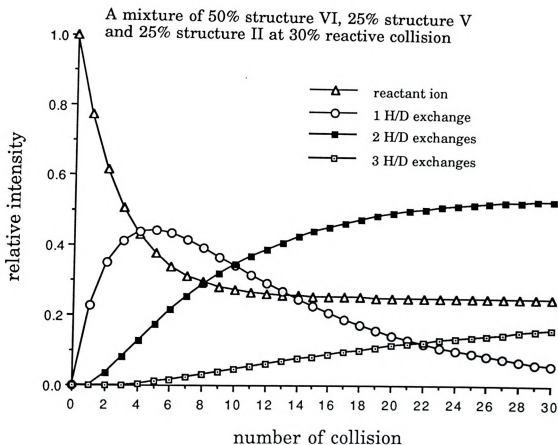


Figure A-32 A simulated collision-product plot for a mixture of dichlorobenzene anions originated from *m*-dichlorobenzene. The calculations are based on an H/D exchange reactivity of 30% reactive collision. The mixture contains anions of 50% structure VI, 25% structure V and 25% structure II.

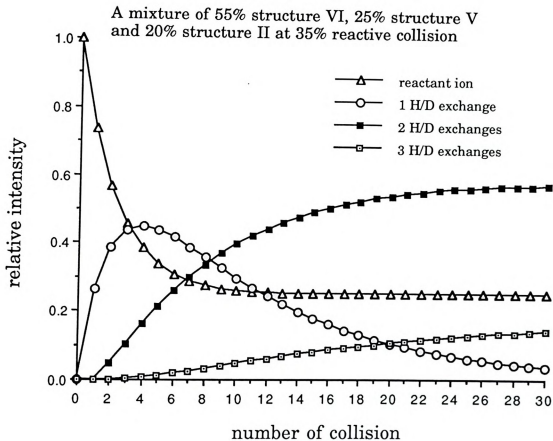


Figure A-33 A simulated collision-product plot for a mixture of dichlorobenzene anions originated from *m*-dichlorobenzene. The calculations are based on an H/D exchange reactivity of 35% reactive collision. The mixture contains anions of 55% structure VI, 25% structure V and 20% structure II.

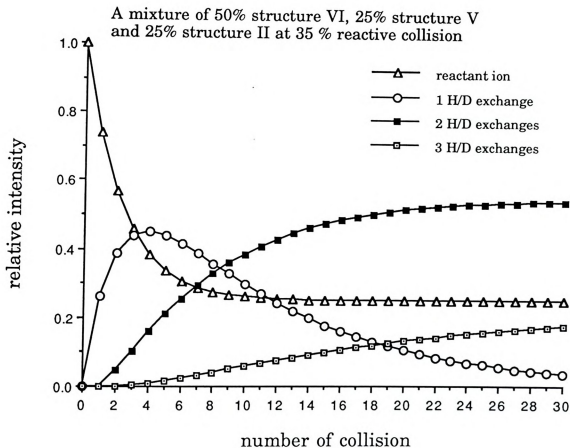


Figure A-34 A simulated collision-product plot for a mixture of dichlorobenzene anions originated from *m*-dichlorobenzene. The calculations are based on an H/D exchange reactivity of 35% reactive collision. The mixture contains anions of 50% structure VI, 25% structure V and 25% structure II.

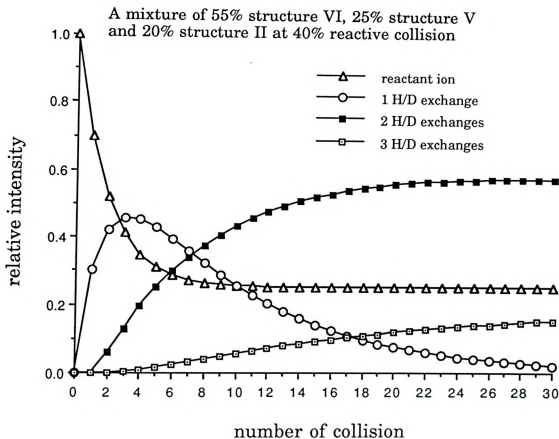


Figure A-35 A simulated collision-product plot for a mixture of dichlorobenzene anions originated from *m*-dichlorobenzene. The calculations are based on an H/D exchange reactivity of 40% reactive collision. The mixture contains anions of 55% structure VI, 25% structure V and 20% structure II.

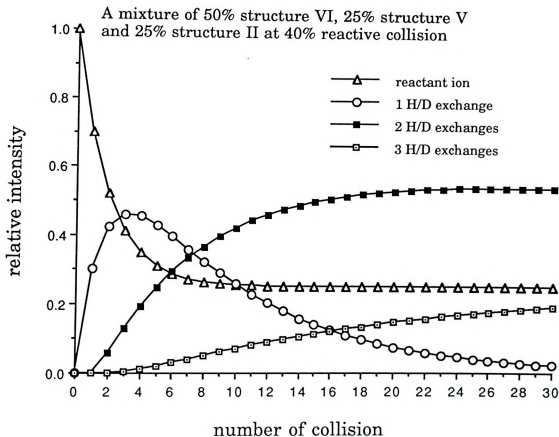


Figure A-36 A simulated collision-product plot for a mixture of dichlorobenzene anions originated from *m*-dichlorobenzene. The calculations are based on an H/D exchange reactivity of 40% reactive collision. The mixture contains anions of 50% structure VI, 25% structure V and 25% structure II.

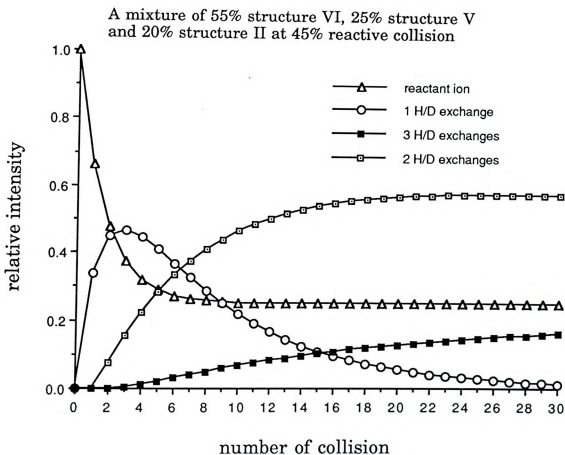


Figure A-37 A simulated collision-product plot for a mixture of dichlorobenzene anions originated from *m*-dichlorobenzene. The calculations are based on an H/D exchange reactivity of 45% reactive collision. The mixture contains anions of 55% structure VI, 25% structure V and 20% structure II.

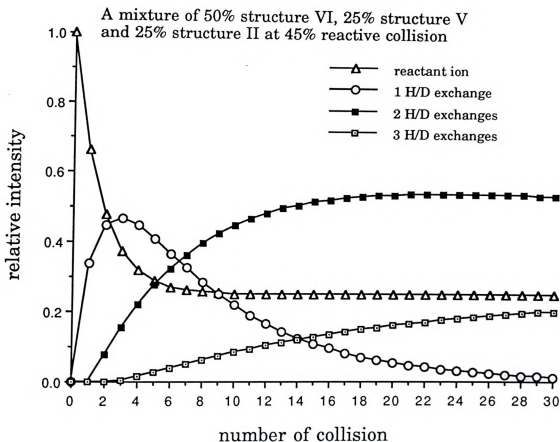


Figure A-38 A simulated collision-product plot for a mixture of dichlorobenzene anions originated from *m*-dichlorobenzene. The calculations are based on an H/D exchange reactivity of 45% reactive collision. The mixture contains anions of 50% structure VI, 25% structure V and 25% structure II.

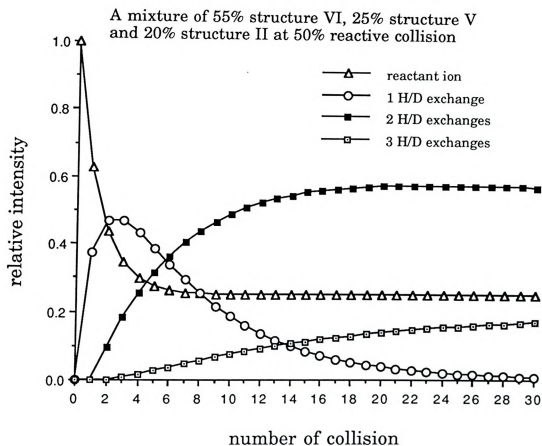


Figure A-39 A simulated collision-product plot for a mixture of dichlorobenzene anions originated from *m*-dichlorobenzene. The calculations are based on an H/D exchange reactivity of 50% reactive collision. The mixture contains anions of 55% structure VI, 25% structure V and 20% structure II.

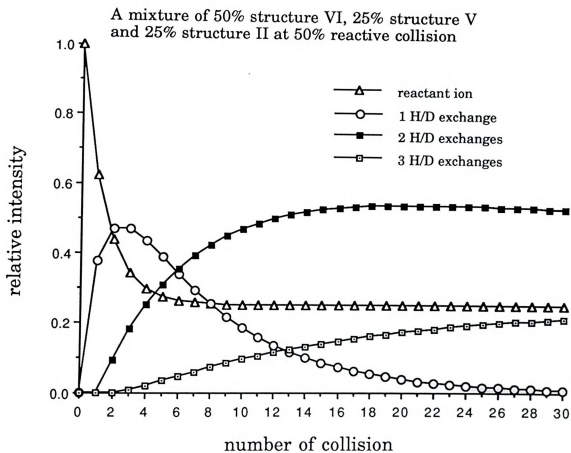


Figure A-40 A simulated collision-product plot for a mixture of dichlorobenzene anions originated from *m*-dichlorobenzene. The calculations are based on an H/D exchange reactivity of 50% reactive collision. The mixture contains anions of 50% structure VI, 25% structure V and 25% structure II.

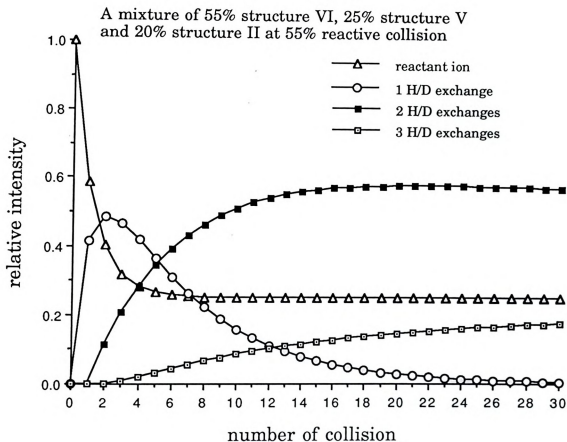


Figure A-41 A simulated collision-product plot for a mixture of dichlorobenzene anions originated from *m*-dichlorobenzene. The calculations are based on an H/D exchange reactivity of 55% reactive collision. The mixture contains anions of 55% structure VI, 25% structure V and 20% structure II.

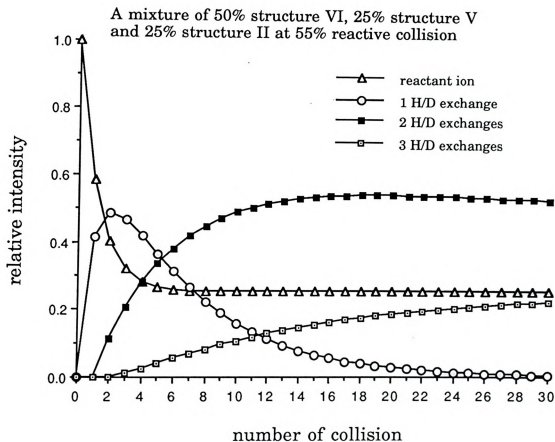


Figure A-42 A simulated collision-product plot for a mixture of dichlorobenzene anions originated from m-dichlorobenzene. The calculations are based on an H/D exchange reactivity of 55% reactive collision. The mixture contains anions of 50% structure VI, 25% structure V and 25% structure II.

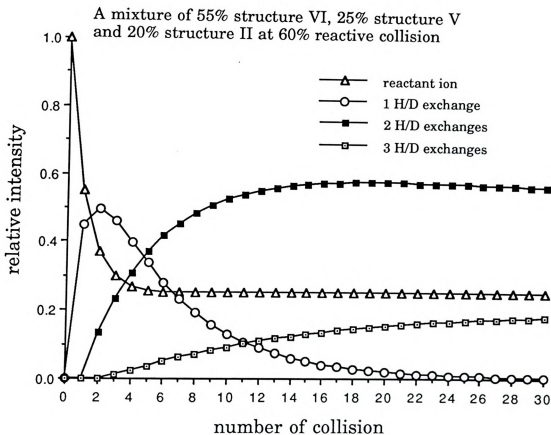


Figure A-43 A simulated collision-product plot for a mixture of dichlorobenzene anions originated from *m*-dichlorobenzene. The calculations are based on an H/D exchange reactivity of 60% reactive collision. The mixture contains anions of 55% structure VI, 25% structure V and 20% structure II.

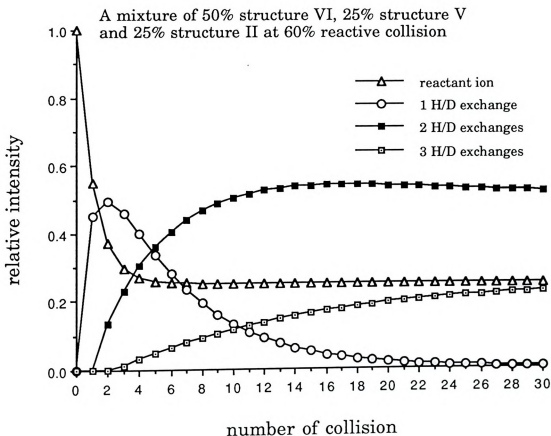


Figure A-44 A simulated collision-product plot for a mixture of dichlorobenzene anions originated from *m*-dichlorobenzene. The calculations are based on an H/D exchange reactivity of 60% reactive collision. The mixture contains anions of 50% structure VI, 25% structure V and 25% structure II.

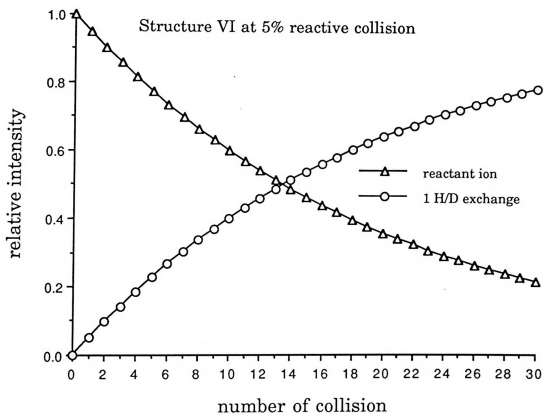


Figure A-45 A simulated collision-product plot for the structure VI of p-dichlorobenzene based on an H/D exchange reactivity of 5% reactive collision.

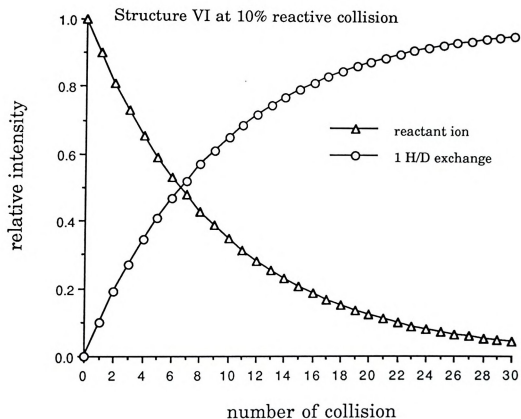


Figure A-46 A simulated collision-product plot for the structure VI of p-dichlorobenzene based on an H/D exchange reactivity of 10% reactive collision.

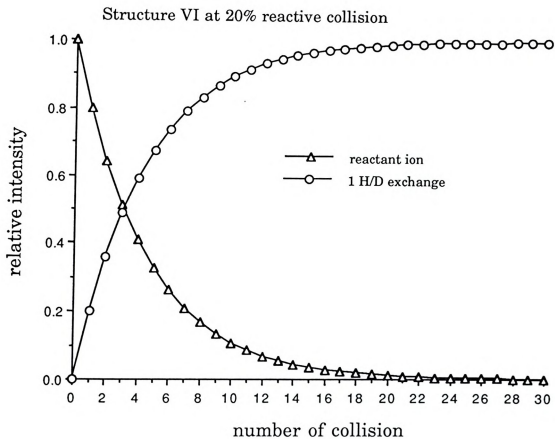


Figure A-47 A simulated collision-product plot for the structure VI of p-dichlorobenzene based on an H/D exchange reactivity of 20% reactive collision.

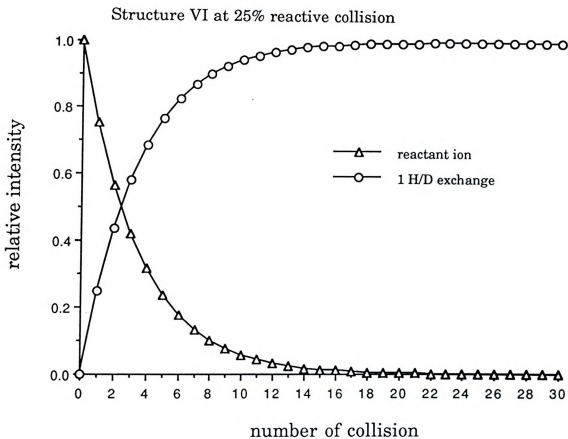


Figure A-48 A simulated collision-product plot for the structure VI of *p*-dichlorobenzene based on an H/D exchange reactivity of 25% reactive collision.

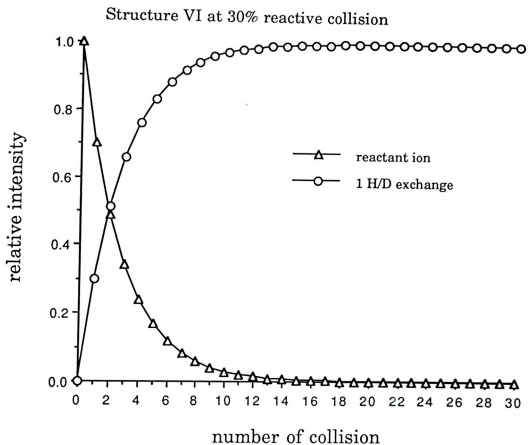


Figure A-49 A simulated collision-product plot for the structure VI of p-dichlorobenzene based on an H/D exchange reactivity of 30% reactive collision.

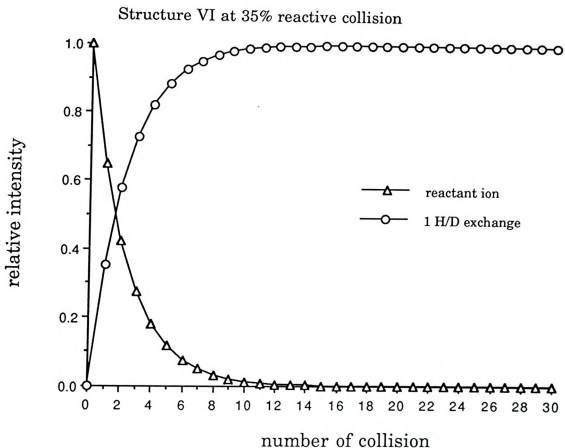


Figure A-50 A simulated collision-product plot for the structure VI of p-dichlorobenzene based on an H/D exchange reactivity of 35% reactive collision.

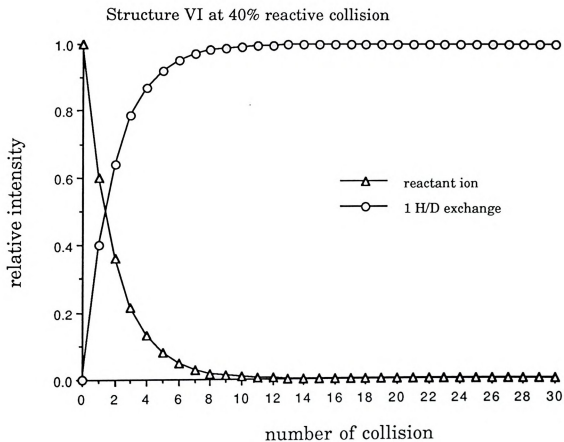


Figure A-51 A simulated collision-product plot for the structure VI of p-dichlorobenzene based on an H/D exchange reactivity of 40% reactive collision.

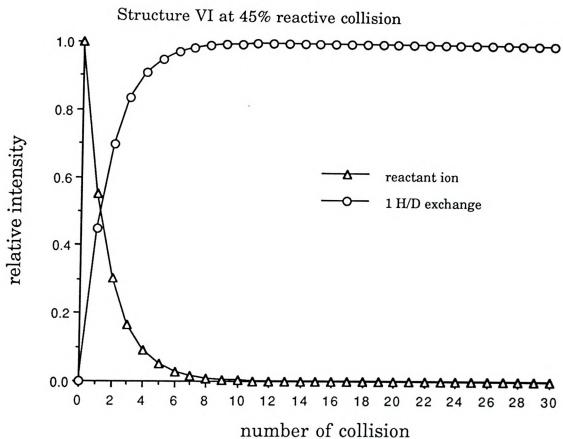


Figure A-52 A simulated collision-product plot for the structure VI of p-dichlorobenzene based on an H/D exchange reactivity of 45% reactive collision.

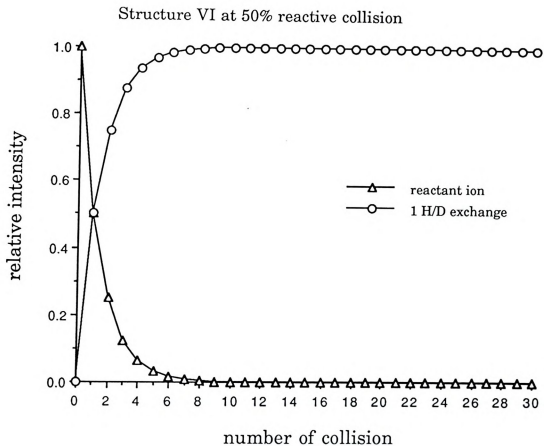


Figure A-53 A simulated collision-product plot for the structure VI of p-dichlorobenzene based on an H/D exchange reactivity of 50% reactive collision.

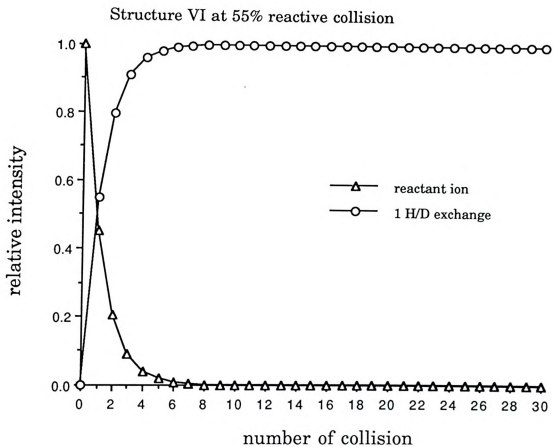


Figure A-54 A simulated collision-product plot for the structure VI of p-dichlorobenzene based on an H/D exchange reactivity of 55% reactive collision.

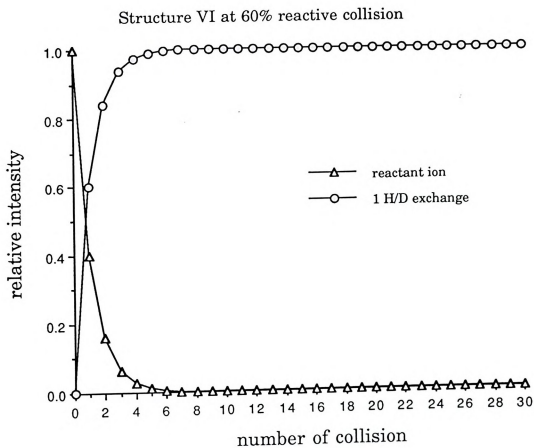


Figure A-55 A simulated collision-product plot for the structure VI of p-dichlorobenzene based on an H/D exchange reactivity of 60% reactive collision.

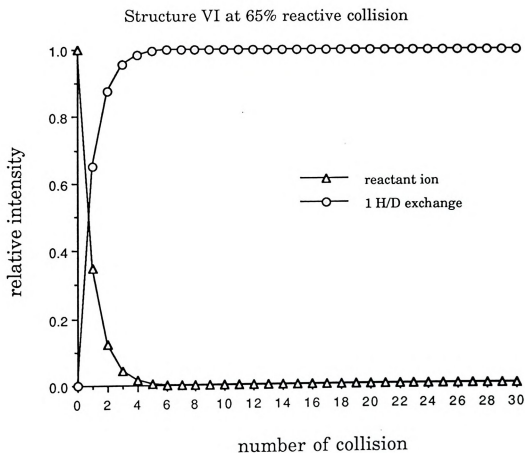


Figure A-56 A simulated collision-product plot for the structure VI of p-dichlorobenzene based on an H/D exchange reactivity of 65% reactive collision.

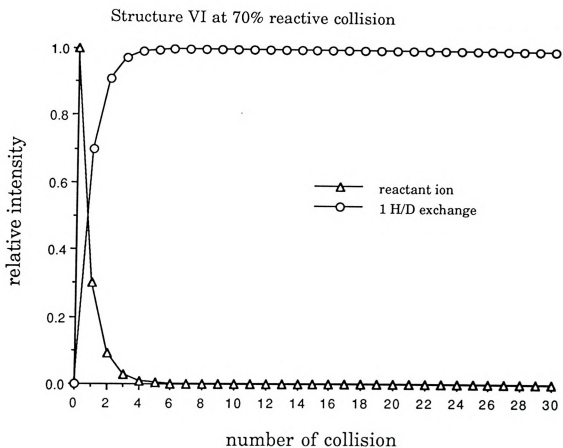


Figure A-57 A simulated collision-product plot for the structure VI of p-dichlorobenzene based on an H/D exchange reactivity of 70% reactive collision.





MICHIGAN STATE UNIV. LIBRARIES



31293009081856